Energimyndigheten

Slutrapport

Energimyndighetens titel på projektet – svenska
Soldriven fjärrvärme med groplager för svenska förhållanden

Energimyndighetens titel på projektet – engelska
Solar district heating with pit storage for Swedish conditions

Organisation
Högskolan Dalarna
Sustainable Energy Research Centre (SERC)
79188 Falun

Namn på projektledare
Chris Bales

Namn på eventuella övriga projektdeltagare
Urban Persson, Puneet Saini, Fredric Ottermo, Luis Sánchez García, Joakim Byström, Erik Björkland

Nyckelord Solar thermal, district heating, pit thermal energy storage, case study, screening, GIS analysis

Förord

Detta projekt (P2022-00461) har finansierats av Energimyndigheten med avseende på Högskolan Dalarnas och Högskolan i Halmstads deltagande. Absolicon AB har medfinansierat projektet med egna medel.

Contents

Sammanfattning

Storskalig solvärme för fjärrvärme har ökat snabbt under detta sekel och är idag en kommersiell industri i Danmark med över 100 system i drift. Flera av dem har storskalig värmelagring i form av groplager, vilket innebär att en större del av värmebehovet kan täckes med solvärme. Tidigare har ekonomiska faktorer inte varit lika bra i Sverige som i Danmark, men med högre bränslepriser, samt med andra konkurrerande användningsområden för biomassa, har förutsättningarna för solvärme ökat även här.

Inom projektet har man jobbat med geografiska och geologiska data från bl.a. SGU för att ta fram vilka platser i Sverige som har potential för att kunna bygga groplager. Kartläggningen visar att de allra flesta fjärrvärmesystem har potentiella områden för groplager inom rimligt avstånd från nätet. Endast 86 fjärrvärmeområden har ingen potential alls. Trots avsaknad av tillförlitliga data för hela landet avseende grundvattennivå eller -flöde, som båda är viktiga faktorer för ekonomisk lönsamhet, är resultaten dock optimistiska. Föga förvånande för ett vidsträckt land som Sverige, visar kartläggningen att det finns stora skillnader, dock att det generellt sett finns bättre förutsättningar i södra Sverige än i norra.

Man uppskattade också hur stora andelar solvärmesystem med groplager potentiellt sett kan leverera till de fjärrvärmeområden som har lämpliga förutsättningar. Om alla dessa fjärrvärmeområden skulle bygga system som täcker 20% av sitt årliga värmebehov skulle solvärme bidra med 15% av hela Sveriges fjärrvärmebehov. Om alla med förutsättningar byggde system som täcker 40% av behovet skulle motsvarande siffra vara hela 36%.

Förstudierna för Råneå, Härnösand och Söderhamn visar att värmekostnaden från solvärmesystemen är något högre än de aktuella värmekostnaderna i dessa system med det aktuella ränteläget. Eftersom värmekostnaden för solvärmesystem nästan uteslutande utgörs av investeringen, varierar kostnaden i princip enbart med ränteläget. En lägre räntenivå eller en liten årlig ökning i bränslepriserna skulle göra dessa system lönsamma. Lönsamheten, så som för många andra tekniker, är bättre för större system än för små. Förstudierna visade också att integrering av en värmepump lönar sig om platsen för groplagret ligger i utkanten av fjärrvärmeområdet och om det finns rökgaskondensering i systemet.

I praktiken finns även andra faktorer som kan försvåra uppförandet av ett groplager vid de platser som kartläggningen identifierat. Kartläggningens resultat är teoretiska med antagandet att inga av dessa negativa faktorer föreligger. Noggranna geologiska undersökningar behövs om man vill ta nästa steg för att försäkra sig om att en plats är lämplig för groplager.

Summary

Large-scale solar district heating has increased fast recently and is a commercial industry in Denmark with over 100 systems. Pit stores with high solar fraction exist in several of these systems. Some economic factors in Sweden are not as good as in Denmark. However, recent events have forced up the price of biomass in Sweden and other competing uses for the forest resource point to greater competition and thus higher prices, resulting in better viability for solar.

The project has used geographic and geological data from e.g. SGU to identify which areas in Sweden that are potentially suitable for pit stores. The results from the screening process show that the vast majority of district heating areas have potentially suitable areas for pit storage within a reasonable distance from the network. Only 86 district heating areas do not. As there is no reliable data for the whole country for ground water level and flow, both important factors for economic viability, the results are optimistic. As to be expected, the results show large variations over the country, but in general there are more suitable areas in the south than north.

The project also estimated how much heat solar and pit storage systems could potentially deliver to the district heating areas with suitable areas. If all of these identified district heating areas installed solar and pit storage systems covering 20% of their demand, 15% of Sweden's total district heating demand would be supplied by solar. If all networks with potential areas for pit storage installed systems covering 40% of the local demand, the equivalent figure is 36%.

Pre-feasibility studies for Råneå, Härnösand and Söderhamn show that the heat cost for solar heating systems is slightly higher than the current production heat cost in these networks, given the current interest rate. As the heat cost for solar is mostly dependent on the investment cost, it varies over time in principle only with the interest rate. A lower interest rate or small annual increases in fuel costs would make the studied solar heating systems economically viable. Costs, as for many other technologies, are lower for larger systems. Integration of a heat pump in the system is cost-effective if the site of the pit store is in the periphery of the network and the district heating system has exhaust gas condensation.

In practice there are many additional factors that can hinder building a pit store in the sites identified as suitable in the screening. The results of the screening are theoretical and are based on the assumption that none of these negative factors exist. Detailed on-site geological measurements are needed if one wants to take the next step in actually building a pit store.

Background

Large-scale solar district heating has increased fast recently and is a commercial industry in Denmark with over 100 systems. Pit storage with high solar fraction exist in several of these systems. Some economic factors in Sweden are not as good as in Denmark. However, recent events have forced up the price of biomass in Sweden and other competing uses for the forest resource point to greater competition and thus higher prices, resulting in better viability for solar.

Sweden's potential for solar district heating was shown in a recent study by the Swedish Energy Agency to be 0.17 – 6.0 TWh depending on assumptions[1]. This report highlighted the fact that large scale storage was key to achieve a higher potential as they are used not only by solar but other heat production units. Another conclusion was that solar heat has higher potential economically in the smaller district heat networks where pellet boilers are used in single plants and to a lesser extent those with wood chip boilers. Systems with waste incineration waste heat and multiple heat sources are less likely to have solar being cost-competitive, but the value of large scale storage is significant in these systems.

There are a number of different types of large-scale storage: pit storage, borehole storage, tanks, old caverns for oil storage and aquifers. As pit stores have been shown to be cost-effective and practically feasible in Denmark and additionally not well studied for Swedish conditions, this type was chosen as the focus of this project.

The project consisted of the following stakeholders and was active October 2022 to February 2025:

Dalarna University, working mainly on the techno-economic pre-feasibility case studies for three networks and project management, but also supporting in the spatial analysis. Chris Bales and Puneet Saini.

Halmstad University, focusing on the spatial analysis but also supporting in the case studies. Urban Persson, Luis Sánchez García, Fredric Ottermo

Absolicon, focusing on project dissemination and identification of suitable networks for the case studies. Joakim Byström, Jonatan Mossegård, Karin Forsell.

PlanEnergi, Danish contracted consultant with long experience of solar district heating as well as pit storage projects, supporting the project in all aspects with key data and advice. Daniel Trier, Geoffroy Gauthier.

Luleå energi, Härnösand energi och miljö samt Söderhamn nära took part in the project with data and discussions around the case studies.

Solar District Heating (SDH) and Pit Thermal Energy Storage (PTES)

Solar District Heating (SDH) is the integration of heat from solar collectors into the district heating system. It has a long history in Sweden with the first systems installed in the 1980's. After a number of installations, the focus for development moved into Europe and now the majority of the systems are in Denmark, Germany and other countries [2].

Many solar district heating systems use diurnal thermal storage and replace fuel from the heat production units during mid-season periods and summer, resulting in solar fractions of 10-20% [2]. Long-term storage, often referred to as seasonal storage is needed to increase the solar fraction further. Pit stores, borehole storage, aquifers and rock caverns are possible technologies. There are a number of studies in the literature on this, many related to borehole and aquifer storage [3]. However, pit thermal energy storage (PTES) can result in lower capital cost per m^3 especially at larger volumes (>50 000 m^3). Solar district heating combined with PTES is receiving more attention in Denmark and Germany due largely to favourable policies as well as technology development [4].

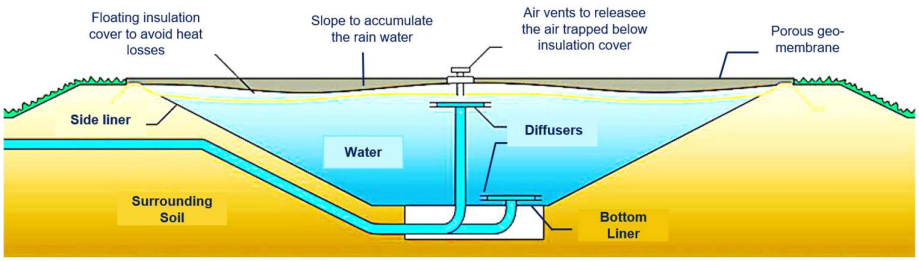

Figure 1. Cross-section of PTES showing the liner, insulated lid, embankments made from soil dug from the pit as well as diffusers inside the store.

Figure 1 shows a very schematic cross-section of a PTES. To get reasonable costs, the soil removed from the pit is used to build embankments above ground to increase the volume of the storage at the same time as to minimize (soil) transportation costs. The slope of the pit is made to avoid the sliding down (erosion) both during construction and operation. It is dependent on the type of soil, but is normally 25°- 30°. The bottom and sides are lined with a polymeric liner to keep the storage water in and ground water out but there is no insulation on these sections. The top has a floating lid with a vapour and liquid barrier and is normally the most expensive part of the construction. This kind of storage requires a number of geological criteria to be fulfilled to be both possible and cost-effective. The focus of this project is to use these criteria to identify possible places in Sweden that are relatively close to the district heating networks.

There are a number of recent and ongoing research, innovation and demonstration projects involving PTES. The Austrian GigaTES project analyses the limitations and possibilities of Austrian conditions and developed new storage concepts some of which are based on the simple pit stores assumed in this project [5]. These new concepts are possible to build in many more places and require less space but are more expensive. The EU Project Treasure [6] plans to have seven PTES demonstration projects in five countries in order to find better ways to plan and design pit stores in practice. Two other EU projects focus on large scale underground storage, though not PTES: EU Uses4Heat project [7] focusses on borehole and aquifer storages while the Interstores project [8] focusses on caverns and reusing existing structures. Additionally the Internation Energy Agency has a recently started Task 45 in the energy storage area: "Accelerating the Uptake of Large Thermal Energy Storages" [9]. The focus is on numerical simulation, materials database and testing as well as construction and performance test standards.

District Heating Database and Spatial Analysis

As a first prerequisite to meet the project objectives and assess a national potential for SDH and PTES in Sweden, information on existing and currently operating Swedish district heating systems was assembled. As a basis for this, an available, but somewhat outdated, database (known through e.g. the Heat Roadmap Europe project series [10, 11] as the Halmstad University District Heating and Cooling database [12]), was revised and updated for the Swedish context. This revision included most importantly a re-count of the total number of systems, an update of annual heat deliveries, as well as a conversion from geographical point source locations to polygon areas by means of geographical modelling.

A second prerequisite to carry out the investigations, was the availability, access, and preparation, of relevant datasets necessary to identify suitable SDH and PTES areas (in vicinity of district heating systems). For this purpose, several national datasets on key geological parameters (as provided e.g. by the Swedish Geological Survey (SGU) and Lantmäteriet), were identified and gathered. By preparation according to certain criteria derived by expert consultancy, literature references etc. [13-15], unique for each input dataset, a spatial analysis sequence was arranged and carried out based on the principle of eliminating non-suitable areas (screening process).

The approach associated with this part of the project may, in short, be described as ranging from the assembly of existing numerical and geographical data on the built environment, heat demand densities, district heating infrastructures etc., through the understanding and management of geological data parameters and associated criteria for SDH and PTES

suitability, to the spatial analysis and rendering of results which quantify and locate the national potential according to a set of given scenarios.

Aims, Scope and Research Questions

The aim of the project was to show how pit storage can help in replacing biomass in the district heating networks by allowing greater use of solar and waste heat. The focus was on three research questions:

- How many, and which, of Sweden's current district heating networks have good conditions for developing solar thermal + pit storage?
- What is the techno-economic feasibility for selected case studies considering detailed design of solar field + pit storage system?
- What is the anticipated potential for solar thermal and pit storage solutions, on national level?

The project limited the analysis to areas within a reasonable distance of the existing district heating networks and to the readily available geological data, which did not include water table depth or flow. These latter two aspects were not covered due to lack of data despite the fact that they are important. They need to be checked in a later stage of project development. However, the depth to bedrock, soil type and slope data as well as land use could be found for all relevant areas, and these could be used for a screening of possible sites for PTES relatively close to district heating systems. This screening process results in areas where PTES is potentially possible. In reality many of these areas would not in practice be feasible due to many possible reasons such as land ownership, water flow, variation in soil types and soil depth within the identified site.

Method

The project used a mixture of methods to achieve the aims and answer the research questions. The cornerstone in the GIS methodology to identify possibly suitable sites for PTES was to estimate the extent of district heating networks and then define buffer areas around these networks where PTES might be located. In order to do this the database of existing district heating systems in Sweden was updated. Geological data for these buffer areas was downloaded from SGU and criteria for geological conditions needed for PTES were defined. These were then used in a screening process to identify possible areas suitable for PTES relatively close to district heating networks.

In parallel, pre-feasibility case studies were made for three district heating systems. The experience from these were used in the analysis of the screening and estimation of the technical potential for solar district heat and use of PTES.

Updated Database of Swedish District Heating Systems

This section presents a concentrated account of the procedure, data, and associated modelling, by which the database on Swedish district heating systems was updated. A more thorough and detailed account may be found in the project conference paper presented at the 2024 International Sustainable Energy Conference in Graz, Austria [16].

The update aimed at producing two main outputs: (1) a tabular list of all known district heating systems currently in operation in Sweden (the database), and (2) a geographical version of this database which depicts the anticipated spatial outstretch (polygon areas) of these systems. Whereas the former would be an update of the available but somewhat outdated Halmstad University District Heating and Cooling database, version 5 [12], with a latest data year of 2016 for the Swedish context, the latter would be an update – and improvement – of an already existing geographical dataset originating from the sEEnergies EU Horizon 2020 project [17], published in February 2020 and named the "D5.1 District Heating Areas" dataset [18], which itself was established in parts on methodological approaches and heat demand density data developed in the preceding Heat Roadmap Europe EU Horizon 2020 project [10, 19, 20].

For the first output, the outdated original Halmstad University District Heating and Cooling database, version 5, hereafter referred to as the "HUDHC_v5", listed 386 unique Swedish district heating systems, of which 372 with data on delivered heat, and summed up a total annual district

heat deliveries volume (Q_s) in Sweden of 47.1 TWh/a, as outlined in Table 1. The information gathered for the original reference itself was based mainly on 2015 records published by former Svensk Fjärrvärme (Swedish District Heating Association), now managed by the Swedenergy [21], and complemented by the Swedish Energy Market Inspectorate [22].

Table 1. Input datasets for the updated database on Swedish district heating systems

Dataset	Nr [n]	Match to original reference	Q_s [TWh/a]	Heat deliveries time reference	Ref.
Original reference (HUDHC_v5)	386	-	47.1	2015	[12]
Public dataset (EMI)	486	379	51	Avg. 2016–2021	[23]
Internal dataset (Swedenergy)	520	386	51.5	Avg. 1996–2021	[24]

As can be seen in Table 1, the update utilised two additional new datasets, one acquired from public sources (Swedish Energy Market Inspectorate [23]) and one from non-public sources (Swedenergy [24]). In addition, a third dataset, internal, provided by Profu AB as complement to the public report [1], was used as an auxiliary information source on Swedish district heating systems which use refined versus non-refined biomass fuels for heat production. This list counted a total of 248 systems, of which 90 use refined, and 158 use non-refined, biomass fuels.

The update procedure itself consisted to a large extent of data management, where the establishment of alignment and coherency between the input datasets in terms of system names, city names etc., was a necessary first step in order to facilitate comparison and to assign unique system identifiers. A notable area of challenges in this context is the frequent habit of annotating, that is naming, Swedish district heating systems in contemporary statistics, not by the actual system name (typically the town or city name), but rather by (1) the combined name of several cities, or (2) the name of the district heating company in charge of the operation. This may be natural and sufficient practice from a traditional reporting perspective but very inappropriate from a geographical mapping perspective, which purports to position each system uniquely on the map.

Another key activity of this procedure involved the determination of reasonable and representative annual heat delivery data, reported by year over different time horizons in the different input datasets, as also indicated in Table 1. This was necessary in order to derive average values, where the principle followed was to use as recent data as possible (predominantly averages of time series data from 2019 to 2023) and refraining from normal-year corrections for this very reason. It should further be noted that the

internal dataset from Swedenergy [24] was used only for reference in this context.

In summary, as presented in Table 2, this part of the update procedure resulted in a tabular list with a total of 547 Swedish district heating systems, considered active and currently in operation. An additional 17 systems were identified but could not be associated with any recent operational data and therefore omitted. Two of these systems are among those listed in the Profu auxiliary list, although these are mainly smaller systems given their marginal shares of both total population and annually delivered heat volumes. In terms of population, the total number of people who are registered as residents in cities associated with Swedish district heating systems amount to no less than 7.72 million, which is approximately 73% of the total population. The sum of heat deliveries from all systems was found at 52.7 TWh per year.

In total, the tabular list consists of 27 fields, mainly referring to various ID-numbers, names (city/town/village, municipality (LAU2), regional administrative units (NUTS3)), geographical coordinates (point source locations), Profu AB auxiliary list indicators, population, status columns, and annually delivered heat in energy volumes.

Table 2. Overview table of input datasets used for the updated database on Swedish district heating systems (tabular list)

Input datasets	**SEDHS_ID [n]**	**Population [Mn]**	**Q_s [TWh/a]**
Not in Profu list	**319**	**6.75**	**47.5**
Only in Public dataset (EMI)	126	0.44	4.3
In both Public dataset (EMI) and HUDHC_v5	160	6.22	41.9
Only in HUDHC_v5	33	0.09	1.3
In Profu list	**228**	**0.97**	**5.2**
Only in Public dataset (EMI)	42	0.14	0.7
In both Public dataset (EMI) and HUDHC_v5	142	0.74	4.1
Only in HUDHC_v5	44	0.09	0.4
Output dataset (Tabular list)	**547**	**7.72**	**52.7**

Geographical representation

For the second output, a geographical representation of the tabular list, the main objective was to create a feature class layer (georeferenced dataset) with polygon areas which resemble the modelled spatial coverage of Swedish district heating systems, here referred to as District Heating Areas (DHA). The reason for this objective was, on the one hand, to have a preliminary understanding of network locations and sizes, as opposed to merely a point coordinate for the city main square or central post office (the geographical representation in the tabular list). Although integration of solar collector fields and seasonal storages often will benefit from central network connection, e.g. connection to main heat production sites where distribution network pressurization installations and wide pipe diameters often are found, decentral connection may also be a feasible alternative given favorable conditions. On the other hand, a spatial representation of district heating systems was helpful also for the subsequent lineation of analytical boundaries for the screening process.

The rendering process followed the principal methodology developed in the sEEnergies EU Horizon 2020 project, documented among other in [25]. This basically consists of a spatial combination of satellite imagery (share of built-up area per hectare), energy statistics (heat demand for residential and service sector buildings), and the tabular list (locations of district heating systems), as illustrated thematically in Figure 2.

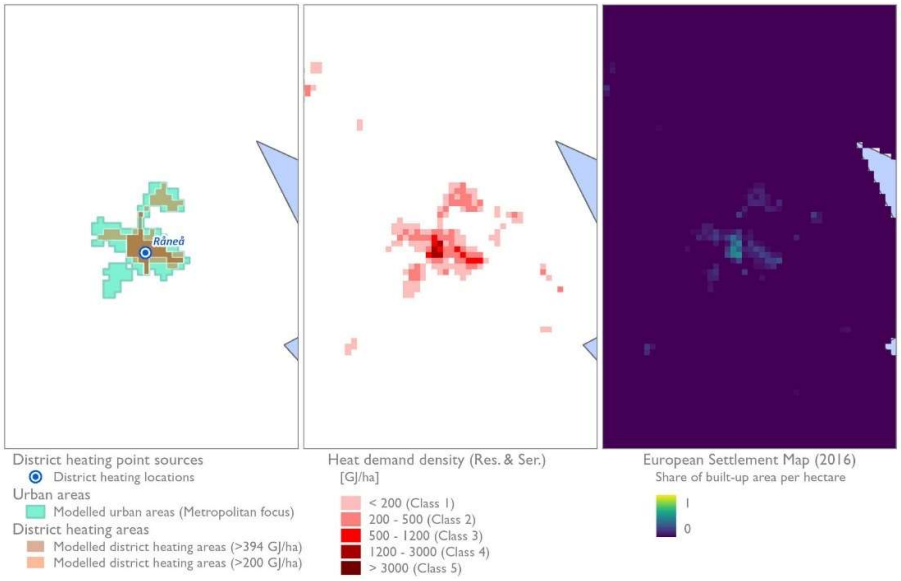

Figure 2. Three maps of the town Råneå in the Northern part of Sweden to illustrate the rendering process of Urban Areas and District Heating Areas (left) based on residential and service sector heat demand densities at the hectare level (centre), in turn based partly on underlying satellite imagery quantifying the relative share of built-up areas per hectare (right).

Satellite imagery interpreted as shares of built-up areas per hectare was retrieved from the publicly available European Settlement Map [26, 27]. In preparation for the rendering process, raster grid cells were converted to polygons and subjected to several requirements. For example, parts smaller than four hectares were removed and a coherent polygon area of nine hectares was required to qualify as an Urban Area. For Sweden, a total of 11,240 Urban Areas were rendered and attributed a location name by use of the publicly available GeoNames dataset [28].

Regarding heat demand data, and heat demand density data in particular, a total national heat demand for space heating and hot water preparations was anticipated at some 98.3 terawatt-hours, based on energy statistics for data year 2015 [29] and modelled electricity use for heat pumps (according to the Stratego project approach, documented in [30]). However, given the relative uncertainty of this latter approach, a more modest, and purely statistics-based, national heat demand volume of 78.9 terawatt-hours per year was used as project reference. This reference volume was used as benchmark for two raster datasets depicting Swedish heat demand densities at the hectare level: (1) , the original 2015 Heat Roadmap Europe dataset [19, 20, 31], with a total volume of 81.1 TWh/a; and (2) the corresponding 2015 baseline dataset from the sEEnergies project [32], with a total volume of 78.1 TWh/a. For the project, a new heat demand density raster dataset was created, by calculating, at hectare raster cell level, the arithmetic average of the two abovementioned datasets, both of which were associated with certain imperfections. The total heat demand volume of this resulting new dataset amounted to 79.7 terawatt hours.

To render district heating areas, the known total yearly district heat demand (i.e. annual heat deliveries: QS = 52.7 TWh/a as presented in Table 2 above), was distributed consecutively over the total population of raster grid cells, starting at the cell with the highest value (~6.55 GWh) and then down towards the point where the accumulated distribution reached the total yearly district heat demand. This point occurred at a heat demand density level of 394 GJ/ha. The idea behind this mode of distribution was that district heating systems have been built where feasibility conditions are at their best (high heat densities would correspond to high economic feasibility), which not necessarily is the case in a country like Sweden, where additional preferences other than pure economic viability may have influenced system investment decisions.

Thus, a heat demand density threshold level at 200 GJ/ha was used in order to incorporate as many as possible of these smaller systems that exist but are below this theoretical value of 394 GJ/ha. At the chosen heat demand density threshold level of 200 GJ/ha, which may be seen together with the

theoretical level of 394 GJ/ha for the city of Enköping in Figure 3, the rendering process generated a total of 464 district heating areas. Why not 547, i.e. one for each of the tabular list systems? Most important is that some larger District Heating Areas (DHA), especially in the larger cities of Sweden, span more than one district heating system. Secondly, in quite a few rural locations, heat demand densities still weren't high enough (above 200 GJ/ha) to have a defined DHA based on this method, although district heating systems exist. In some instances, district heating areas were in fact rendered but not at the given point source location of the system, which therefore generated no match in the spatial join process.

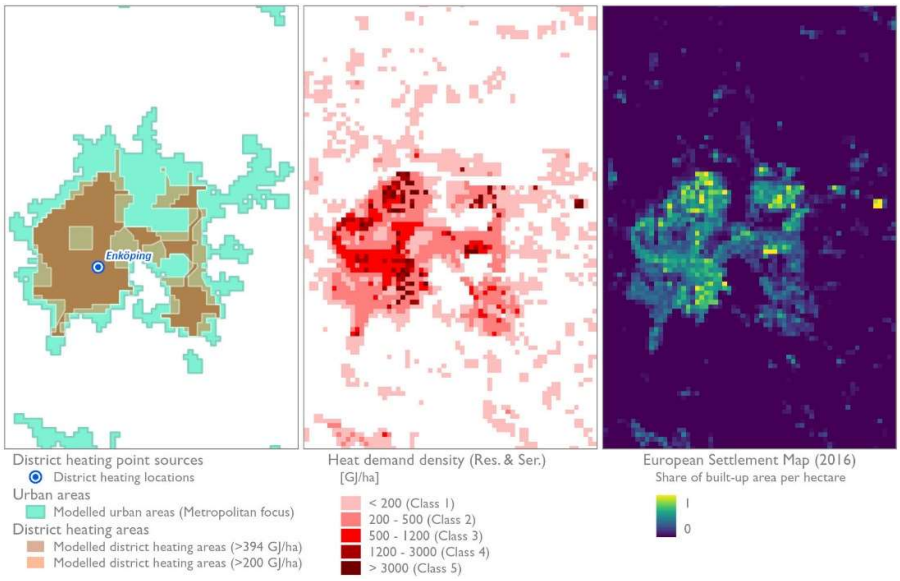

Figure 3. Three maps of the city of Enköping in mid-Sweden to illustrate the rendering process of Urban Areas and District Heating Areas (left) based on residential and service sector heat demand densities at the hectare level (centre), in turn based partly on underlying satellite imagery quantifying the relative share of built-up areas per hectare (right).

Dynamic Boundary Buffers

The next step in preparation for the spatial analysis to determine the potential for pit stores in Sweden, a boundary layer, i.e. the lineation of analytical boundaries for the screening process, needed to be created. For this purpose, so-called "dynamic boundary buffers" were created reflecting cost-effective heat transmission distances which surround each DHA and delimit the area analysed for the screening process.

By relating such a desired heat transmission threshold distance, $L_{threshold}$ [m], to a unit cost of heat transmission, C_{unit}, 50 SEK/MWh in this case, an expression was derived for this purpose:

$$L_{threshold} = C_{unit} \cdot \frac{P_{max} \cdot \tau}{\lambda + \sigma \cdot z \cdot P_{max}^{w} + \phi \cdot z^{\delta} \cdot P_{max}^{3+w \cdot \delta}} \qquad \text{Equation 1}$$

Where P_{max} is the maximum heat capacity for transmission [MW], τ is the hours of operation (8760 for seasonal storage) [h], λ is the intercept of an associated heat cost function [SEK/m], σ the corresponding slope of the same heat cost function, [SEK/m^2], and where z and w are coefficient and exponent respectively for an associated expression for optimum diameter, D, and where ϕ and δ are coefficients in an associated expression for total heat transmission cost. A detailed description of the derivation of the threshold distance has been provided as a separate attachment to this report (File name: Heat transmission threshold distance.pdf).

By application of this expression, where the product $P_{max} \cdot \tau$ was set to correspond to the annual heat delivery volume of any given district heating system (Q_s), at an anticipated solar fraction of 80%, resulted in the boundary layer shown in Figure 4: at left by detail over the Malmö/Lund region in Skåne, and at right as a dissolve feature layer for all of Sweden.

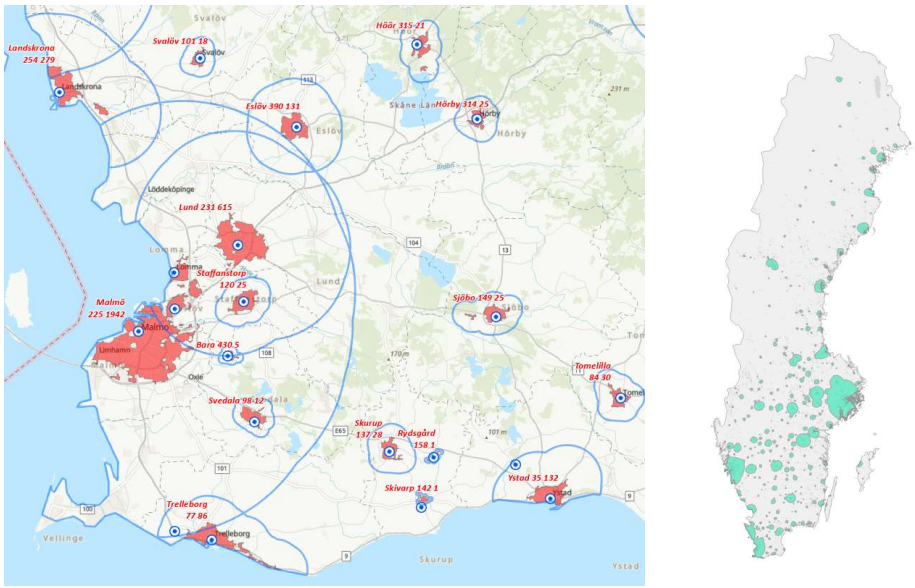

Figure 4. Dynamic boundary buffers drawn around modelled district heating areas in the Malmö/Lund region (left) and for the nation (right) at an anticipates solar fraction of 80%.

Hereby, the boundary layer provided the geographical study boundaries within which all other datasets were to be considered in the screening process (no analysis to be performed outside these study boundaries). The land area covered by the boundary input dataset (39.7 kkm^2) represents approximately 8.8% of the total Swedish land area (~450 kkm^2), which may be observed in the national-level map displayed at right in Figure 4. Hereby,

the required computational time for the spatial analysis modelling was significantly reduced in comparison to model runs that would have had to relate to the national boundaries of Sweden.

Collector Area and Store Size for Different Solar Fractions

A key practical constraint in the installation of solar heating systems is the required land area for installation of solar collectors and storage in proximity to the DH network. For national potential analysis, calculations are made to determine the required solar collector area, storage volume, and land area required for different solar fractions.

The calculations are made for three distinct solar fractions (20%, 40%, and 60%) for each district heating (DH) system, which represents as follows:

- 2**0% Solar Fraction:** Focuses on potential cases where solar collectors can be used to meet heat demand during summer. This typically requires a storage tank; however, for systems with high annual heat demand (>100 GWh), the required storage volume would favor the use of PTES instead of tank storage.
- **40% Solar Fraction:** Solar heat in summer and then typically a few months in autumn discharged from PTES.
- **60% Solar Fraction:** This represents a high solar contribution scenario, where a majority of the annual heat demand is met by solar system, ie well into the winter season.

Calculations for solar collector area

To calculate the required collector area and storage volume, simplified approach is used, due to the limited input (annual heating demand) available for DH systems in Sweden, which was obtained from the updated database of Swedish district heating systems. The calculations followed the pre-feasibility guidelines outlined in [33]. These were based on studies for Denmark and further south in Europe and thus not completely applicable for high latitudes, but are the best available. The underlying assumptions for these calculations are detailed in Table 3
.

Table 3: Assumptions considered for tabular calculations

Parameters	Value	Unit	Remarks
Collector's characteristics	$\eta = 0.78$ $a_1 = 2.6$	W/m^{2}K	Single glazed FPC from [34]
Mean fluid temperature in the collector	75	ºC	Average of supply and return temperatures
Reference GHI for calculations	1000	kWh/ (m^2.year)	

The annual collector output (Q_{coll}) is calculated using the following equation.

$$Q_C = 0.45 \cdot GHI \cdot C_f \quad \text{Equation 2}$$

Where, C_f is correction factor derived based on figure 2.3.4 in [33].
A single-glazed flat plate collector is utilized as the reference to calculate the thermal output based on specified mean temperature. Based on the efficiency of collector, and annual GHI, the specific thermal output is derived (Q_{coll}). the collector aperture area required (A_{apr}) at any solar fraction (SF%) is defined using the following equation.

$$A_{apr} = \frac{Annual\ heat\ demand \cdot SF\%}{Q_{coll.}} \quad \text{Equation 3}$$

Where SF% represents the solar fraction % (i.e 20%, 40%, 60%). The land area required (A_{land}) is then defined as using the following equation.

$$A_{land} = A_{apr} \cdot 3 \quad \text{Equation 4}$$

Calculations for PTES

The storage volume is calculated as a function of $A_{apr.}$ for different solar fractions as shown in Figure 5

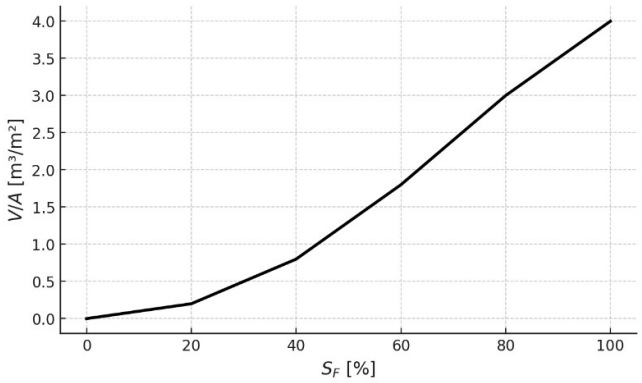

Figure 5: Correlation of collector aperture area and thermal storage for different solar fractions based on [33]

For PTES, a truncated inverted pyramid geometry is assumed to estimate the height and other geometric dimensions. Based on table 10 in [35], for a specific volume, the lid area is calculated based on Figure 6. The land area is calculated as 1.5x the lid area to account for area required for the construction area required to build the pit.

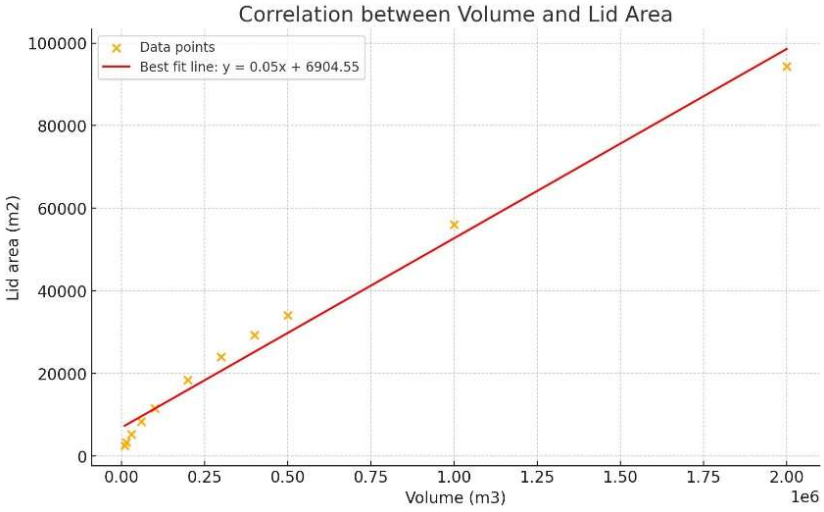

Figure 6: Co-relation of storage volume and lid area used for calculations of land area required for PTES for different solar fractions.

Case Studies

Overview

To assess the techno-economic feasibility of integrating PTES into a DH network, dynamic simulations are conducted. The system's performance depends not only on the thermal storage itself but also significantly on how the storage interacts with the connected energy system. Therefore, it is important to simulate the charging and discharging behavior of the PTES, along with its interaction with the surrounding ground

Out of the initially selected possible case study networks, three locations were chosen after applying geological filters, ensuring that suitable land is available for PTES installation. These locations are: a) Råneå b) Härnösand c) Söderhamn

The simulation tool TRNSYS is used, and a model was developed to simulate the coupled system, consisting of solar collectors, PTES, and the district heating network [36]. Some simplifications have been applied in the model to ensure that the most important physical processes and boundary conditions related to the storage system are captured, while keeping the model computationally efficient enough for integration into broader system-level simulations.

System typologies and constraints

The simulated solar district heating system combines flat plate collectors with a PTES. The solar collectors transfer the heat to a closed water-glycol loop. Heat is then transferred to the PTES via a heat exchanger, and charging takes place either through the top diffuser, or through the middle diffuser if the outlet temperature from the solar field is lower than the temperature at the top of the storage. This charging strategy helps to maintain the stratification by preserving temperature layers within the PTES [37]

The stored heat is discharged from the PTES to the district heating network. The discharge process is managed via heat exchangers, with the return flow from the district heating network sent to the discharge heat exchanger. This water return from the district heating network is heated under two different scenarios:

Scenario 1: If the boiler does not have heat recovery (i.e flue gas condenser), the system operates in one of the following modes:

a) Return-Supply mode. If the maximum temperature in PTES temperature is high enough to meet the required supply temperature of the district heating system, the heat is directly supplied to the network through return-to-supply mode i.e the return water is heated to the required supply temperature in the network, and heat is then fed to the network's supply pipe.

b) Return-Return mode. If the maximum temperature in PTES temperature is lower than required supply temperature, the system switches to return-to-return heating as shown in Figure 7. In this case, the PTES is used to preheat the colder return water from the district heating network and then send the heated water back to the network's return line, before it enters the boiler. The boiler then increases the temperature to the required supply level. This preheating strategy is particularly beneficial because it allows the storage can be cooled down to the lowest temperature (return temperature from DH network), ensuring that all possible heat in the storage is delivered to the network

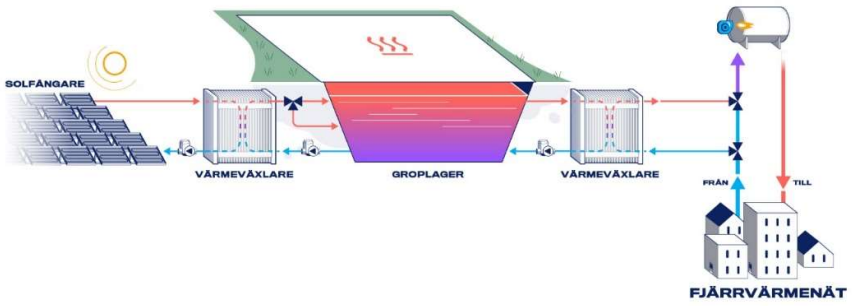

Figure 7: Schematic of system in return-return heating mode.

Scenario 2: If the boiler has heat recovery, then:

a) Return-Supply Solar Only mode. The return-to-return heating strategy is not used because it would increase the inlet temperature to the boiler, thereby reducing the potential for heat recovery from the flue gas. In such cases, only return-to-supply heating is modelled, as shown in Figure 8, meaning that the heat supplied from the PTES must always be at or above the required supply temperature of the district heating network. The main drawback of this approach is that it creates a limited window for discharging heat from the storage once it becomes fully charged during summer. This is because the temperature required in the network gradually increases after summer and exceeds the maximum temperature that can be provided by the storage. Therefore, to fully utilize the storage, the system design must carefully size the storage volume to ensure that the stored heat can be completely discharged within this limited window, when the supply temp in network is lower than the max possible temperature in PTES (90 ºC). This constraint also places a cap on the achievable solar fraction that can be covered by the solar + PTES system. If the storage is too large, some of the stored solar heat may become unusable, reducing the overall system's effectiveness.

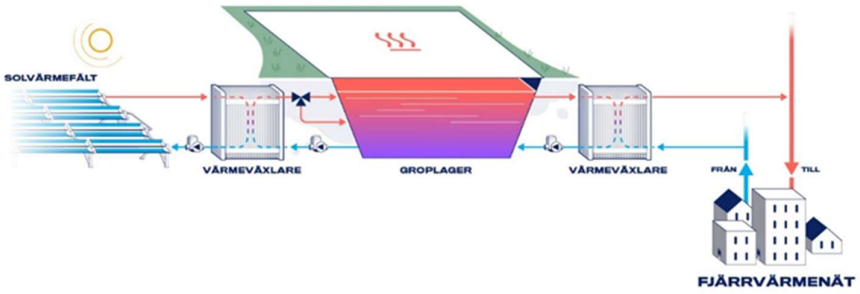

Figure 8 Schematic of the system in supply-return heating mode

b) Return-Supply Solar and Heat Pump mode. For return to supply heating systems, integrating a heat pump into the system, as shown in Figure 9, can be highly beneficial. There are two reasons for this. Firstly the heat pump can raise the outlet temperature from the PTES to match the required supply temperature of the district heating network, thereby increasing the amount of usable heat extracted from the storage. Secondly the heat pump requires a low-temperature heat source that can be provided from the middle layers of the PTES. After extracting heat, the cooler return flow from the heat pump evaporator is sent back to the storage, lowering its minimum temperature and thus increases the energy capacity. This

increases solar collector performance during the next charging cycle (as the collectors operate more efficiently with a lower return temperature), and reduces thermal losses from the storage to the surrounding ground. However, the main drawback of this approach is the increased capital expenditure associated with installing the heat pump, and higher operational cost due to use of electricity by HP.

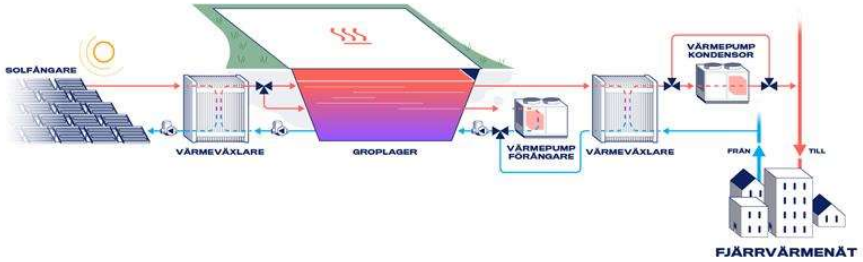

Figure 9 Schematic of the system in supply-return heating mode with heat pump. Evaporator and condenser of heat pump are shown as separate units for ease of illustration.

It is important to note that even with the addition of a heat pump to the system, the available discharge window for the PTES remains narrower compared to systems where return-to-return heating is possible. This is primarily because heat pumps used in district heating applications typically have an upper-temperature limit of around 95° [38, 39] . As a result, the heat pump cannot fully bridge the gap if the network requires significantly higher supply temperatures, particularly in colder periods. Therefore, the solar fraction that can be provided with a solar and HP system is also limited, unless there is a boiler located nearby, which is not the case here.

Limitation due to pipe size in network at connection point

Another important factor that limits the achievable solar fraction in the district heating system is the size of the available pipes used to transfer heat from the storage to the network. For instance, if the geologically suitable site for PTES is located far from the central boiler plant, and the closest available pipe to feed heat into the network has a limited diameter, the discharge capacity of the system is constrained. This hydraulic bottleneck restricts how quickly heat can be delivered from the storage to the network, effectively slowing down the discharge process. As a consequence, the PTES remains at higher temperatures for a longer period, which increases thermal losses to the surrounding ground as well as limiting possible solar fraction. In contrast, systems without such pipe size limitations can discharge more quickly, minimizing storage losses.

Waste heat availability

If part of the district heating network's heat demand is already covered by waste heat sources (e.g., from industrial processes), that portion of the demand is excluded from the target for replacement by the solar collector + PTES system. This prioritization ensures that the available waste heat, which is often low-cost and resource efficient, is fully utilized in the network before solar and storage systems are integrated.

Boundary conditions for case studies

Table 4 shows the integration type and constraints applicable for analysed case studies:

Table 4: Summary of various constraints and integration for different case studies

	Råneå	**Härnösand**	**Söderhamn**
Heat recovery in the boiler	No	Yes	Yes
Integration type	R-R/R-S	R-S	R-S
Heat pump in the system	No	Yes	Yes
Limitation due to discharge pipe size	No	Yes	Yes
Waste heat as a heat source in the network	No	Yes	No

In discussion with the district heating companies, suitable sites for PTES and solar field were identified based on the geological conditions and availability of land. As shown in Figure 10, the system in Råneå is the simplest among all the case studies, where the PTES location was found very close to the boiler central (200 meters) , allowing direct access to the largest pipe in the network. The boiler does not have any heat recovery system, which allows the storage to be discharged in both return-to-supply (R-S) and return-to-return (R-R) modes.

In the cases of Härnösand and Söderhamn, the geologically suitable locations for PTES were found in the southern parts of the cities, while the boiler centrals were located in the northern parts. Consequently, the most suitable and closest available relatively large pipe sizes were DN250 for Härnösand and DN200 for Söderhamn. These sizes and distances to the connection point were used for the simulations. And/or co-generation plants Boilers in both cases exhaust gas condensation, meaning only return-to-supply (R-S) heating is feasible for storage discharge, with or without heat pumps.

Figure 10: Location of suitable area for PTES (yellow box) and boiler central (red box) for Råneå (left), Härnösand (center), and Söderhamn (Right). Distances are not represented to the scale.

Initial sizing using simple Python model

The simulation process is carried out in two steps. The first step aims to approximate the required system size (solar collector area and storage volume), which then serves as the basis for more detailed simulations in TRNSYS.

A simple Python model was developed to perform a sensitivity analysis across a range of collector areas and storage volumes, based on a given heat load profile. This Python model incorporates a simplified heat balance, accounting for heat available from the solar collectors, the heating demand, and thermal losses from the storage on hourly basis.

The storage is modeled using a simplified two-node approach, representing an ideal thermocline that moves up or down depending on the charging and discharging processes. This two-node model is less accurate for the return-to-supply (R-S) heating mode, because real thermal storage exhibits continuous temperature gradients rather than a sharp division between two uniform layers. In reality, only the uppermost (hottest) portion of the storage can deliver the required supply temperature, meaning the usable storage volume for discharge is smaller than what a two-node model would suggest.

Based on the defined ranges of solar collector areas and storage volumes, hourly simulations are performed for each combination. The results are then plotted to identify a suitable system size: the point at which the majority of the heat collected by the solar field can be effectively delivered to the network. This pre-sizing step helps to narrow down feasible system configurations, making the subsequent TRNSYS simulations more focused only on a few selected sizes. A comparative analysis is made between heat output from the Python model with the results from the TRNSYS model.

TRNSYS model

The model was developed in TRNSYS to perform dynamic, multi-year simulations aimed at capturing the long-term performance of the system. Each simulation runs for a period of five years, with a time step of 5 minutes, allowing for detailed representation of system dynamics and seasonal variations. Unless otherwise stated, results are for the fifth year when ground temperatures and losses from PTES have stabilized.

The key inputs and components of the model are outlined below:

- Input Data: The heat load data consists of an hourly profile for heat demand, obtained for each case study from utility, along with corresponding supply, return, and ambient temperatures. Weather data for the simulation is sourced from Meteonorm.
- The solar collector model applied in the simulation is a single-glazed flat plate collector, with thermal properties obtained from [34].To account for shading effects caused by the collector array, the solar shading component (Type 30) is used.
- The thermal storage model is a combination of two TRNSYS component models. Type 1300 represents a detailed model of a fluid-filled storage volume, capable of simulating an inverted truncated cone geometry. Type 1301 simulates the thermal behavior of the surrounding ground using a two-dimensional nodal grid, capturing heat transfer between the storage and the soil. Although many existing PTES systems use an inverted truncated pyramid geometry, modeling the storage as a truncated cone simplifies the heat transfer calculation to two dimensions, significantly reducing computational complexity and simulation time while preserving reasonable accuracy. See [40] for detailed descriptions.
- Heat pumps are represented using an equation block, where the peak capacity is defined as an input parameter. The actual operating capacity is then calculated dynamically based on real-time source and sink temperatures. A model based on a 6 MW heat pump from [41] was used to calculate the operational capacity and COP.
- Pipes are simulated using TRNSYS Type 31. The following pipes are simulated: (a) between the solar field and storage, and (b) between storage and the network. The former is simulated with the assumption that both the solar field and storage are located in proximity to each other, with a fixed trench length of 100 m (200 m for both supply and return pipes). For the pipe between storage and the network, the distance is based on the case study conditions, determined after locating the area for PTES, and distance of connection point.

Table 5 shows the most important parameters used in the model for various components.

Table 5: Key components' specifications used for the TRNSYS model

1. **Solar collectors**	
Type	Single glazed flat plate collector, Type 539
Thermal characteristics	Optical efficiency: 85%, a_1: 3.08 W/m²K, a_2: 0.013 W/m²K²
Shading	Simulated using Type 30, collector height: 2.2 m, row distance of 4.5 m, and collector row length of 100 m
2. Thermal storage	
Type	Inverted conical storage (Type 1300-1301)
Size	For given storage volume, storage height and ratio of radii calculated from [35]
3. Ground properties	
Conductivity	2.52 kJ/hmK
Density	2100 kg/m³
Specific heat	1.3 kJ/kgK
Far field and deep earth distance	30 m
4. Storage Model	
Number of storgae nodes	25
Smallest node size	0.1 m
Number of inlet diffusers for charging	2 (node 1, 12)
Number of diffusers for discharging	1 for system without HP, 2 for system with HP (node 1 and node 12)
5. Storage Insulation	
Insulation extension	4 meters away from the edge of PTES
R_top_insulation	1.39 hm²K/kJ
Utank_top	0.82 kJ/hm²K
Utank_edge	12 * Utank_top
Utank_bottom	36 * Utank_top
6. Network pipe	
Pipe density	7850 kg/m³
Thermal conductivity of pipe	150 kJ/hmK
Specific heat of pipe	0.47 kJ/kgK
Insulation thickness	75 mm
Insulation density	60 kg/m³
Thermal conductivity of insulation	0.0792 kJ/hmK
Specific heat of insulation	1.2 kJ/kgK

System controls

The most important system controls are explained below

*Solar field***:** The solar collector pump operates based on the incident solar radiation (G) on the collector surface after shading, with three control conditions:

- If G < 100 W/m², the pump remains off: $\dot{m} = 0$
- For 100 ≤ G < 600 W/m², the pump operates in fixed temperature difference mode, maintaining ΔTset (20°C). To do this, the system calculates the collector output using solar radiation and collector properties from the previous time step.
- For G ≥ 600 W/m², the pump operates in fixed outlet temperature mode, targeting Tout,set = 95°C. If the required flowrate exceeds $\dot{m}_{max}$ = 30 kg/h/m², the outlet temperature is allowed to rise above the set point.

Diffusers: The outlet temperature from the charging heat exchanger is continuously compared to the temperature in the top layer (node 1) of the PTES:

- If the outlet temperature from the heat exchanger is higher than the top layer temperature of PTES, flow is directed to the top diffuser.
- If the HX outlet temperature is more than 10°C lower than the top layer temperature, flow is directed to the middle diffuser.

Storage discharge:

- The maximum flowrate in PTES is restricted by the pipe size at the connection point, to limit the velocity in pipe below 2 m/s.
- In R-R heating mode, PTES is allowed to discharge only if the top temperature of the pit is at least 5°C higher than the district heating return temperature. If this condition is not met, the discharge pump remains off.
- In R-S mode, PTES is allowed to discharge only if the top temperature of the pit is at least 5°C higher than the required supply temperature. If not, the discharge pump is turned off.
- In systems with a heat pump and operating in R-S heating mode, the middle node temperature in PTES is also checked. If the middle node temperature is below 35°C, then the PTES does not have enough energy for HP's evaporator, so the discharge pump stays off. If the middle node temperature is 35°C or higher, the required supply temperature is compared to the maximum temperature the heat pump can provide.
    - If the heat pump can meet the required supply temperature, both the discharge pump and heat pump are turned on.

- If the heat pump cannot meet the required supply temperature, both remain off.
- When the heat pump is on, the allowed flowrate in PTES is calculated from the operating temperature of the previous time step, based on the operating capacity of the heat pump. The HP operational capacity and COP is calculated based on the evaporator's outlet temperature and the condenser outlet temperature.

Model simplifications

The following simplifications are made in the modelling work:

- The solar collector and PTES performance are simulated in detail, but the impact of generated heat on existing components (e.g., boilers/combined heat and power plant) is not modelled. The boiler is assigned to fixed efficiency, without considering part-load conditions or their effect on efficiency.
- The modelling is limited to thermal analysis, excluding hydraulic aspects such as pressure drops and pipe velocity in simulations.
- Only single glazed, fix tilt, South facing flat plate collector technology is used as solar collectors for modelling. However, there is potential to use concentrating collectors, which offer advantages such as low stagnation and potentially lower snow-induced radiation losses. However, their impact has not been considered in this analysis.
- The effect of snow accumulation on PTES/solar collectors is not modelled. However, as a conservative estimate, it is assumed that solar collectors do not produce any heat from December to February.
- The annual demand is provided by utilities for a specific year. However, the weather data used for simulation is based on a Typical Meteorological Year, derived from Meteonorm, and does not correspond to a specific year. This discrepancy introduces some uncertainties in the results.

Key performance indicators and economic inputs

Levelized cost of heating: LCOH is a comparative indicator representing the cost of solar heating including capital, operation, and maintenance costs during the system's lifetime. If the LCOH of solar heat is lower than the LCOH of the existing boiler-based system, it implies that the solar system implementation will have positive returns.

LCOH is calculated based on the following equation

$$\boldsymbol{LCOH} = \frac{\boldsymbol{CAPEX} + \sum_{n=1}^{N}\left(\frac{\boldsymbol{EX_{O\&M}}}{(\mathbf{1}+\boldsymbol{IR})^{n}}\right)}{\sum_{n=1}^{N}\left(\frac{\boldsymbol{Q_{yield}}}{(\mathbf{1}+\boldsymbol{IR})^{n}}\right)} \qquad \textbf{Equation 5}$$

$\boldsymbol{CAPEX}$ = Capital cost of technology used (including installation and commissioning) (€]
$\boldsymbol{EX_{O\&M}}$ = operation and maintenance cost per year (€/year]
IR=Interest rate (%)
SD=degradation rate (%] of each technology
N= Project lifetime (years)
$\boldsymbol{Q_{Yield}}$ =Heat yield of the solar system per year (kWh/year)

Net present value: NPV considers the cash inflows and cash outflows over the life of a project to assess the economic benefits of the project. The calculation formula is given in the following eq.

$$NPV = \int_{1}^{N} \frac{B-C}{(\mathbf{1}+\boldsymbol{DR})^{n}} - Capex \qquad \text{Equation 6}$$

Where B is the benefit in year n, DR is the discount rate, and C is annual cost of the system.

The economic boundary conditions considered for analysis are shown in Table 6.

Table 6 Economic boundary conditions considered for calculations.

Component	**Cost range**	**Units**	**Remarks**
Capex solar collectors	550-200	€/m^2	Based on the correlation derived based on input from manufacturers. The collector cost is calculated as (190 000-x)/600, where x is the aperture area in m^2.
Capex PTES	40-90	€/m^3	Based on the data in [35] with a 1.5x factor to account for increased costs as recommended by consultants.
Capex heat pump	400	€/kW	Based on inputs from manufacturers, for capacities relevant for case studies.
Opex. (not including. El cost)	0.50%	of capex per year	
El. cost	100/150	€/MWh	
Interest /Discount rate	0%-7%		Based on inputs from utilities
Economic lifetime	15-30	years	

Potential for Pit Stores in Sweden

This section presents a concentrated account of the procedure, data, and associated screening process, by which the potential for PTES in Sweden was carried out. A more thorough and complementary account may be found in the project conference presentation given at the 2024 Smart Energy Systems Conference in Aalborg, Denmark [42].

The main aim of the screening process (a preliminary geographical investigation based on spatial analysis) was to provide a first order assessment of viable locations for large-scale PTES in vicinity of Swedish district heating systems. For this reason, early project activities involved discussions and consultancy advice to determine which input data parameters to include in the assessment. Several datasets were considered and investigated, e.g. decisive geological data parameters such as soil depth and soil type, given that PTES are constructed by the excavation of soil where a substantial part of the storage volume (the pit) is located below the soil surface. Additional considerations included for example the slope of the land and the character of available land areas.

Screening based on geological criteria and land use

Eventually, four key input datasets were selected for the screening process, as presented in Table 7, and prepared for further analysis (these four key input datasets are also presented graphically in four national maps in Appendix section "Input datasets for the screening process", see Figure 48, Figure 49, Figure 50, and Figure 51). During the discussions, several other input datasets were also considered, for example ballast production sites (where existing excavations potentially could be used), central heat production sources (additional heat to perhaps be stored), as well as model of the Swedish ground water table (developed in the project), all of which later were assigned complementary status. An illustration of these complementary datasets is presented in Figure 52 in the appendix section.

The analytical sequence (the internal order of the datasets, as arranged in Table 7) was not random, but deliberately arranged according to a logic that aimed to begin with those datasets for which there are less alternatives concerning selection criteria. This logic was motivated by the principle to postpone, as far as possible, the introduction of parallel routes through the model (which eventually leads to multiple alternative results, i.e. "scenarios"). As they only involve one single selection criteria set-value each, the first and second input datasets were: elevation of the land (used for the calculation of slope); and soil depth (used to exclude soils too shallow) - see Table 8.

Table 7. Input datasets for the screening process

Input dataset	Name/Description	Geometry	Sources
1	**Elevation** (Höjddata)	Raster (50x50m)	[43, 44]
	The dataset consists of elevation values, meters above sea level, for each cell in a 50 m by 50 m raster grid.		
2	**Soil depth** (Jorddjup)	Raster (10x10m)	[45, 46]
	The dataset consists of soil depth values, meters below ground level, for each cell in a 10 m by 10 m raster grid.		
3	**Soil type** (Jordart)	Feature class layer (Polygon)	[47, 48]
	The dataset contains all soil types ("Jordartstyper") available for Sweden in the SGU ground layer JG2.		
4	**Land use**	Feature class layer (Polygon)	[49]
	The dataset is based on interpreted satellite imagery (Sentinel 2 and Landsat 8) and annotated by use of 44 defined land use classes.		

For the third and the fourth datasets (soil type and land use, respectively), both were associated with more than one selection criteria, in fact, two in each case, as also detailed in Table 8. This elaboration of alternative "screenings" served the purpose of sensitivity analysis with respect to the effect of including more or less clay and silt soil type fractions, on the one hand, and more or less forest and artificial land areas on the other, elaborations which in both instances induced parallel model routes with regard to these latter two parameters.

Table 8. Screening datasets created by application of criteria on used input datasets

Screening datasets	Name/Description	Count	Geometry
1	**Required slope**	1	Raster (50x50m) Converted to dissolved polygon
	Criteria: Cells with slopes larger than 15% are excluded from the analysis. Description: Slope calculated for each grid cell as percent rise relative to surrounding cells.		
2	**Required soil depth**	1	Raster (10x10m) Converted to dissolved polygon
	Criteria: Cells with soil depth less than 10 meters are excluded from the analysis. Description: Soil depth is defined by one default value. Alternative values may be investigated.		
3	**Required soil types**	2	Feature class layer (Polygon) Dissolved
	Criteria: Screening 1: Exclusion of clay and silt in all forms (as well as rock, water and organic soils). Screening 2:, Same as screening 1 but with partial inclusion of clay and silt (courser fractions). Description: The two datasets represent different selections of soil types according to each corresponding screening criteria (See appendix Table 24 for more details).		
4	**Available areas**	2	Feature class layer (Polygon) Dissolved
	Criteria: Screening 1: Only agricultural and semi natural areas. Screening 2: Same as screening 1 but with the addition of forest areas and some artificial surfaces (e.g. industrial and commercial areas, airports, port areas, road and rail networks and associated land etc.). Description: The two datasets represent different selections of land use classes according to each corresponding screening criteria (See appendix Table 25).		

As for the second input dataset, that of soil depth, this was accessed as part of the "soil depth model" ("Jorddjupsmodell"), developed by the Swedish geological survey (SGU) [46]. The soil depth input dataset is an interpolation based among other on the analysis of soil depth information

from well drilling, exploration drilling, mapping observations, and seismic surveys etc. (see also appendix Figure 49).

The third input dataset, the ground layer JG2 from the SGU soil type dataset (Jordarter 1:25 000-1:100 000) [48], provides a comprehensive picture of the distribution of soil types in or near the soil surface, however, with an unfortunate lack of coverage in some northern areas of the country. The layer refers to the type of soil that can normally be expected at mapping depth, i.e. about 0.5 m below the ground surface, and which is estimated to have a thickness well exceeding 0.5 meters. Noteworthy, SGU assembles data also on deeper, underlying soil layers (Jordart, underliggande lager (JD3)), but due mainly to limited and random coverage, the JD3 layer was omitted for the national potential study. The lack of coverage in some northern areas of the ground layer JG2 was considered of lesser significance, given the scarcity of district heating systems in these areas, but in a few instances it did in fact have an influence. A closer look in appendix Figure 50 provides an indication of affected areas. See further also appendix Table 24 for a complete listing of soil type classifications, by a detailed JG2 legend and also by a more aggregated JBAS legend.

The source for Input dataset 4 in Table 7 was the Corine Land Cover (CLC) dataset made available by the European Environment Agency, here referring to Version 20 (V20u1), which represents the publication of final and corrected CLC2018 data [49]. The CLC inventory, which was first introduced in 1990 (CLC1990 dataset), aims to standardize data collection on land in Europe in the support of environmental policy development, and follows a 6-year update cycle [50]. The dataset itself relies on satellite imagery (Sentinel 2 and Landsat 8 for the CLC2018 version) which, by means mainly of photo-interpretations, image processing, in-situ data integrations, cartographic generalisations etc., facilitates the identification of different land uses, such as for example built-up areas (residential, tertiary, commercial, industrial etc.), agricultural areas, forest lands, and several others. In fact, the CLC dataset employs a categorisation of 44 different land use classes (Label 3 level), divided into five main Label 1 categories, as outlined in Table 9. In addition, appendix Table 25 provides a complete listing of all classes as well as the used screening criteria.

Table 9. Land use classes in the Corine Land Cover database, by Label 1, with Label 3 count (Note: "No data" and "Unclassified" Label 1 categories omitted in this presentation)

CLC Label 1	Count of CLC Label 3
Agricultural areas	11
Artificial surfaces	11
Forest and semi natural areas	12
Water bodies	5
Wetlands	5
Grand Total	**44**

The spatial analysis was performed in a GIS (Geographical Information System), ESRI's ArcGIS Pro in this case, and the resulting suitable land areas were identified by sequential elimination of unsuitable areas. This means that the result datasets were created in sequence so that every new result layer included the results from the previous layer and so on. Hereof the naming convention of the result dataset, as shown in Table 10. If, at the end of the screening process, no suitable land areas were to remain, the conclusion would be that no (techno-spatial) potential exists for any given particular location. If, on the other hand, suitable land areas are present after completing the sequence, this would mean that a potential exists.

As can further be seen in Table 10, the applied modelling sequence generates four final result datasets, result datasets 4.1 to 4.4, all of which outline suitable land areas within the boundary layer that meet the particular criteria requirements under each respective combination of criteria screenings. For the sake of convenience, these four final results datasets are synonymously labelled and referred to as the four project scenarios. In short, these four scenarios, may be characterised as Scenario 1 – All conservative; Scenario 2 – Progressive soil type, conservative land use; Scenario 3 – Conservative soil type, progressive land use; and Scenario 4 – All progressive.

It should be noted that despite not representing final results in the sense of suitable areas, the produced result datasets from the first (flat land), the second (deep soil and flat land), and the third (apt deep soil and flat land) screening steps, may be regarded as bonus model spin-offs.

Table 10. Result datasets from the screening process

Result datasets	Name/Description	Count	Geometry
1	**Flat land**	1	Feature class layer (Polygon)
	Description: The dataset is an exact copy of screening dataset 1 (dissolved polygon) and consists of areas with required slope. 1.1: Flat land.		
2	**Deep soil and flat land**	1	Feature class layer (Polygon)
	Description: The dataset consists of one dissolved polygon layer which outlines areas with required soil depth and required slope. 2.1: Deep soil and flat land		
3	**Apt deep soil and flat land**	2	Feature class layer (Polygon)
	Description: The two datasets are dissolved polygon layers and consist of areas with required soil depth and required slope, and which meet one of two required soil type criteria. 3.1: Apt deep soil and flat land under required soil type screening 1 criteria. 3.2: Apt deep soil and flat land under required soil type screening 2 criteria.		
4	**Suitable areas**	4	Feature class layer (Polygon)
	Description: The four datasets are dissolved polygon layers and consist of areas with required soil depth and required slope, and which meet of one of two required soil type criteria and one of two available areas criteria. 4.1: Suitable areas under required soil type (3.1) and available areas under screening criteria 1. 4.2: Suitable areas under required soil type (3.2) and available areas under screening criteria 1. 4.3: Suitable areas under required soil type (3.1) and available areas under screening criteria 2. 4.4: Suitable areas under required soil type (3.2) and available areas under screening criteria 2.		

After the screening process was completed, final result datasets 4.1. to 4.4 were subjected to a post-treatment procedure integrated into the GIS modelling, with the primary purpose to identify and remove rendered suitable areas whose shape or total size would not allow the construction of

PTES according to certain project boundary conditions. Secondarily, to equip the datasets with some calculated quantity fields.

Further limitation based on shape and size

The two most essential project boundary conditions, both based on Danish practice and experience (see e.g. ref. [13]), concerned, on the one hand, a minimum required land area of 15,000 m^2 (referring to total PTES land area, A_{PTES} $[m^2]$, at square or mildly rectangular surface design), and, on the other hand, a minimum storage volume of 50,000 m^3.

For this end, the concept of roundness, R_d [-], was developed in an attempt to define a quantity by which mathematically to determine whether a suitable area of a given shape and size in fact could host a pit storage of the preconceived size and form. The definition of roundness is the ratio of a polygon area (area of the suitable area) to the one of a circle with the same circumference as the considered polygon:

$$R_d = \frac{4\pi A}{C^2} \qquad \text{Equation 7}$$

where A and C are the area and the circumference of the polygon in question. To qualify and be sufficiently large according to project boundary conditions, a suitable area would have to be larger or equal in size than that of the following quota:

$$Suitable\ area_{Sufficient}\ [m^2] >= \frac{15{,}000\ [m^2]}{{R_d}^2} \qquad \text{Equation 8}$$

By this definition, we realise that perfectly square-shaped candidate polygons with areas close to 15,000 m^2 will in fact have been rejected, which is not optimal. However, the definition used guarantees that any unsuitably shaped polygons with areas close to 15,000 m^2, i.e. extremely thin, narrow, or irregular by any other measure, will not be accepted. At this stage, we have considered the latter effect as most important.

For the relationship between required total PTES land area, A_{PTES}, and a corresponding PTES storage volume, V_{PTES} $[m^3]$, the project investigated and summoned experiences from Danish PTES installations, supported by consultancy advice, combined with own GIS measurements, and arrived at the following correlation for the experienced-based interval from Dronninglund Sunstore 3 (~18,000 m^2 and 60,000 m^3), through Höje Taastrup (~19,000 m^2 and 70,000 m^3), Marstal Sunstore 4 (~19,500 m^2 and 75,000 m^3), Toftlund (~20,000 m^2 and 85,000 m^3), Gram (~23,500 m^2 and 122,000 m^3), and, the world's largest at current, Vojens (~31,000 m^2 and 210,000 m^3):

$A_{PTES} \leq 31{,}000\ m^2$: $V_{PTES} = 12{,}582e^{0.00009 \cdot A_{PTES}}$ Equation 9

For larger areas, that is larger than 31,000 m^2, a linear extrapolation was used up to a project maximum volume limit set at 2 Mm^3:

$A_{PTES} > 31{,}000\ m^2$: $V_{PTES} = 8.628 \cdot A_{PTES} - 49{,}835$ Equation 10

Storage heat capacity calculations, Q_{PTES}, used a water density of 1000 kg/m^3, a specific heat capacity of 4190 J/KgK, and a ΔT of 40°C.

Results

Database of Swedish District Heating Systems with Required Collector Field and Store Sizes

The resulting and updated database on Swedish district heating systems distinguishes in terms of summation between three principal levels: the district heating system (DHS) level; the district heating area (DHA) level; and the aggregated district heating area (DHA*) level. The latter of these, indicated by a star annotation, and as illustrated for the southern part of Skåne län in Figure 11, was added to facilitate final summation of national potentials without the risk of double-counting due to overlapping DHA´s.

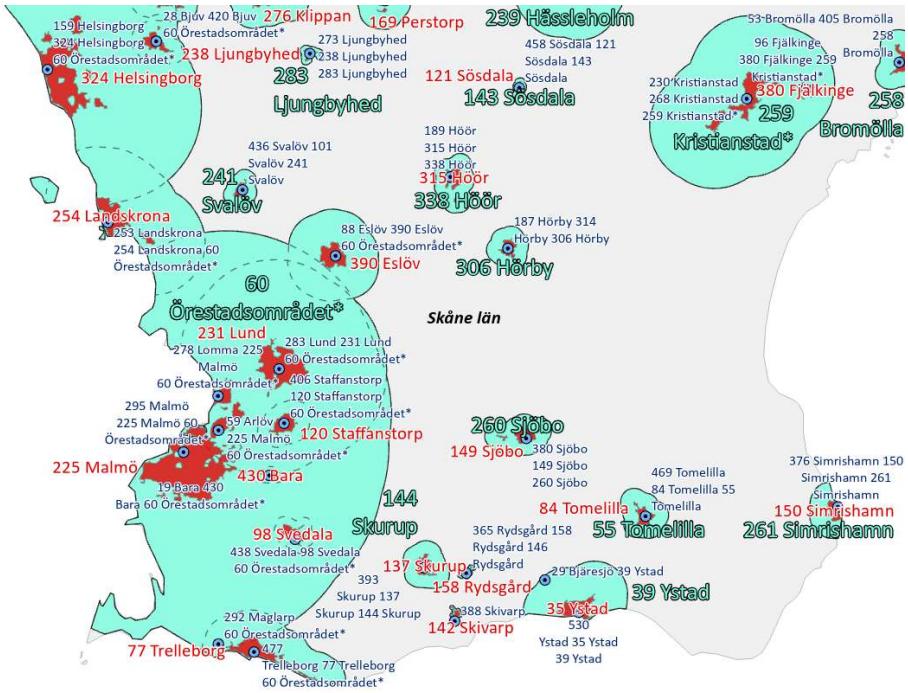

Figure 11. ID-numbers and names for Swedish district heating systems by system level (blue circles), district heating area level (red), and by aggregated district heating area level with dynamic buffer areas (green), exemplified for the southern part of Skåne län.

In total, as also presented above in Table 2, 547 unique district heating systems are currently in operation in Sweden. By means of geographical location and spatial association, 476 of these systems belong to (i.e. are located within) an aggregated district heating area, whereas 385 system belong to unique district heating areas, as presented by NUTS2 and NUTS3 administrative areas in Table 11.

Table 11. Total count of Swedish district heating systems (DHS), the number of DHS associated to aggregated district heating areas (DHA*), and to unique district heating areas (DHA), by administrative areas, with summation of total population (Pop.) and annual district heat deliveries (Qs)

Administrative areas	**DHS [n]**	**DHA* [n]**	**DHA [n]**	**Pop. [kn]**	**Qs [GWh/a]**
Mellersta Norrland	**55**	**41**	**32**	**254**	**2,294**
Jämtlands län	28	18	12	79	777
Västernorrlands län	27	23	20	174	1,517
Norra Mellansverige	**81**	**73**	**58**	**538**	**4,349**
Dalarnas län	27	26	22	178	1,516
Gävleborgs län	32	27	21	192	1,635
Värmlands län	22	20	15	169	1,198
Östra Mellansverige	**98**	**86**	**69**	**1,301**	**10,215**
Örebro län	21	16	14	249	2,018
Östergötlands län	21	19	15	371	2,864
Södermanlands län	21	17	14	199	1,567
Uppsala län	23	23	16	268	1,779
Västmanlands län	12	11	10	214	1,986
Övre Norrland	**56**	**48**	**45**	**393**	**3,891**
Norrbottens län	24	21	20	158	2,090
Västerbottens län	32	27	25	235	1,802
Småland med öarna	**82**	**69**	**52**	**539**	**4,086**
Gotlands län	6	5	5	28	212
Jönköpings län	30	25	21	234	1,639
Kalmar län	24	19	15	141	1,197
Kronobergs län	22	20	11	136	1,039
Stockholm	**32**	**31**	**23**	**2,245**	**13,101**
Stockholms län	32	31	23	2,245	13,101
Sydsverige	**56**	**53**	**46**	**1,057**	**6,182**
Blekinge län	11	9	7	130	643
Skåne län	45	44	39	927	5,540
Västsverige	**87**	**75**	**60**	**1,395**	**8,544**
Hallands län	13	9	7	159	968
Västra Götalands län	74	66	53	1,236	7,576
Grand Total	**547**	**476**	**385**	**7,723**	**52,663**

From Table 11 it may be concluded that 71 DHS could not be associated to an aggregated district heating area, and, likewise, that 162 systems could

not be associated with a unique DHA, for reasons explained above in the method section. Table 26 in the Appendices shows this information from the perspective of DHA*, ie how many DHS and DHA exist there.

Case Studies

Eight locations were identified for potential case studies. The location and annual heating demand of these potential case studies are depicted in Figure 12 and Table 12. Each case study was passed through following filters for locations close to DH network boundary a) Soil depth b) Soil type c) access to identified land.

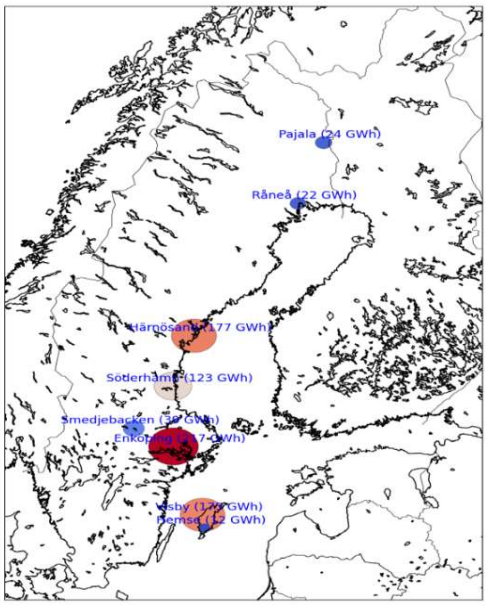

Figure 12: Locations and annual heat demand of case studies. the annual heat demand is based on the Swedish DH data base and can differ from the actual demand received from utilities.

Table 12: Annual heat demand and geo-suitability for case studies. It is important to note that the annual heat demand is based on the Swedish DH data base and can differ from the actual demand received from utilities. In Visby, an existing quarry was investigated as a potential site for heat storage; therefore, the geo-properties were not evaluated.

Location	Annual heat demand (GWh)	Soil type	Soil depth	Access to land
Söderhamn	123	Yes	Yes	Yes
Råneå	22	Yes	Yes	Yes
Pajala	24	No data available	Yes	-
Hemse	12	Yes	No	-
Enköping	217	Yes	Yes	No
Härnösand	177	Yes	Yes	Yes
Smedjebacken	39	No	Yes	-

Råneå

System description: The district heating system has an annual heat demand of 25.9 GWh for the chosen year, which is slightly higher than the nominal load in Table 12. The peak load is 7.51 MW with an average summer load of 2 MW. To meet this demand, a new 4.5 MW pellet boiler is installed to serve the base load year-round. Additionally, there are two other pellet boilers with a combined capacity of 3.9 MW to supplement the system during higher demand periods. For peak loads, a 6 MW Oil boiler is available. The cost of pellets is 2890 SEK per ton, with a calorific value of 4.94 MWh per ton, leading to an approximate heat cost of 650 SEK/MWh. Investment for the system are subject to a 7% interest rate. The variation of demand, supply, return and ambient temperature is shown in Figure 13.

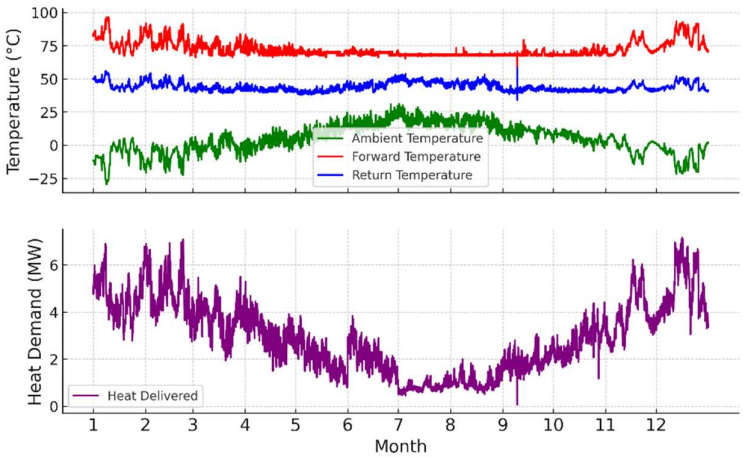

Figure 13: Variation in heat demand and temperatures for Råneå. The data is available on hourly scale for Year 2022. The sudden increase in heat demand in June is attributed to the outdoor hot water baths

Key results

The summary of two different system sizes is shown in Table 13, which provides an overview of the collector area, storage volume, and the corresponding solar fraction achieved. For a solar fraction of 20%, only a relatively small tank is required to store the collected thermal energy. However, as the solar fraction increases to 44%, a PTES with a volume of 25 000 m³, combined with a solar field of 25 000 m² is needed.

Table 13: System size for 2 different solar fractions for Råneå case study

	Case A	**Case B**
Solar field m^2	13000	25000
Storage m^3	3000	25000
Annual heat delivered MWh	5034	10021
Solar fraction	20%	44%

The 5-year performance of system for Case B (44% solar fraction) is shown in Table 14.

Table 14: Five years performance of system designed for 44% solar fraction case.

Year	Heat charged into PTES MWh	Heat losses from PTES MWh	Heat discharged to the network MWh	% heat losses	% Solar fraction
1	-13705	2090	10993	15%	42%
2	-13179	1708	11416	13%	44%
3	-13085	1594	11472	12%	44%
4	-13046	1534	11502	12%	44%
5	-13020	1437	11516	11%	44%

Heat losses are initially higher during the first year of operation; however, as the system reaches thermal equilibrium with the surrounding ground, these losses gradually decrease to approximately 11% in 5th year of operation. As shown in Figure 14. While the top losses remain relatively constant throughout the year, edge losses exhibit a significant reduction over time.

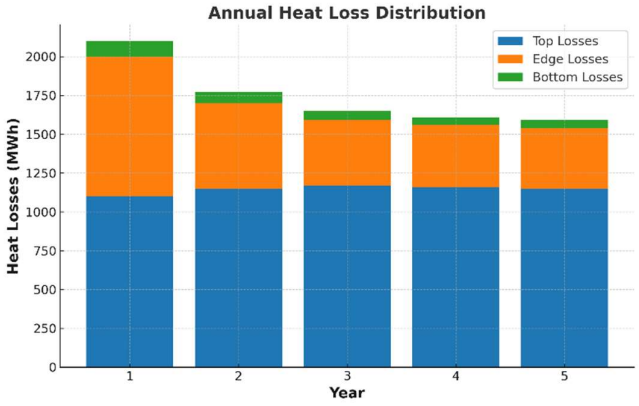

Figure 14 Variation of PTES heat losses over the years from top lid, edge, and bottom

The temperature distribution across different storage nodes is shown in Figure 15. During the summer months, the storage remains stratified, with a temperature difference (ΔT) of 20°C between the top layer (node 1) and the bottom layer (node 25) of the storage. However, most of the stored heat is gradually discharged between September and October.

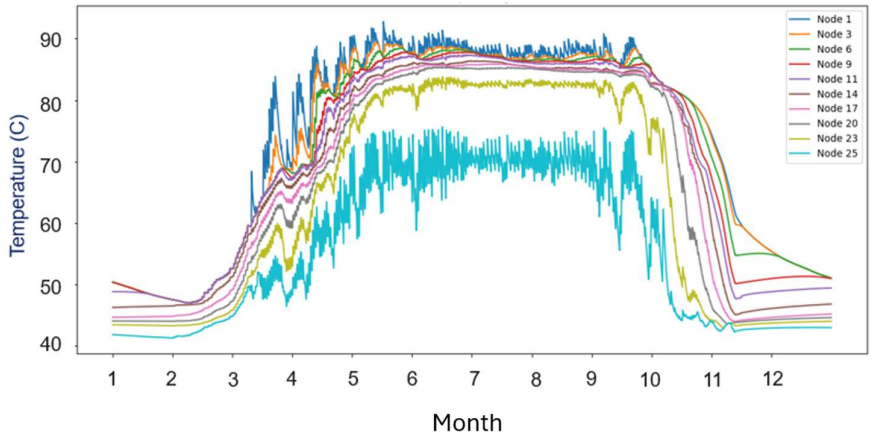

Figure 15 Variation of temperatures in different layers of PTES. Node 1 represents the top layer of PTES; and Node 25 is the bottom layer.

Increasing the collector area and storage volume can further increase the solar fraction, but the system experiences diminishing returns at higher solar fractions, as illustrated in Figure 16. For instance, with a collector area of 40 000 m² and a storage volume of 120 000 m³ (a ratio of 3:1 compared to the recommended 2:1 based on guidelines for 60% solar fraction), the solar fraction achieved is only 49%. This limitation arises primarily due to the seasonal distribution of solar irradiation in northern regions. Unlike more southerly locations, where solar energy is more evenly distributed, northern regions receive a significant portion of their solar irradiation within a shorter summer period. As a result, a substantially larger thermal storage capacity is required to capture and retain this energy for use during the colder months. Therefore, storing energy for extended periods leads to higher thermal losses due to prolonged heat dissipation as well as larger storage

voluems (19% heat losses for 49% solar fraction). These factors collectively reduce the overall effectiveness of increasing storage volume and collector area in achieving high solar fractions in northern climates.

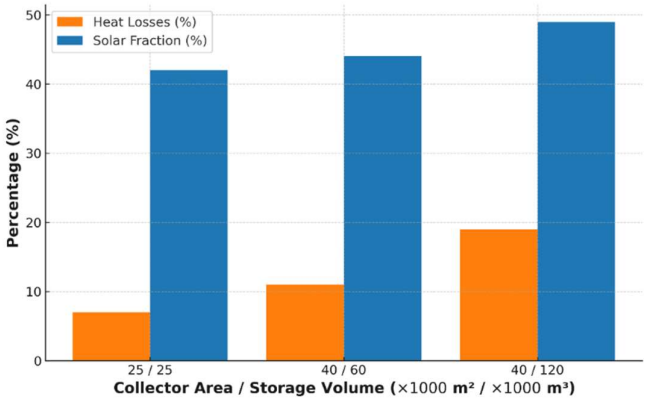

Figure 16 Effect of increasing system size on PTES heat losses and solar fraction

Figure 17 illustrates the CAPEX and LCOH for two cases with different solar fractions (SF): 20% SF (Case A) and 44% SF (Case B). Case A employs a tank-based thermal storage system, which has a higher capex per unit volume compared to PTES used in Case B. Case A has an LCOH of 100 €/MWh, compared to 86 €/MWh for Case B.

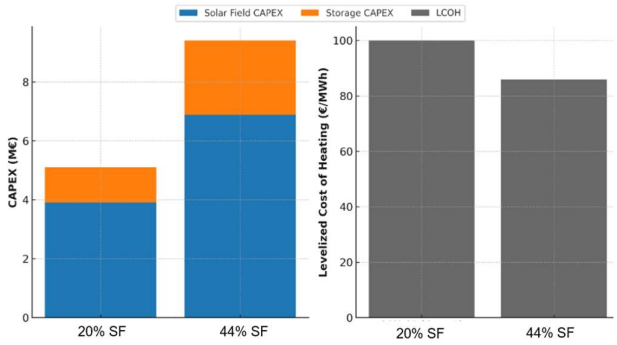

Figure 17 Capex and LCOH for analysed cases. LCOH are calculated for 20 years economic life time, and 7% interest rate.

The LCOH is highly sensitive to both the interest rate and the economic lifetime of the system, as shown in Figure 18. For an economic lifetime of 25 years, which is same as the technical lifetime of the system, LCOH remains competitive with conventional fuel-based heating at interest rates below 4%.

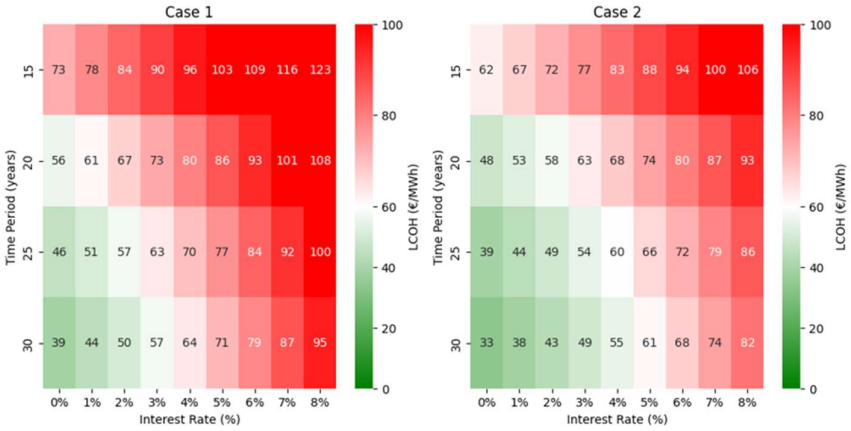

Figure 18 Effect of economic lifetime, and interest rate on LCOH for 2 analysed cases. The left figure is for 20% SF, and the right figure is for 44% SF case.

Härnösand

The total annual heating demand in 2023 is 208 GWh, with different heat sources contributing to meet this demand. The district heating network supplies a total of 1867 residential buildings and 212 industrial buildings.

Industrial waste heat provides 30 GWh, with nearly constant availability throughout the year. The turbine condenser and flue gas condenser contribute the largest share, at 128 GWh, powered by wood chips. The pellet boiler supplies 5.5 GWh and is only used during summer when the CHP plant is off. Another wood chip boiler accounts for 33 GWh, used for top-up effects in addition to CHP plant. The oil boiler contributes a minor share of 0.6 GWh, used only for peak demand. Variation in the heat demand, and supply/return temperatures are shown in Figure 19 and Figure 20 respectively.

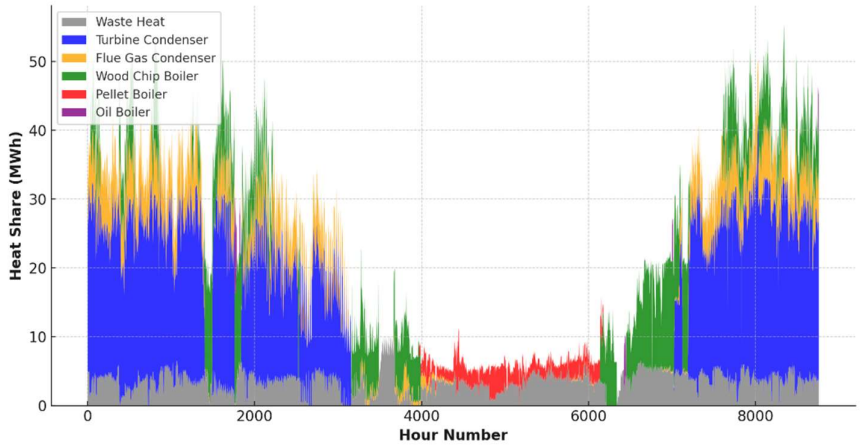

Figure 19: Variation of heat demand, and various fuel sources used to meet the heat demand in Härnösand.

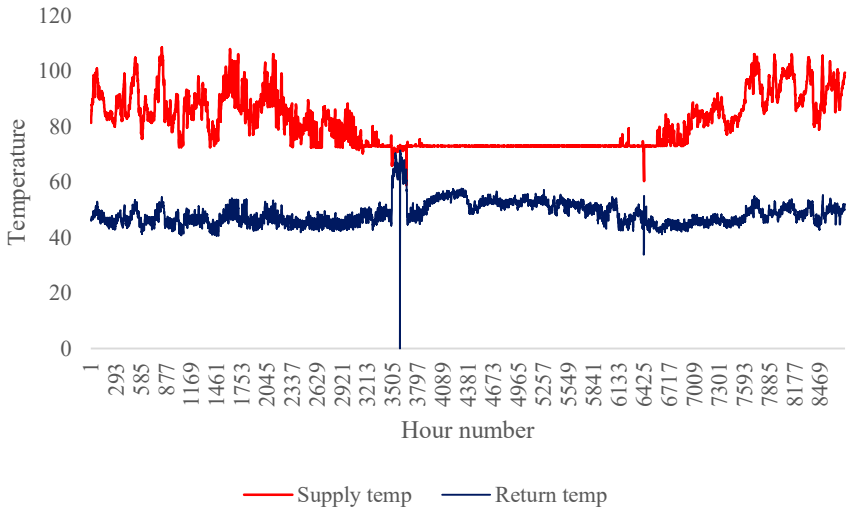

Figure 20 Variation of supply and return temperature in DH network

As shown earlier in Figure 10, the location available for PTES is away from the boiler central. This limits the maximum heat that can be discharged from storage to the network. The available pipe sizes and the maximum flow considered to limit velocity in the pipes are shown below. A DN250 pipe size was chosen for the simulation study with trench length of 2.3 km.

Table 15: Details of pipe sizes, distances, and corresponding maximum available flow near the PTES location.

	Total pipe length (m) (supply + return)	Max allowed pipe flow kg/h
DN100	580	28000
DN125	1440	50000
DN150	2700	81000
DN250	**4600**	**281000**
DN400	6200	904000
DN500	7880	1580000

Simulation results for DN250 pipe size without HP

The maximum temperature that can be discharged from PTES to the network is 95°C, the heat load seen by PTES for a DN250 pipe size is 54 GWh. Figure 21 shows the variation of heat demand seen by PTES (restricted by the flow, temperature, and waste heat).

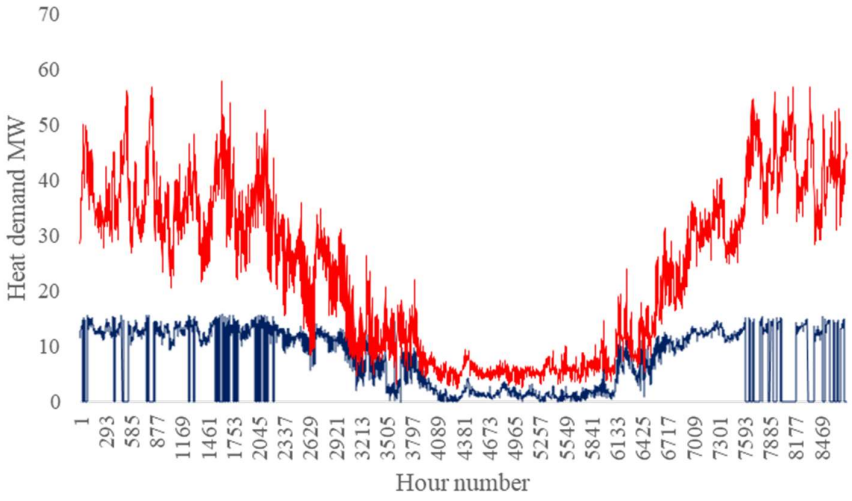

Figure 21: Variation of network's total heat demand (red curve), and the demand curve restricted by maximum flow, temperature, and without waste heat (blue curve).

Different system sizes were tested based on the following two criteria:

- Ensuring the solar collector output remains within the expected range (400 kWh/m²·year).
- Verifying that the storage is significantly discharged.

A smaller storage volume would be used more frequently and efficiently. However, it would only meet a small fraction of the total potential demand, limiting the overall contribution of stored heat to the district heating system. On the other hand, an oversized storage system would result in a large amount of remaining heat at the end of the year. This excess heat would lead to higher heat losses, ultimately reducing the overall efficiency of the system. The size of the system chosen is shown in Table 16, and the multi-year performance of the system is shown in Table 17.

Table 16: Specifics for the chosen system

Solar field	55000	m^2
Number of collector rows	247	
PTES Volume	500000	m^3
Longer side length for PTES	184	m
Shorter side length for PTES	59.2	m
Radii Ratio	3.1	

Table 17: Multi-year performance of the designed system

Year	Heat into PTES MWh	Heat losses MWh	Heat discharged MWh	Heat losses %	Number of storage cycles
1	-29588	10068	17695	-34%	2.03
2	-28689	7473	20933	-26%	2.40
3	-28352	6948	21292	-25%	2.44
4	-28206	6674	21456	-24%	2.46

The designed system meets 10% of the network's demand and 38% of the load seen by storage. The specific collector output is 390 kWh/m². However, the average temperature in the storage remains high, leading to greater heat losses compared to a system where heat can be discharged over a longer period, such as an R-R integration, or a system with a heat pump.

The energy content of the storage is shown in the Figure 22. The grey lines indicate instances when heat is discharged from the storage. As observed, when the last discharge occurs, the remaining storage capacity is 1600

MWh, which corresponds to 18% of the maximum capacity, and thus 82% of the heat is discharged from the storage. The variation of LCOH for this case is shown in Figure 23.

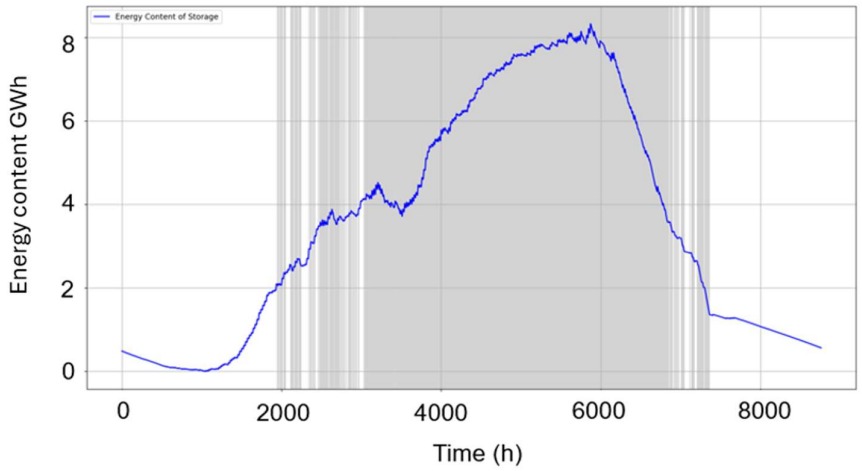

Figure 22: Energy content of the storage (blue curve). The energy content is calculated based on the storage volume, minimum and maximum temperature of the storage for given year. The grey lines indicate instances when heat is discharged from the storage.

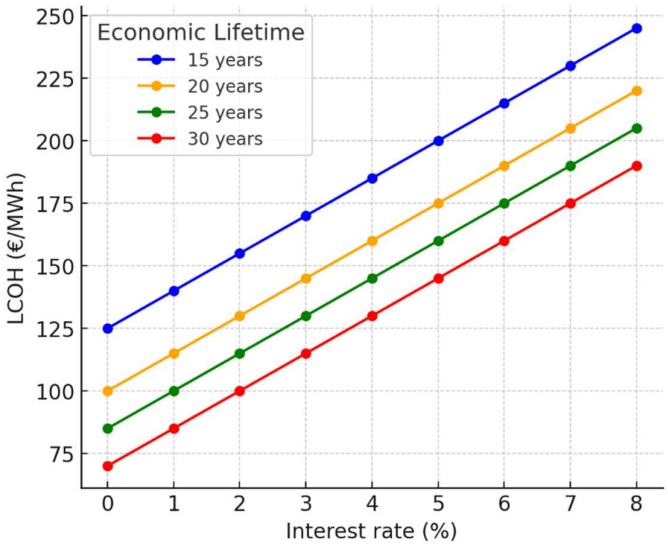

Figure 23 Variation of LCOH with interest rate, and economic lifetime considered for economic analysis

To reduce heat losses and improve discharge efficiency, a HP can be integrated. This would allow for better utilization of stored heat, ultimately enhancing the overall efficiency of the solar district heating system.

Simulation results for system with HP

The results of the sensitivity analysis using the Python model for various solar collector sizes and storage volumes is shown in Figure 24. Delivered energy refers to the heat delivered to the DH network. Capacity reserve refers to the percentage of heat available in the system that is not discharged, either because the storage is full or there is no immediate demand. A lower capacity reserve, such as 5%, indicates that 95% of the heat collected from the solar collectors is effectively utilized within the network. This ensures efficient energy use while minimizing wasted heat.

The results show that for collector areas up to 30 000 m², the required storage volume remains below 2 500 m³, effectively absorbing most of the heat from the collectors. As the collector area increases, the need for storage also rises to accommodate seasonal load demands. A system with an 85,000 m² collector area and a 300 000 m³ storage volume is selected to maximize heat absorption for TRNSYS modeling.

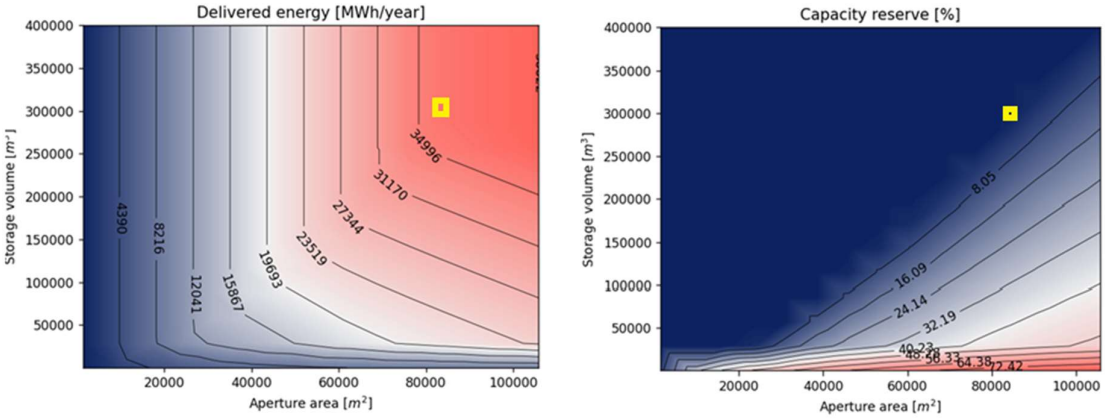

Figure 24 Result of the sensitivity analysis for various solar collector sizes and storage volumes. Heat delivered is shown in the left, whereas heat not utilized from solar collector (capacity reserve) is shown in the right, as a % of available heat from solar collectors. The yellow marked rectangle shows the system size chosen for TRNSYS simulations.

As HP capacity decreases, heat utilization from storage declines, negatively impacting the total heat delivered. This is due to the limited heat provided by PTES for the evaporator and for pre-heating the HP condenser. Without any HP, the system would deliver 24 GWh of heat, which increases to 45 GWh if an HP when a 15 MW capacity is integrated. The larger the heat pump capacity, the lower the storage losses, allowing the storage to be

cooled down to lower temperatures. To determine the optimal HP capacity, the LCOH of heating is compared for different system sizes, and the results are shown in Figure 25.

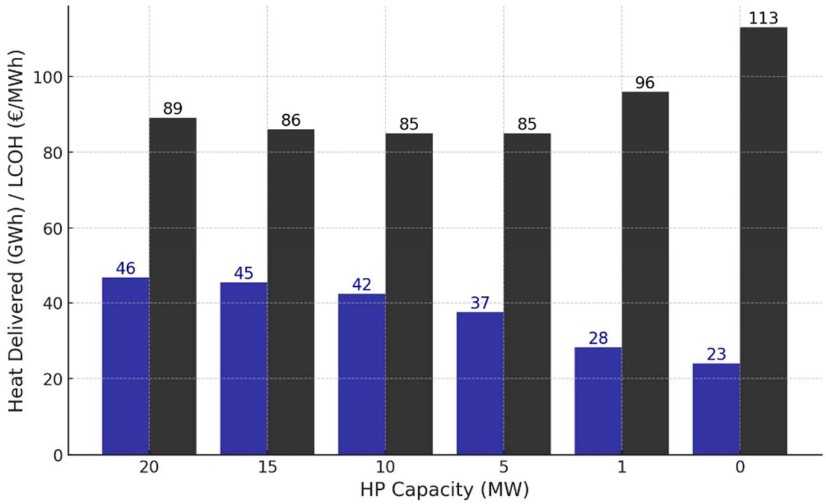

Figure 25: Effect of HP capacity on LCOH and heat delivered to the DH network, based on the TRSNYS simulations. The LCOH is calculated at 5% interest rate, for 20 years economic lifetime.

Based on the above sensitivity analysis, the following system size was chosen:

- Solar collector area: 85 000 m^2
- Storage volume: 300 000 m^3
- HP peak capacity: 15 MW

For chosen configuration, the total heat delivered to the network is 45.3 GWh, and the Sankey diagram is shown in Figure 26. The heat pump supplies 15.7 GWh heat with an SPF of 2.3 and a further 7.7 GWh are supplied from the top of the PTES before the temperature is raised by the heat pump in the condenser.

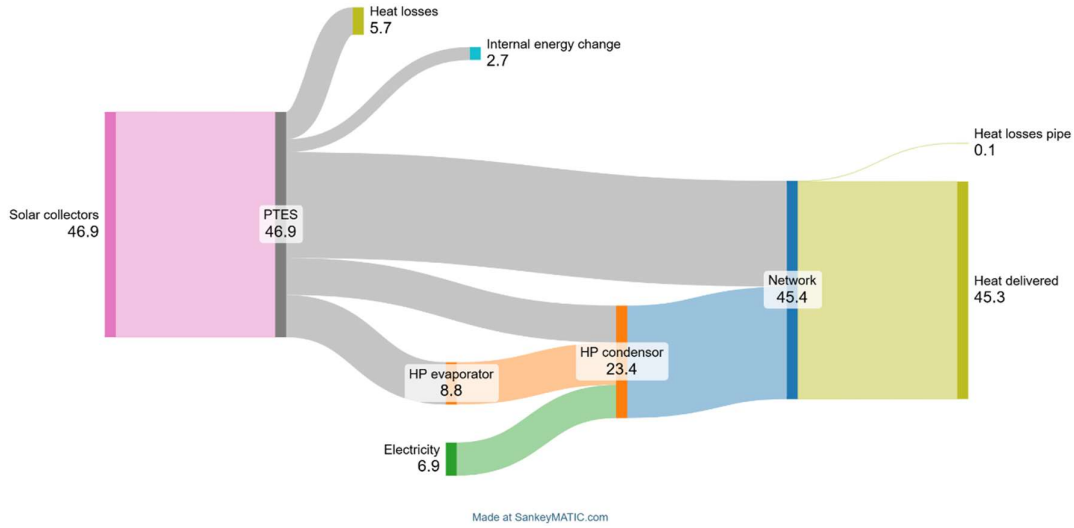

Figure 26 Sankey diagram to visualize various energy flows for simulated configurations.

Comparing the results from the sensitivity analysis using the simple Python model, the heat delivered is within 8 %: 35 GWh for the Python model and 38 GWh with the TRNSYS model. This shows a close match between the sensitivity and detailed results.

The heat pump operates for 2700 hours over the course of the year. The annual electricity use of the heat pump is 6.9 GWh. The seasonal coefficient of performance of the heat pump is 2.2. The total capex of the system is 40.2 M€ as shown in Table 18. The LCOH comparison is done for 2 different values of electricity prices.

Table 18: Capex and opex of the designed system

Parameter	**Value M€**
Solar collectors capex	14.9
PTES capex	16.8
Heat pump capex	6
Pipe capex	0.644
Contingency	2
Total capex	**40.2**
Opex/y case 1 (100 €/MWh)/y	0.7
Opex/y case 2 (150 €/MWh)	1

The LCOH variation for case 1 and case 2 is shown below. Electricity cost has a significant impact on the LCOH. For example, for economic lifetime of 20 years, and with a 4% IR, the LCOH increases from 80 €/MWh to 88 €/MWh when the electricity cost rises from 100 €/MWh to 150 €/MWh.

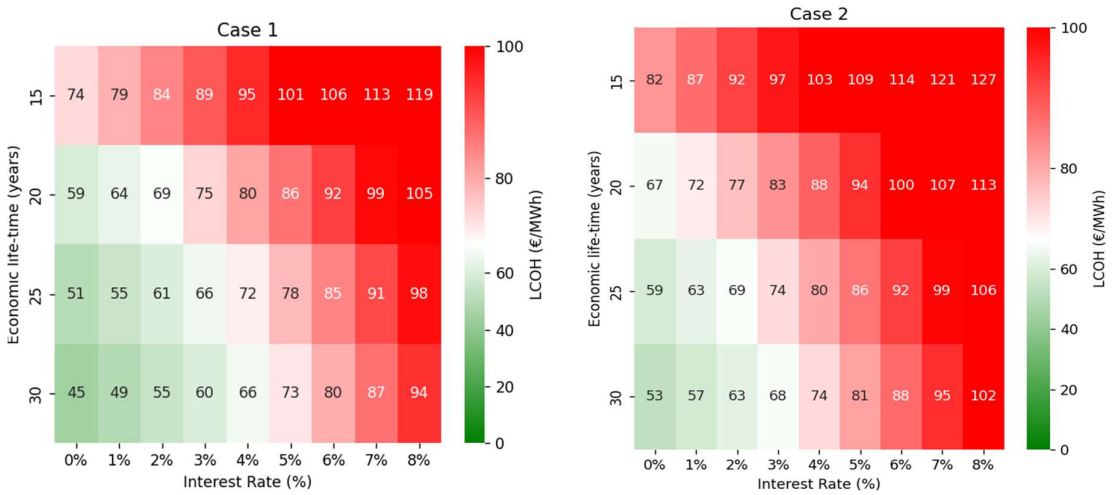

Figure 27 Variation of LCOH for two cases.
Case 1 considers an electricity price of 100 €/MWh, while Case 2 assumes 150 €/MWh.

Söderhamn

The total annual heating demand in 2020 is 143 GWh, with various heat sources contributing to meet this demand, as shown in the figure below. The heat from the CHP plant serves as the primary source, while pellet boilers are used during the summer period.

The district heating network operates at varying temperatures throughout the year, with summer operation temperatures ranging between 70-75°C and winter temperatures as high as 115° - 120°C. The primary fuel source is wood chips, with an average cost of 40 €/MWh. During the summer period, pellets are used at an average cost of 60 €/MWh. The boiler efficiency of pellet boilers is 85%.

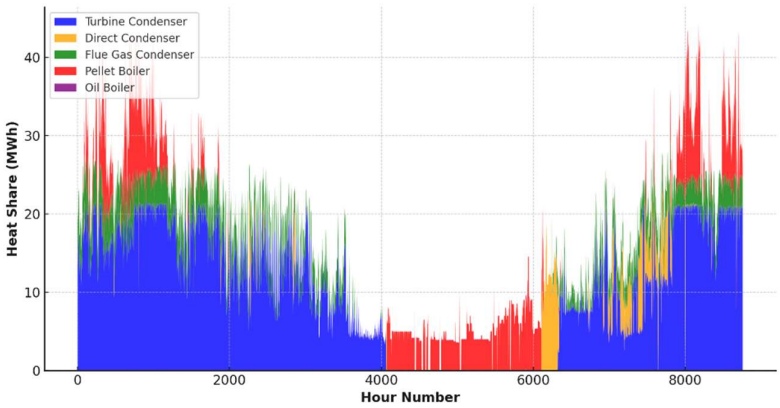

Figure 28 Heat demand and share supply from various heat sources for Söderhamn in 2020.

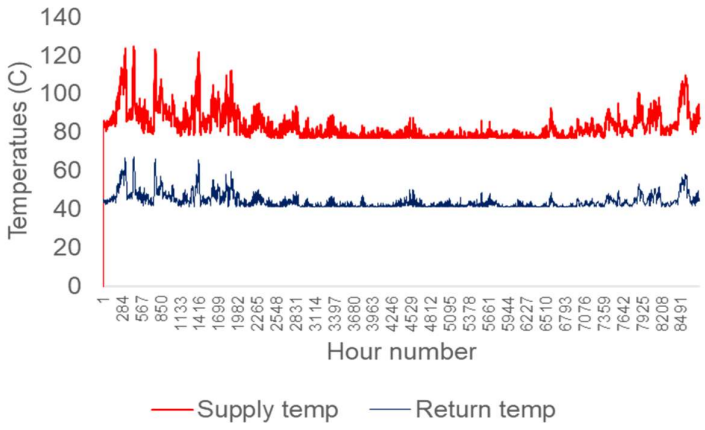

Figure 29 Supply (red) and return temperatures (blue) for Söderhamn in 2020.

Two cases were analyzed, as explained below.

Case 1: System designed to only meet the summer demand.

The first case aims to meet the heat demand exclusively during the summer period, with the objective of completely shutting down the pellet boiler. The system's operational window is focused between Week 24 and Week 33, during which the pellet boiler is intended to remain off.

In this setup, a solar collector system is used to supply heat directly to the district heating network or store it in an existing buffer tank plus an additional new tank. If solar heat is not available, and the storage tank is

fully discharged, an electric heater is activated to maintain the required heat for the network. This system does not require seasonal storage since it is designed only for summer operations.

Based on the sensitivity analysis aimed at maximizing heat utilization from the solar collectors, the selected system configuration consists of a solar field aperture of 35 000 m² and a storage volume of 7000 m³. This setup ensures an optimized balance between solar heat collection, storage capacity, and electric heating requirements. The design system delivers 14.8 GWh of heat, achieving a solar fraction of 10% over the year.

The heatmap illustrates the solar fraction and the required heater capacity across different start and end weeks of operation. For the selected system size (35 000 m² solar field and 7 000 m³ storage), a significant portion of heat (85%) is provided by solar energy between Week 24 and Week 33. The corresponding maximum required electrical heater capacity is 8 MW, with an annual electricity consumption of 1100 MWh. Extending or shifting the operational window would require larger heaters, with capacity requirements reaching up to 20 MW in some cases.

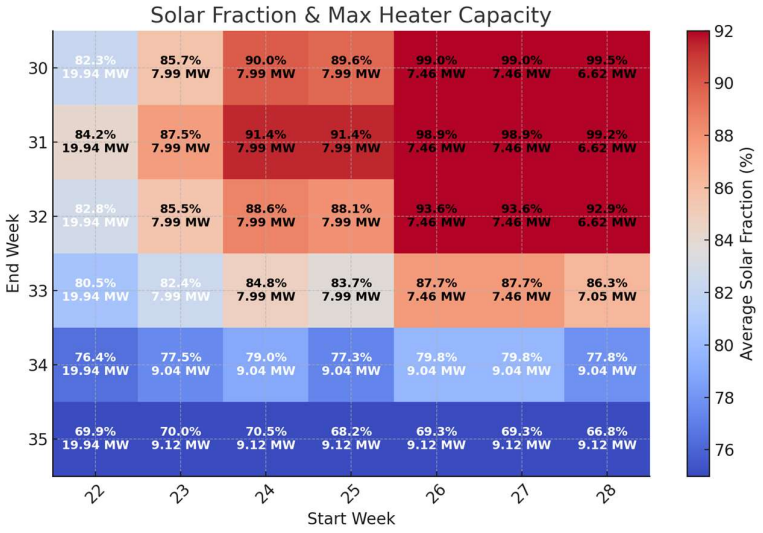

Figure 30 Solar fraction and required electrical heater capacity for different shut-off periods. The X-axis represents the start week when the pellet boiler is turned off, while the Y-axis represents the end week until the remains off. The % in the box shows Solar fraction during this period, and the number below shows the maximum heater capacity (MW) needed to cover any remaining heat demand.

The total system capex is 12.8 M€, and the variation of LCOH is shown below:

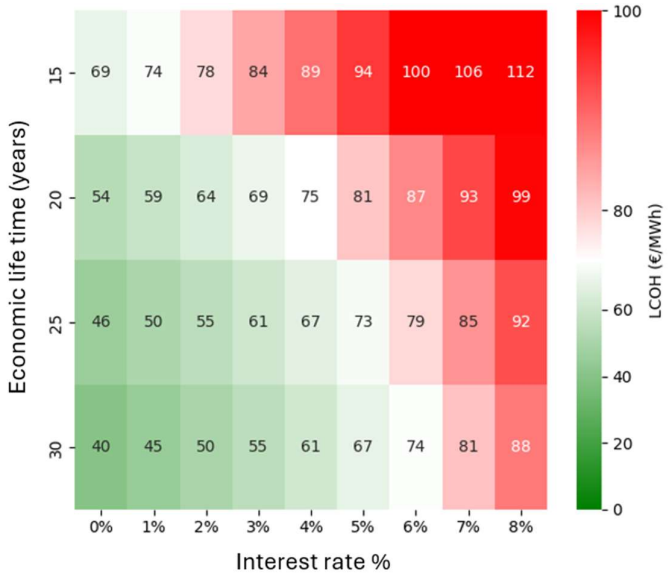

Figure 31 Variation of LCOH for a range of interest rates (0-7%) and economic lifespan (15-30 years) of the system.

Case 2: System with seasonal storage

In this case, the solar field is designed to meet most of the demand as seen by the PTES with a connection point in the network with pipe size of DN200. As for Härnösand, the maximum heat transfer is also restricted.

A sensitivity analysis was performed on temperature and a flow-constrained load profile to obtain initial insights into sizing for TRNSYS modeling. The sensitivity results for a larger storage/solar field showed that for a solar collector field of 85 000 m² and a storage volume of 200 000 m³, 95% of the heat from solar collectors is utilized. This size was chosen for the TRNSYS simulations. Based on the sensitivity analysis of the heat pump (HP) size, an 8 MW HP was selected as optimal.

The results of the TRNSYS model are shown in the table below.

Table 19: The results of the simulations for selected configuration

Parameter	Value
Solar collector area	85 000 m²
Storage volume	200 000 m³
Heat pump capacity	8 MW
HP max temperature	95°C
Heat delivered to the network	41 GWh
Renewable fraction (total network demand)	29% (solar + HP)
Solar fraction (only solar heat)	27%
% heat difference between python and TRNSYS simulations	12%

The results showed that during weeks 22 to 33 (approximately hours 3600 to 5600), the solar field, PTES and HP are capable of meeting most of the summer heat demand. However, there are a few instances where the required power exceeds the heat transfer capacity of the available piping, leading to minor deficits. This result confirms that the designed system can achieve pellet boiler-free operation during summer as can be seen in the monthly plot of energy supplied (Figure 32). Due to the limited pipe size, the storage is discharged over an extended period, lasting until December.

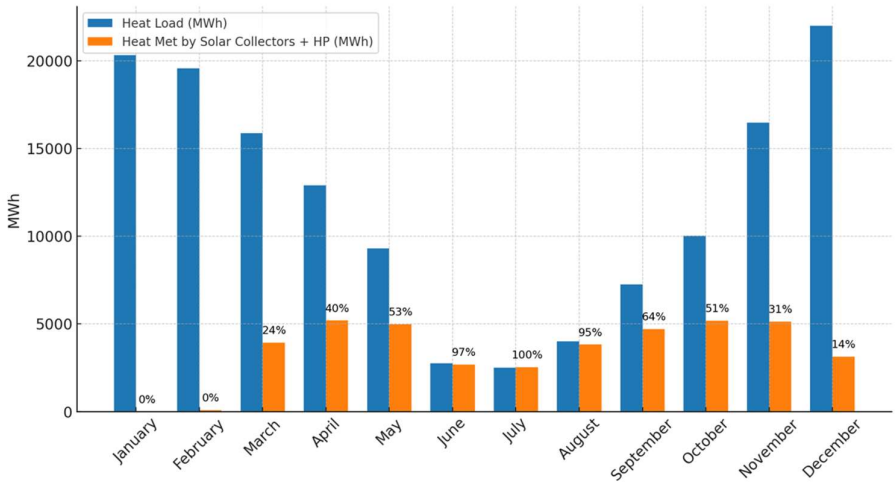

Figure 32 Monthly heat loads for whole network and heat supplied by the solar, PTES and HP system.

The annual electricity consumption of HP is 3312 MWh per year. The scatter plot (Figure 33) illustrates that for most of the year, when the HP operates, the electricity price remains below 100 €/MWh. This indicates that the system effectively utilizes electricity during lower-cost periods, optimizing operational costs.

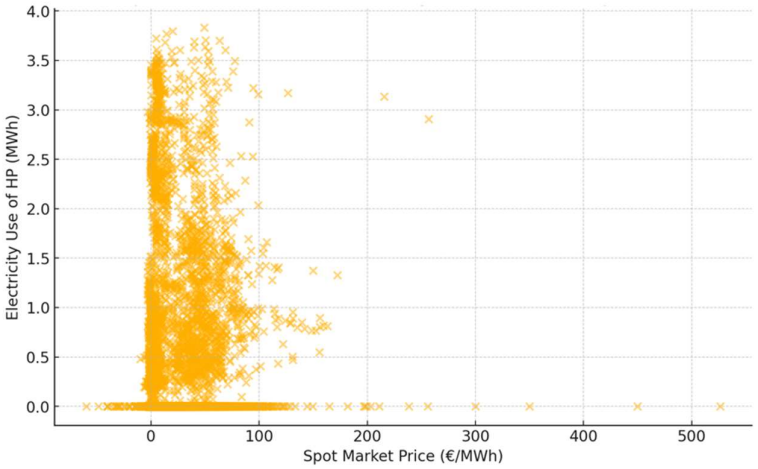

Figure 33 Spot market price of electricity for the hours when the HP is operating plotted against the power used by the HP during the hour. The spot prices are for 2024, for SE2, and without any taxes.

The total system capex as well as LCOH is shown in the table below. The opex is 0.5 M€/year (for electricity cost of 100 €/MWh).

Table 20: Capex for chosen system size

Solar collectors	14.9	M€
PTES	11.8	M€
Heat pump	3.2	M€
Transmission pipe	0.336	M€
Contingency	3	M€
Total capex	**33.2**	**M€**

Figure 34 shows the impact of subsidies on the LCOH. Without subsidies, the LCOH is 75 €/MWh (5% IR, 20 y), which decreases to 52 €/MWh with a 30% subsidy. This highlights the financial benefits of government support for renewable heating projects.

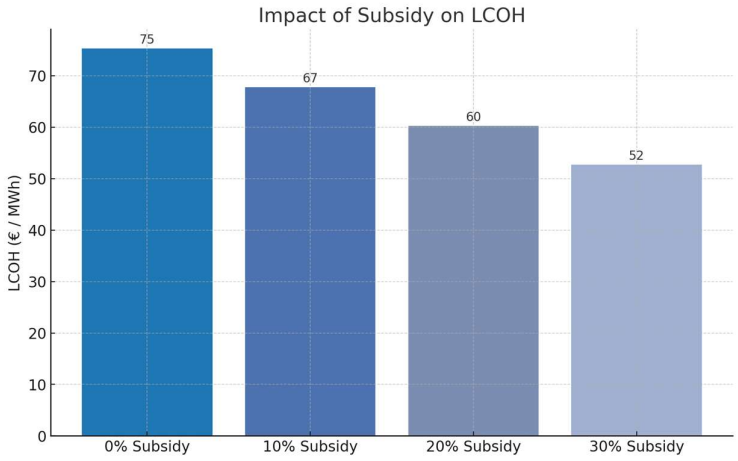

Figure 34 Impact of subsidy rate on LCOH for the Söderhamn case with solar and HP system.

The main economic figure given in this report is the LCOH. To show the impact of rising fuel costs, the NPV was also calculated for a range of annual increase in heat costs from boilers (see Figure 35). As the boiler heat price increases, the NPV of the solar system increases, indicating that the project becomes increasingly profitable with higher fuel price inflation. A 1% increase results in a near-neutral NPV, while a 10% annual increase leads to an NPV exceeding 40 M€, emphasizing the economic viability of investing in alternative heating solutions under rising fuel costs.

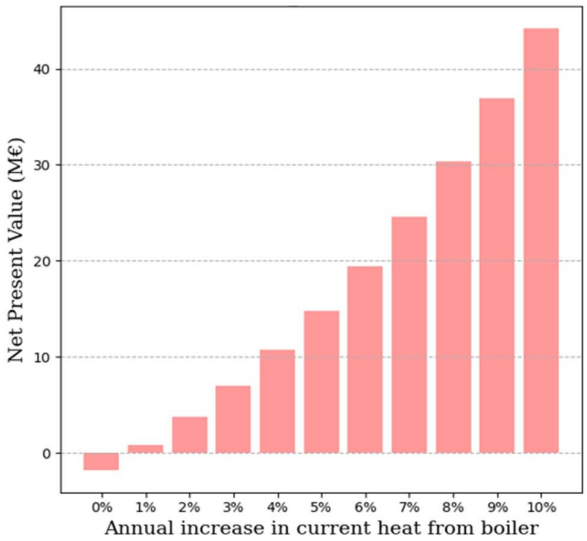

Figure 35 Impact of fuel cost increases on NPV for the Söderhamn case with solar and HP system. NPV is calculated for 5% discount rate, and 20 years economic lifetime.

Potential for Pit Stores in Sweden

As was outlined above in the method section, see e.g. Table 10, the four final results datasets from the screening process were labelled and referred to as four project scenarios: Scenario 1 – All conservative; Scenario 2 – Progressive soil type, conservative land use; Scenario 3 – Conservative soil type, progressive land use; and Scenario 4 – All progressive. In this section, the results in terms of identified suitable areas upon which large-scale pit storages could be built, are presented in accordance with these four scenarios. The main focus in the following report presentation will be on the 1st and 4th scenarios, whereas corresponding data for scenario 2 and 3 are attached in the appendix section where relevant.

To illustrate and describe the results, the following presentation will utilise screen captured map images from the GIS work environment complemented with pivot table summaries based on model exports. Regarding these model exports, all identified suitable areas under each of the four scenarios are designated a unique ID-number in the rendering process, which is exemplified in appendix Figure 55 (see Appendices) for the city of Söderhamn under the first scenario. Although such ID-numbers are superfluous in the sense of project reporting, they constitute in fact key identifiers should the results of this project become relevant and useful for developers, energy planners, municipal heat planners etc. Note that ID-numbers for identified suitable areas are unique for each scenario as each scenario consists of a different amount of differently shaped suitable areas.

The following pages show the maps for the three main urban areas in Sweden around Malmö, Stockholm and Göteborg. It is clear that the buffer areas around these cities with large populations is large due to the high heat demand and the dynamic buffering method that takes this into account. It is also evident that in some cases there are large differences in the size and number of areas that are suitable for PTES between scenarios 1 and 4. This is mostly due to the fact that scenario 1 excludes forested areas, whereas scenario 4 includes them. This difference becomes even more pronounced in northern Sweden where forest areas dominate.

Note that the identified suitable areas, (yellow in the maps) and labelled SA in the tables, represent potential sites for PTES using the available data and screening criteria. As the available data did not contain important data for PTES viability such as ground water flow and the available data has uncertainties, the identified SA's are a likely overestimation of what would in practice be feasible. In addition to ground water flow, there are a number of other practical aspects such land ownership, homogeneity of soil type etc that would reduce the practical realisability of PTES.

The results for the 1st and 4th scenarios are depicted for the southern part of Skåne län in Figure 36.

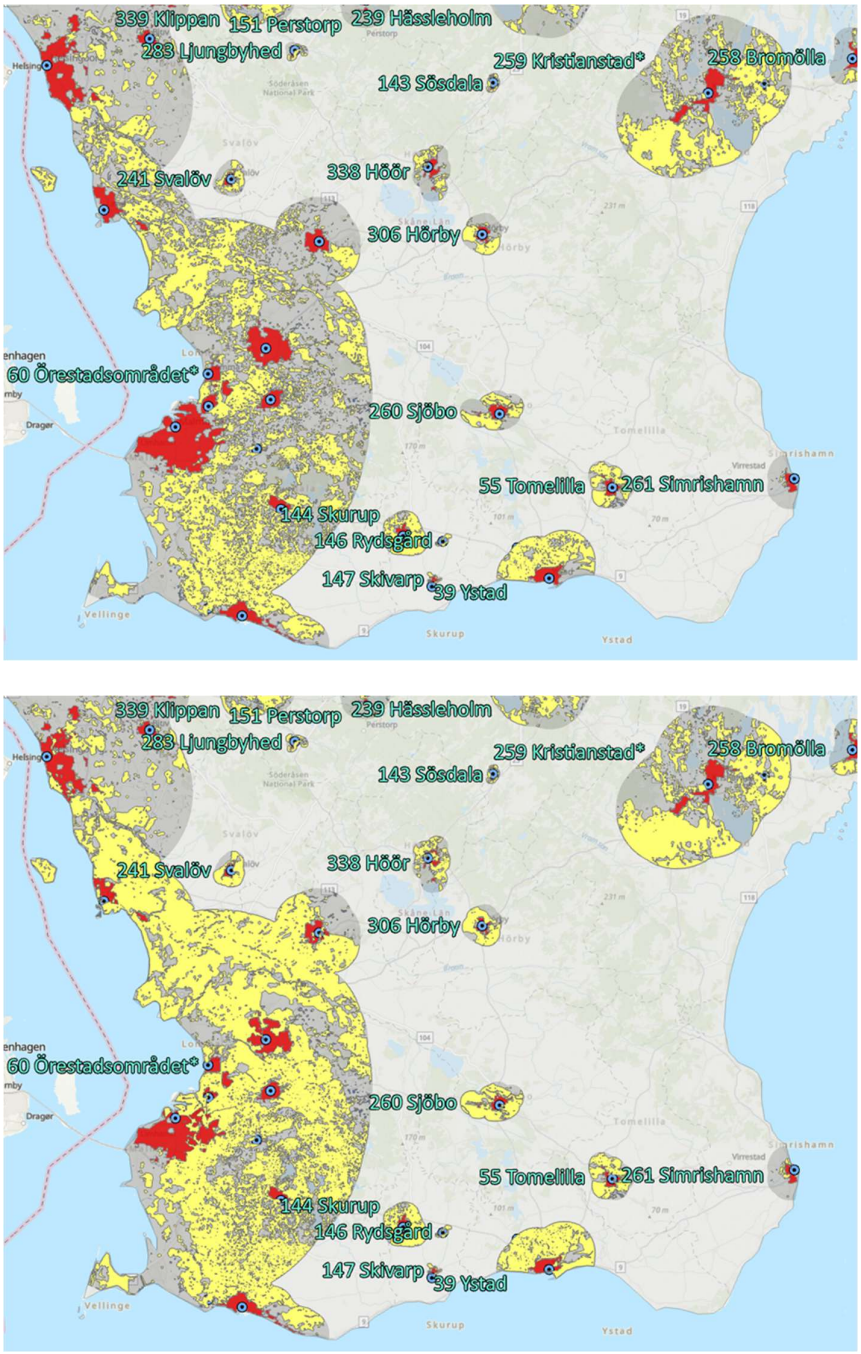

Figure 36. Screen capture map illustrations of suitable areas (yellow) identified in the southern part of Skåne län under the 1st scenario (top) and 4th scenario (bottom). Red areas are the unique DHA and the blues dots are the unique DHS.

The results for the 1st and 4th scenarios are depicted for the larger Stockholm area with surroundings in Figure 37.

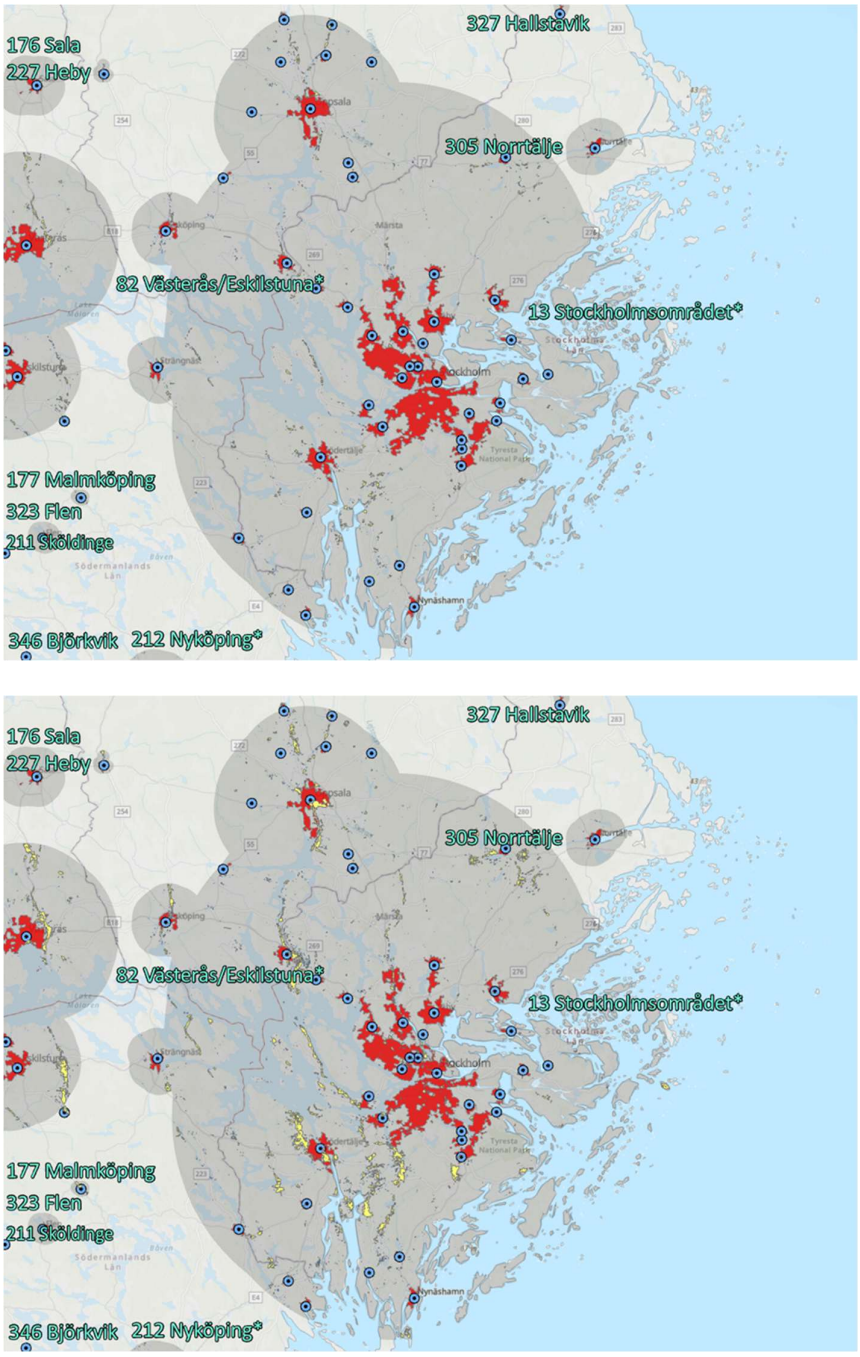

Figure 37. Screen capture map illustrations of suitable areas (yellow) identified in the larger Stockholm area with surroundings under the 1st scenario (top) and 4th scenario (bottom). Red areas are the unique DHA and the blues dots are the unique DHS.

The results for the 1st and 4th scenarios are depicted for the larger Gothenburg area with surroundings in Figure 38.

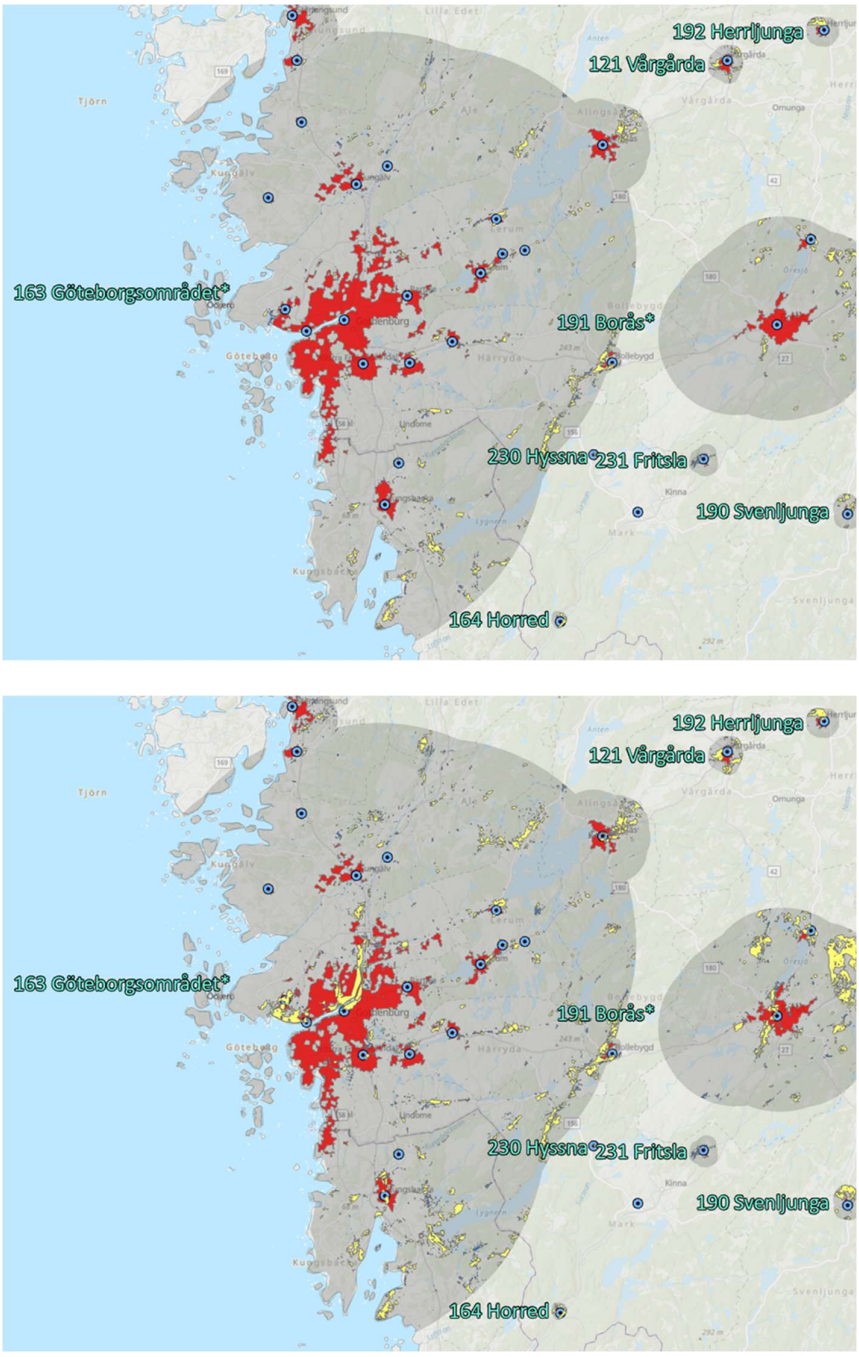

Figure 38. Screen capture map illustrations of suitable areas (yellow) identified in the larger Gothenburg area with surroundings under the 1st scenario (top) and 4th scenario (bottom). Red areas are the unique DHA and the blues dots are the unique DHS.

Three additional screen capture map illustrations for the case study areas are available in the appendices In addition, all scenario results are generated and available in the original as georeferenced datasets, albeit not published or planned for publication at this time. With these datasets it is possible to derive a lot of both statistics on a more general level but also information on a more detailed level.

Table 21. Scenario 1 (Total): Count of aggregated district heating areas (DHA*) and the corresponding total count of district heating areas (DHA) and district heating systems (DHS) within them that have one or more suitable areas (SA).

Administrative areas	**DHA* [n]**	**DHA [n]**	**DHS [n]**	**SA [n]**
Mellersta Norrland	**19**	**23**	**27**	**184**
Jämtlands län	11	11	12	42
Västernorrlands län	8	12	15	142
Norra Mellansverige	**44**	**54**	**53**	**401**
Dalarnas län	18	21	21	148
Gävleborgs län	17	23	22	195
Värmlands län	9	10	10	58
Östra Mellansverige	**31**	**48**	**50**	**612**
Örebro län	8	12	12	217
Östergötlands län	10	16	16	285
Södermanlands län	3	4	5	19
Uppsala län	5	5	6	13
Västmanlands län	5	11	11	78
Övre Norrland	**27**	**35**	**35**	**436**
Norrbottens län	11	13	13	253
Västerbottens län	16	22	22	183
Småland med öarna	**34**	**37**	**39**	**357**
Gotlands län	1	1	1	3
Jönköpings län	17	18	20	187
Kalmar län	9	10	10	101
Kronobergs län	7	8	8	66
Stockholm	**2**	**33**	**45**	**149**
Stockholms län	2	33	45	149
Sydsverige	**32**	**49**	**52**	**1022**
Blekinge län	7	9	9	28
Skåne län	25	40	43	994
Västsverige	**35**	**53**	**60**	**658**
Hallands län	5	5	5	144
Västra Götalands län	30	48	55	514
Grand Total	**224**	**332**	**361**	**3819**

Table 21 presents in summary the main characteristics of the 1st scenario results, considering all outputs with no filtering. It shows the number of DHA*, DHA and DHS that have suitable areas as well as the number of suitable areas. The table splits into the different counties (län) in Sweden as there are significant regional differences due to the wide range in geological characteristics in the counties. In the 1st scenario, 3819 polygon areas, out of a total scenario rendering volume of 37,592 candidate polygons, qualified as suitable areas by meeting the roundness criteria. Altogether, these suitable areas are located within 224 aggregated district heating areas, thus in the vicinity of 361 DHS.

Similarly for the 4th scenario, Table 22 outlines the main characteristics of the results under these screening settings but with no other filtering. The total count of associated aggregated district heating areas that have suitable areas for PTES has increased compared to the 1st scenario from 224 to 269, which corresponds to an approximate 20% increase. The total count of suitable areas amounts here to 4958, which correspond to a relative increase compared to the 1st scenario of ~30%. However, while the sum of all suitable areas amounts to 2,028 square kilometers in the 1st scenario, the corresponding number in scenario 4 is 5,164 km^2, which represent more than a doubling. The impact of accepting certain forest and artificial land areas is more profound in norther parts of the country compared to southern parts.

From the above, it is clear that the generated results for the overall potential for large-scale PTES in Sweden are extensive, with several thousand suitable areas generated under each of the four scenarios. Since many of these suitable areas are larger than what would be required to build a single pit storage according to the stipulated project maximum storage volume (two million cubic meters), anticipated storage volumes and associated storage heat capacities occasionally reach practically unrealistic magnitudes. However, given that the purpose for this part of the project is to establish a first order assessment of a national spatio-technical potential, and not a dedicated techno-economic feasibility study, the numbers have been permitted to ascend into the improbable where considered conditions have so allowed.

Table 22. Scenario 4 (Total): Count of aggregated district heating areas (DHA*) and the corresponding total count of district heating areas (DHA) and district heating systems (DHS) within them that have one or more suitable areas (SA).

Administrative areas	DHA* [n]	DHA [n]	DHS [n]	SA [n]
Mellersta Norrland	**25**	**29**	**32**	**407**
Jämtlands län	11	11	12	61
Västernorrlands län	14	18	20	346
Norra Mellansverige	**53**	**63**	**62**	**754**
Dalarnas län	21	24	24	275
Gävleborgs län	20	26	25	369
Värmlands län	12	13	13	110
Östra Mellansverige	**39**	**56**	**58**	**737**
Örebro län	10	14	14	285
Östergötlands län	12	18	18	278
Södermanlands län	4	5	6	35
Uppsala län	5	5	6	19
Västmanlands län	8	14	14	120
Övre Norrland	**32**	**40**	**40**	**819**
Norrbottens län	11	13	13	395
Västerbottens län	21	27	27	424
Småland med öarna	**43**	**46**	**48**	**457**
Gotlands län	1	1	1	1
Jönköpings län	19	20	22	239
Kalmar län	12	13	13	118
Kronobergs län	11	12	12	99
Stockholm	**2**	**33**	**45**	**317**
Stockholms län	2	33	45	317
Sydsverige	**32**	**49**	**52**	**701**
Blekinge län	7	9	9	43
Skåne län	25	40	43	658
Västsverige	**43**	**61**	**67**	**766**
Hallands län	8	8	7	122
Västra Götalands län	35	53	60	644
Grand Total	**269**	**377**	**404**	**4958**

Supplementary to the above, summary tables for the 2nd and the 3rd scenarios are provided in appendix Table 27 (Scenario 2) and Table 28 (Scenario 3).

Figure 39 scenario 4 (progressive) and Figure 40 scenario 1 (conservative) shows the ratio of potential storage capacity based on the identified suitable areas (Q_{PTES}) to the annual heat demand of district heating areas (Q_S). It can be seen that, in the progressive scenario, the number of DHAs without suitable PTES areas is 86, while this increases to 132 in the conservative scenario. Most of the qualified DHAs have more than enough land available to build a PTES with a capacity exceeding the annual heating demand (R>1). The largest bubble is for Stockholm and the next two largest are Gothenburg and Malmö. It is clear that most DHAs have theoretically more potential PTES storage capacity than annual demand, while a smaller yet significant number with no possibility. Virtually none have an R-value between 0 and 1.

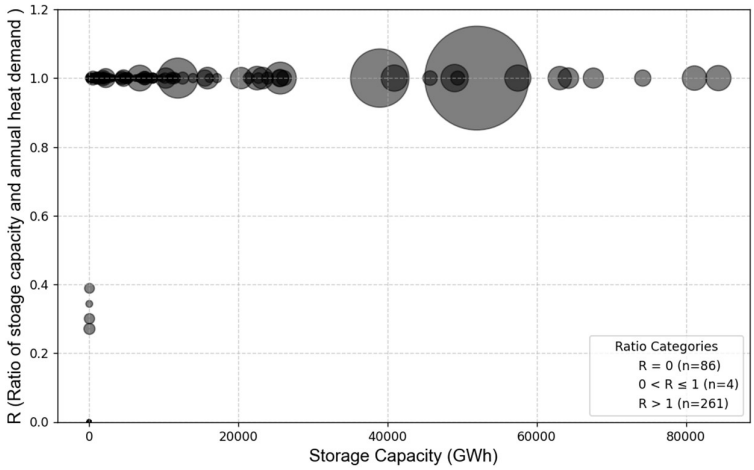

Figure 39 Ratio of storage capacity to annual heat demand for scenario 4. Maximum value of R is capped to 1. The bubble size corresponds to the annual heat demand of DHA.

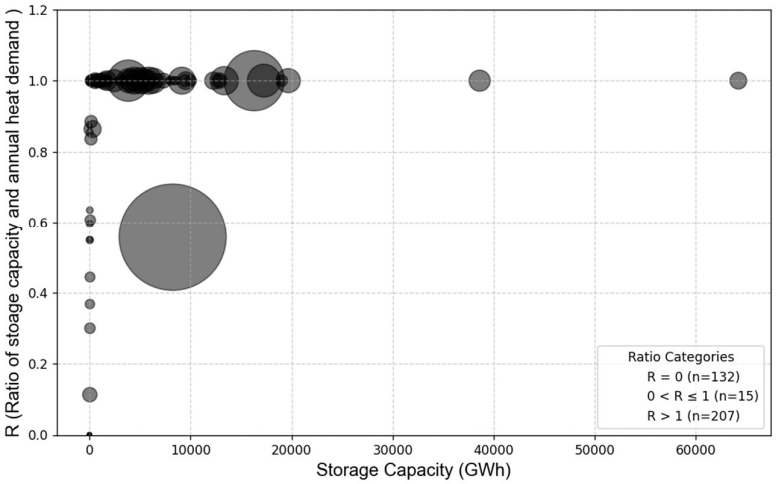

Figure 40 Ratio of storage capacity to annual heat demand for scenario 1. Maximum value of R is capped to 1. The bubble size corresponds to the annual heat demand of DHA.

For the generated suitable areas in the project, the district heating area labelled "Örestadsområdet*", consisting of 18 unique DHS assembled under 15 unique DHA, has by far the largest total suitable area in scenario 1. It has 806 km^2 of suitable areas as shown at left in Figure 41 and 1,274 km^2 in scenario 4 (left in Figure 42). See also Figure 36 for map illustration of the area, where it is obvious that there most of the total area is potentially suitable for PTES.

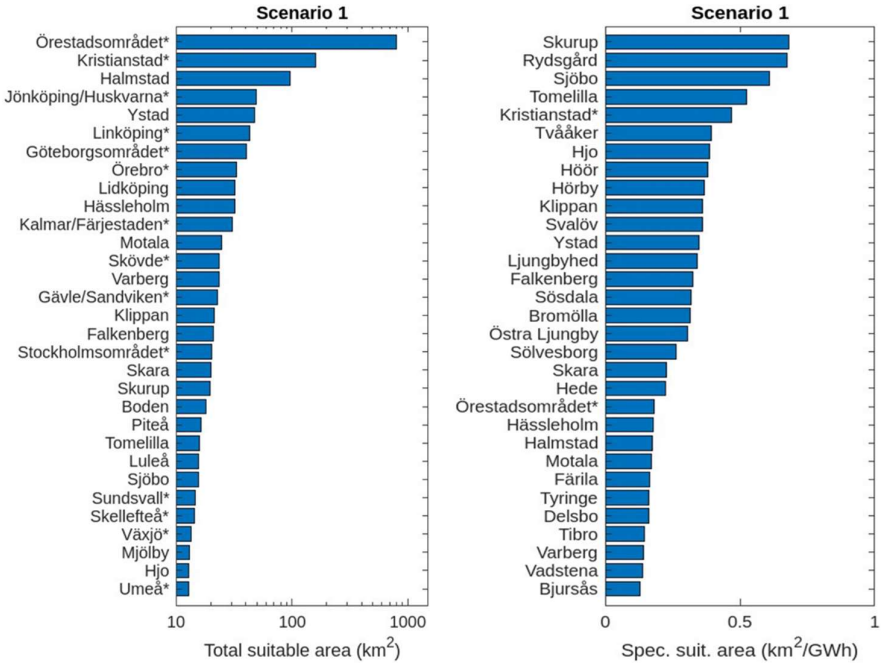

Figure 41. Final results for scenario 1with total sum of suitable areas (km^2) per aggregated district heating areas, at left, and with ratio of total sum of suitable areas (km^2) by sum of annual district heat deliveries (GWh/a) per aggregated district heating areas, at right, both sorted by descending order from highest to lowest values.

Gävle/Sandviken*, at some 23 km^2, appears as the first aggregated area with a more northern location (15th largest area). In scenario 4, on the other hand, as outlined below in Figure 42, it can be seen that northern locations, e.g. Umeå (210 km^2), Luleå (202 km^2), as well as several other, clearly benefit from the inclusion mainly of conifer forest and artificial land areas, which places them at 2nd and 3rd place respectively. This shows that scenario 1 is not so suited to forested areas.

Looking at average sizes of the suitable areas, we find that for the 3819 suitable areas in scenario 1 the average size is 0.53 km^2, while it is 1.04 km^2 for the 4958 identified suitable areas in scenario 4. The 224 aggregated

district heating areas in scenario 1 have an average of 9.1 km^2 per DHA*, whereas the 269 DHA* in scenario 4 have 19.1 km^2 average.

Additionally, the total sum of suitable areas per aggregated DHA with the sum of annual district heat deliveries associated with these is shown on the right side of Figure 41 and Figure 42. For scenario 1, it can be seen that five Skåne län district heating areas (Skurup, Rydsgård, Sjöbo, Tomelilla, and Kristiandstad*) top the list with values in the range of 0.47 to 0.68. A large ratio in this context would indicate a large likelihood of being able to find suitable areas for pit storages that can support the district heating systems within the aggregated area. In scenario 4 this situation is not changed dramatically, although a few northern locations, for example Sveg (0.59) and Piteå (0.50), make it into the top 15, an interval with values ranging from 0.46 to 0.92.

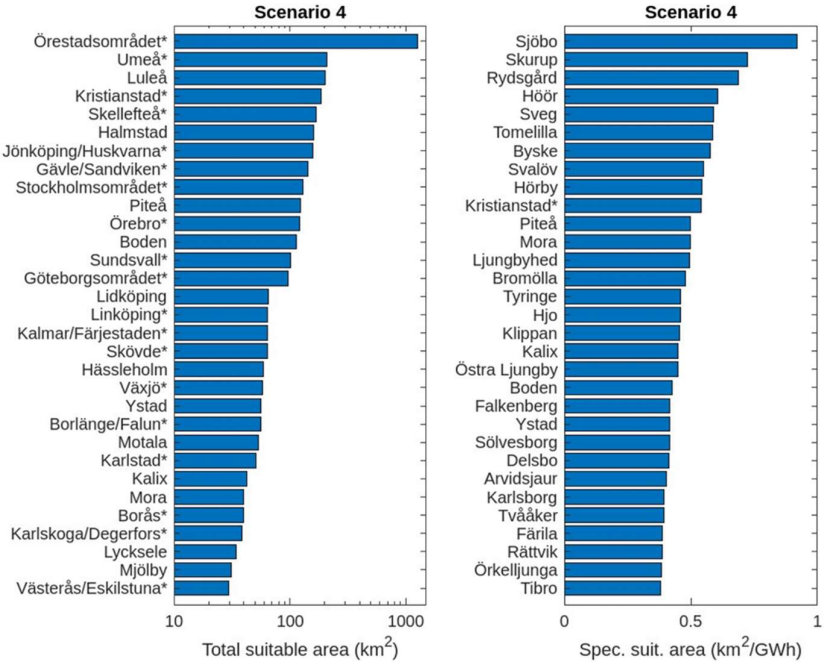

Figure 42. Final results for the 4th scenario with total sum of suitable areas (km^2) per aggregated district heating areas, at left, and with ratio of total sum of suitable areas (km^2) by sum of annual district heat deliveries (GWh/a) per aggregated district heating areas, at right, both sorted by descending order from highest to lowest values.

The character of identified suitable areas can be further described by displaying the distribution of suitable area sizes (polygon areas) by total bin areas, as shown for Örestadsområdet* in Figure 43 for scenario 1 and 4. In both scenarios it can be seen that a majority of the total area is found in very large polygons (probably just one polygon), of an area of above 100 km^2 or more.

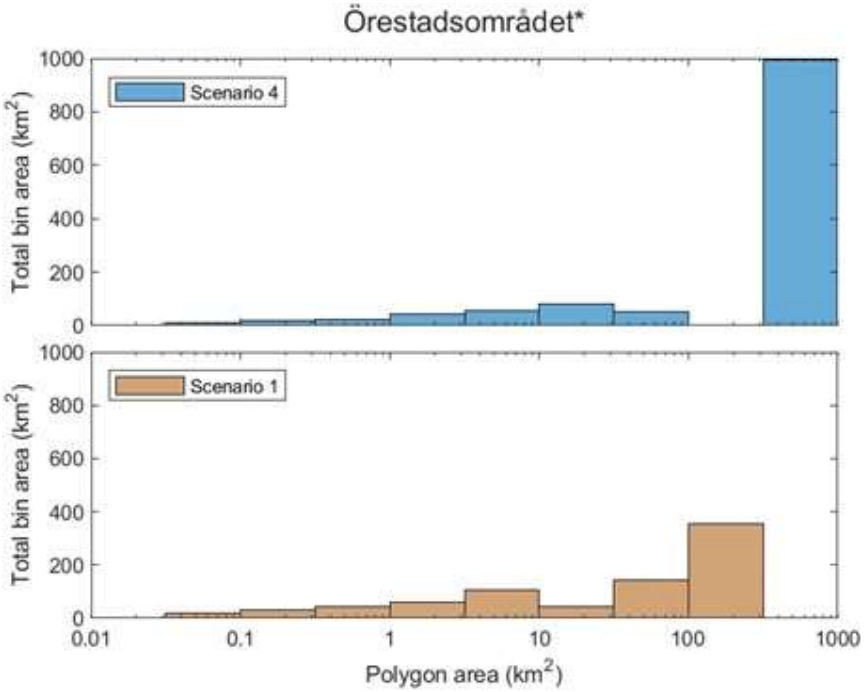

Figure 43. Distribution of suitable area polygon areas (km^2) in the 1st scenario (bottom) and the 4th scenario (top) for the aggregated district heating area of Örestadsområdet*.

In other aggregated district heating areas, for example the larger area of Stockholm with surroundings, "Stockholmsområdet*, as shown in the upper diagram of Figure 44, the situation is very fragmented for scenario 1. The majority of the total suitable areas are found in polygons within the area range 0.1 – 0.3 km^2. For scenario 4, the fragmentation is of the same level as for the aggregated area of Göteborgsområdet*, as depicted in the lower diagram of Figure 44, where the majority of the total area is found in polygons with areas in the range of 1 - 3 square kilometres. Similar figures can be found in the Appendices for Sundsvall*, Kristianstad* and Umeå*.

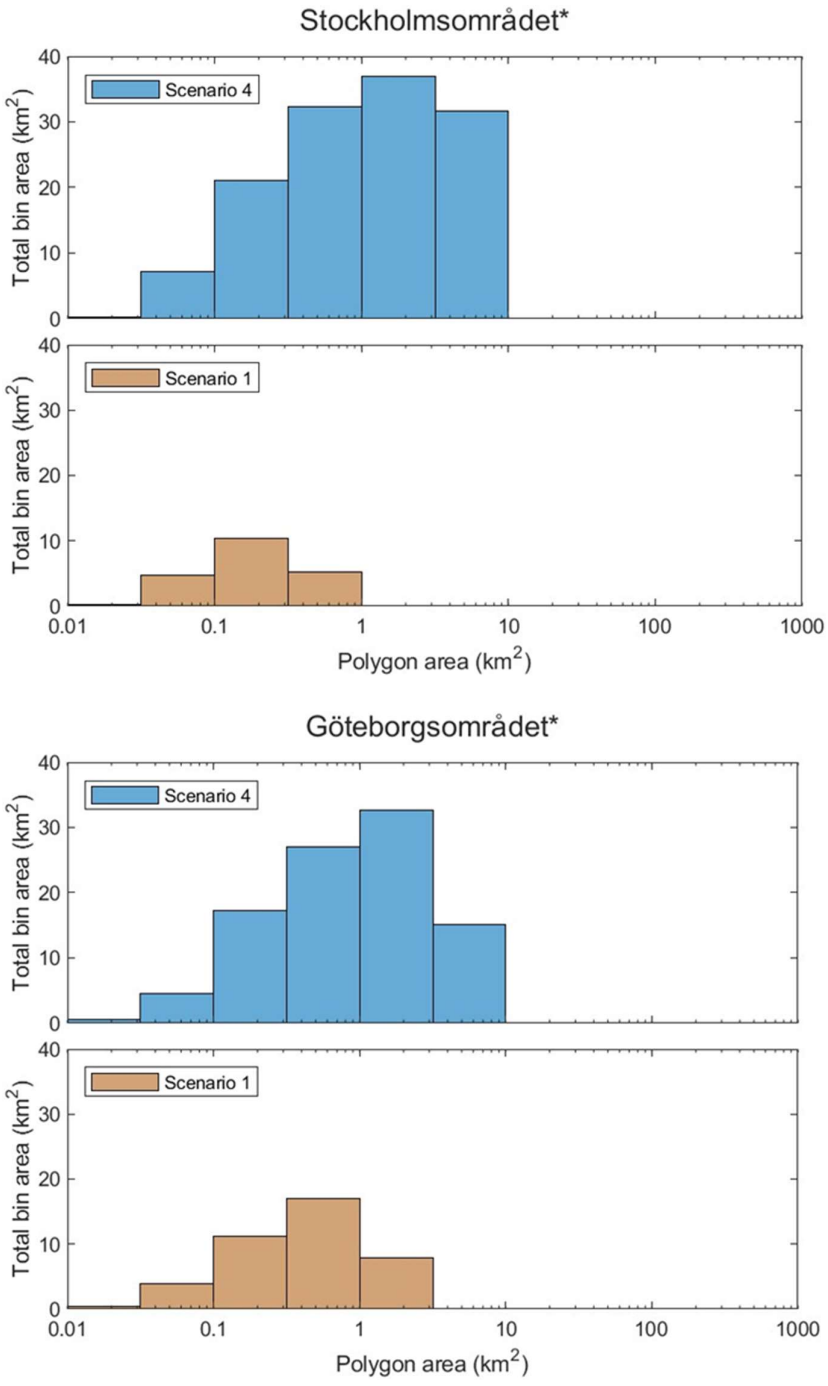

Figure 44. Above: Distribution of suitable area polygon areas (km^2) in the 1st scenario (bottom) and the 4th scenario (top) for the aggregated district heating area of Stockholmsområdet*. Below: Similarly, for Göteborgsområdet*.

A major finding and conclusion from the screening process is that there is a distinct general difference in the availability of suitable areas for the construction and installation of large-scale PTES in Sweden, a difference of latitude one might say, since southern parts of the country display more promising potential than their northern counterparts, as illustrated in the scenario diagram of Figure 45.

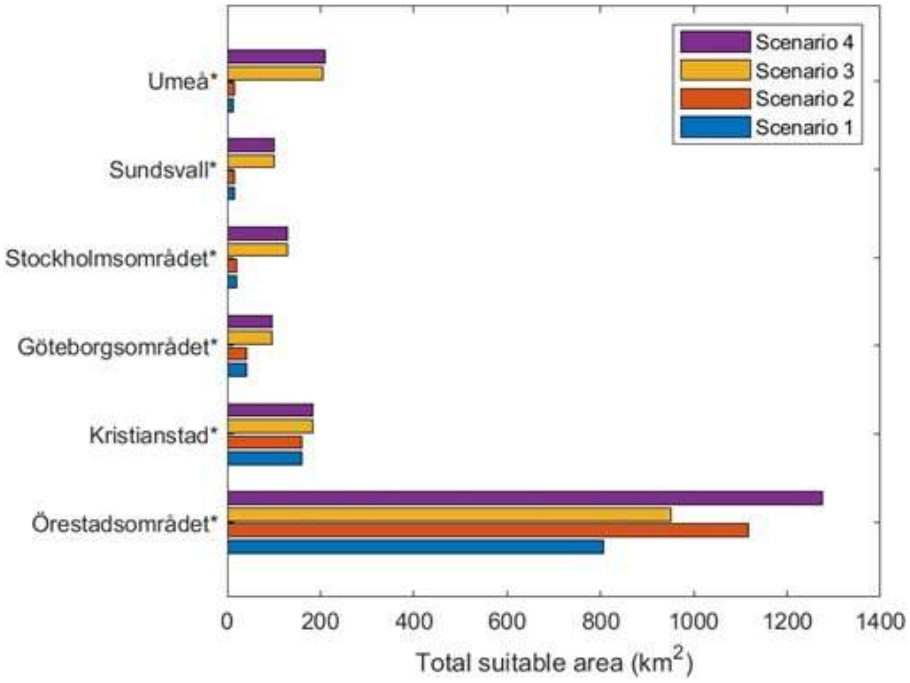

Figure 45. Total suitable area for all four scenarios and six aggregated district heating areas representative of a north-south distribution.

This difference might not exist locally, since the results indicate feasible conditions also in many northern locations. However, generally speaking, and especially if not permitting any exploitation of broad-leaved, conifer, and mixed forest areas, as well as no industrial and commercial areas, airports, ports, road and rail networks etc., the likeliness of finding a suitable PTES land area in the north is considerably smaller than finding one in more southern locations.

The influence of the applied screening criteria concerning soil type (screening dataset 3), on the one hand, and available land (screening dataset 4), on the other hand, are of more relative significance the further north a DHA is located. The differentiated screening criteria for soil type, where the difference merely consisted in the allowance of certain courser fractions of silt and clay, had a minor influence, why the main result scenarios for the national potential may be found in scenarios 1 and 4 respectively.

Potential for Solar and Pit Stores in Sweden

As part of the update of the database of district heating systems, rough estimations of requirements in terms of solar collector areas, PTES volumes as well as surface area were made for all DHS for nominal solar fractions of 20%, 40% and 60% (see method description p18). In order to estimate the technical potential of solar and PTES systems a number of steps in the calculation were made:

1. All DHA that have suitable areas that are larger than the area required for the PTES for the 20%/40%/60% scenarios are considered.

2. Any PTES volume that is less than 50 000 m^3 is filtered out of the analysis because below this threshold other kinds of storage are just as economically viable.

3. All of the scenarios that are left are assumed to produce the 20%/40%/60% fractions of the heat demand of the individual DHAs, independent of what other heat sources are available.

4. The number of DHAs with viable systems and the aggregated supplied heat was calculated.

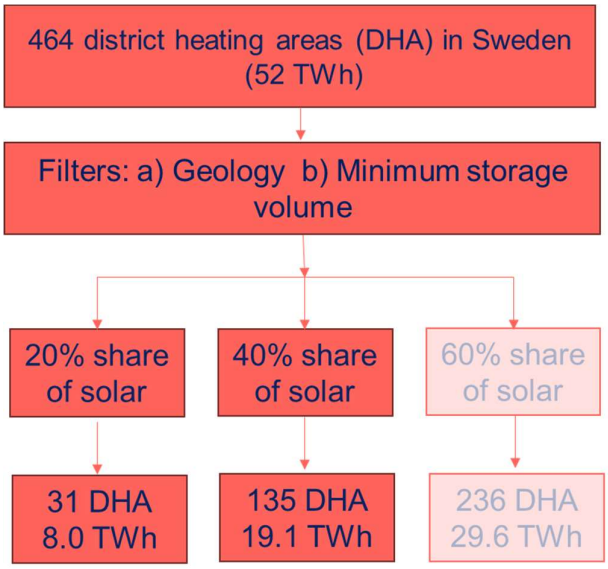

Figure 46. Estimated solar energy contributions and number of systems if all DHS that have enough suitable areas for PTES actually build solar thermal and PTES systems that supply 20%, 40% or 60% of the total heat demand of the DHS. For the progressive screening scenario 4.

The results of this estimate for the optimistic (progressive) scenario 4 can be seen in Figure 46. It shows that only 31 DHAs can have a solar and PTES system that supplies 20% of the heat demand of the DHA. The number is small as nearly all smaller DHAs have too little heat demand to require a PTES larger than 50 000 m^3, the threshold set in the analysis. However, these 31 systems provide a lot of heat as they are for moderate and large DHAs, in all 8.0 TWh (15% of total district heating demand in Sweden).

For the 40% solar fraction there are a lot more DHAs that require more than the threshold volume for PTES, in all 135 DHAs (29% of all DHAs). The systems provide in total 19.1 TWh solar thermal heat (36% of all district heat in Sweden). The values for the nominal 60% are of course significantly large, in total over half the total demand in Sweden. However, the simulations in the case studies have shown that 60% is in practice difficult to achieve, especially in the far north of Sweden and would require much larger PTES as well as collector areas than calculated based on the thumb rules from literature. Therefore the values for 60% solar fraction are toned down in the figure.

Discussion

In a report from 2019 that investigated six Swedish district heating type systems and possible seasonal heat storage solutions for them, Sköldberg et al. [51] investigated at what storage size relative to annual district heat loads, the cost-benefit would be the greatest. According to their findings, a 10% heat storage capacity relative to the annual district heat delivery volume was, perhaps not the most cost-effective, although close to, but indeed the most prevalent. It is, however, not clear whether this value holds when the energy source is from solar collectors. Both the energy costs and the cost for PTES have increased in the last five years. The case study for Söderhamn showed that a solar heating system with PTES and heat pump that supplies 29% of the total demand has a lower heat cost (LCOH of 75 €/MWh) than a smaller system providing 10% of the total demand using a tank storage (LCOH of 81 €/MWh).

On one hand, the calculations for the combined potential of solar collectors with associated pit storages utilised fixed fractions (20%, 40%, and 60%). On the other hand, the spatial analysis of a national PTES potential did not concern itself with this ratio. Hence, the screening process of this work has indeed identified suitable areas where pit storages could be built, as well as estimated sizes and capacities of corresponding storages that could fit on these areas.

What is the usefulness for a DHS operator of knowing that there is enough available land (several square kilometres) to build, let's say, a 5 million cubic meter storage nearby, when perhaps all that is needed – for a cost-effective storage size relative to the given load – is a couple of hectares. Here, all we wanted to be able to say is whether or not, yes or no, there is enough land to build a storage of at least 50,000 m^3. Today, real world large-scale PTES sites range from about this lower end up towards volumes in excess of 200,000 m^3, with Vojens in Denmark as the currently largest PTES in the world at 210,000 m^3.

In the post-treatment of identified candidate suitable areas, we introduced the concept of roundness in order to discard identified areas with undesired shape (polygons with total areas at or above the general project threshold of 15,000 m^2 but with shapes that would not allow a square with this minimum area requirement to fit inside of it). For this study, in the quota expression to determine if a candidate area would be sufficiently large to qualify as a suitable area, we took a conservative stand by having the denominator roundness factor squared. In another context, with a less conservative approach, a plane denominator roundness factor could perhaps suffice.

The spatial analysis is based on the datasets explained in the previous sections. However, there are uncertainties and limitations due to data unavailability that are not addressed in the spatial analysis. One such factor is the groundwater table and groundwater flow, which are crucial considerations for constructing a PTES. If the groundwater table is not lower than the PTES depth, additional costs would be incurred to lower the groundwater level before and during construction. Moreover, groundwater flow could carry heat away from the sides and bottom of the PTES, increasing heat losses. Both of these factors are not accounted for in the spatial analysis.

Another simplification in the analysis is the assumption that soil type remains uniform throughout the PTES depth, as depicted in soil maps. In reality, soil types can vary at different depths, and certain soil layers might not be suitable for PTES embankments. This could necessitate the removal and replacement of unsuitable soil, further increasing the costs. Therefore, for detailed feasibility of PTES for a specific site, a next-level analysis is required that involves making site boreholes and another tests to check whether the potential site, identified here as a suitable area (SA), is in fact feasible from a practical point of view. Land ownership is another issue that is of practical relevance, and for the case of Enköping meant that several suitable areas were not possible in practice. Additionally, the estimation of the potential for solar and pit storage systems assumes that all systems with suitable areas have systems, irrespective of what other heat sources there are in the system.

However, the fact that the identified suitable areas can store more heat that the annual heat demand for most district heating areas means that the potential is high, even if the majority of suitable areas is shown in practice to not be feasible. It is then an economic question as to whether the site is close enough to a good connection point in the network.

The three case studies are distinct from each other, therefore, direct comparison of LCOH between three cases is not recommended. However, a few conclusions can be made from results.

Annual heat demand has significant impact on the LCOH. Comparing Råneå and Söderhamn, as shown in Table 23, it is evident that the system designed for summer demand, which uses TTES, has a higher LCOH than the system that includes PTES. This is primarily due to the higher cost associated with TTES compared to PTES, as well as the higher specific heat cost of solar collectors resulting from the smaller collector areas required for summer demand.

Additionally, the LCOH comparison between both case studies clearly highlights the economies of scale, where a larger collector area and storage volume (as seen in Söderhamn/Härnösand) have a significant positive effect on reducing LCOH.

Table 23: Comparison of LCOH for Råneå and Söderhamn

	Råneå	**Söderhamn**
Annual heat demand GWh	25.9	143
With TTES		
Collector area [m^2]/storage volume [m^3]	13000/3000	35000/7000
LCOH (20y, 5% IR) [€/MWh]	100	81
With PTES		
Collector area [m^2]/storage volume [m^3]	25000/25000	85000/200 000
LCOH (20y, 5% IR) [€/MWh]	86	75

Both the Söderhamn and Härnösand case studies face pipe size limitations, requiring the integration of heat pumps in their systems. For a 20-year period with a 5% interest rate, the LCOH for Härnösand is 86 €/MWh, whereas for Söderhamn, it is 75 €/MWh.

One reason for the higher LCOH in Härnösand is the larger storage capacity required for the same collector area. This can be attributed to industrial waste heat availability during summer in Härnösand, which reduces the summer heat load for solar system, as shown in Figure 47. Assuming the waste heat is preferred to solar heat and always used, an additional PTES volume is required. In contrast, Söderhamn has higher summer demand, reducing the necessity for additional HP capacity and large PTES storage volumes.

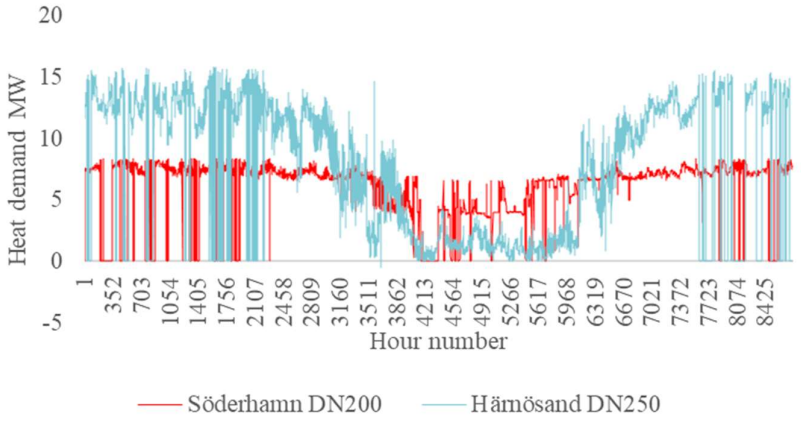

Figure 47: Heat demand variation, restricted by flow and temperature, for Härnösand and Söderhamn.

The costs of PTES and solar collectors have increased in recent years due to inflation and due to costs related to technological development of the PTES lid that make it more robust and thus increasing lifetime and operation costs. This has led to higher PTES costs compared to benchmark costs for the same storage volumes from a few years ago [52]**.** The key conclusion from the economic analysis is that the cost feasibility of the system is highly dependent on the interest rate and economic lifetime. Unlike boiler base systems, a solar thermal system with PTES requires high upfront capital investment but has minimal operational costs, as it utilizes free solar energy. Therefore, the return on investment depends on long-term energy savings and financing conditions. The availability of low-interest loans as part of government support policies, along with a long-term investment vision from utilities, would significantly improve the financial viability of PTES as well as solar collectors.

The integration of HP is technically and economically advantageous especially in return to supply integration mode, as seen in both Härnösand and Söderhamn case. Currently, there are few suppliers that offer heat pumps capable of delivering temperatures up to 95°C [53]. The heat pumps considered for both case studies are theoretical, and their actual commercial availability, suppliers, detailed technical constraints have not been extensively studied in this project. Heat pumps with higher temperature capabilities is an area of development, especially towards industrial applications, and new commercial products are expected in the future.

If PTES and SC are integrated near the boiler such as in Råneå, the flow direction in the network remains unchanged since the return water is preheated before reaching the boiler. However, if the integration is at the periphery of the network (such as in Härnösand and Söderhamn), the flow in the network reverses. This impact of flow reversal on hydraulic parameters and the need for additional controls to maintain network operation needs further evaluation as it was not covered in this project.

In addition to its integration with solar collectors, as analyzed in this project, PTES can also serve as a valuable flexibility resource in existing heating systems. Several possibilities exist with PTES in this regard such as: a) storing waste heat for both short- and long-term use; b) optimizing CHP plant operations by storing surplus heat generated from CHP plants from one period to another (short or long term), enabling a more strategic dispatch of electricity to the grid when el. prices are higher. c) PTES integration with heat pumps can allow participation in the grid balancing market, creating opportunities for additional savings. There was no time left in the project to evaluate this, but this should be evaluated in future studies to assess their feasibility, economic impact, and integration challenges

Conclusions

In this project there have been four main parts: an update of a database of district heating systems; a geographically based screening process for identifying suitable areas for pit stores within a reasonable distance of the district heating systems; an estimation of the potential for PTES within these areas and for solar and PTES systems; case studies of solar and PTES systems for three district heating systems. The conclusions are separated into these four different areas:

Updated database of district heating systems:

- Several sources were used to update an existing database of district heating systems, resulting in a complete list that is consistent with the reported total annual heat supply from district heating (52.7 TWh).
- The new database has 547 identified district heating systems. For all of these, the required solar collector area, PTES volume and land areas were calculated for systems providing 20%, 40% and 60% of the heat demand of the district heating system. A tabular database in excel is the result of this (not published).
- Geographical areas for these systems were created based on heat densities and calibrated threshold values for viability for district heating. This resulted in 464 district heating areas, fewer than the 547 systems as some areas are supplied by several systems.
- Dynamic buffer areas were defined and created for the screening process for identifying suitable areas for PTES. As these are geographically larger, these buffer areas around each district heating area can overlap. These buffer areas are 9% of Sweden's area.

Screening for suitable areas for PTES:

- The screening process was made based on openly available geographical data, mostly from SGU: ground elevation, soil type and depth, land use category.
- Criteria for slope, soil type, soil depth and land use type were defined and used for the screening process. Two variants of criteria for both land use type and soil type were defined giving conservative or progressive (optimistic) results, and thus there are four scenarios for the screening process.
- A "roundness" criterion was developed and used to eliminate possible areas that are long and thin and thus not realistic for PTES.

- Important factors for PTES economic viability such as ground water depth and water flow had no data readily available and so could not be used in the screening. The aggregated results should therefore be considered as overestimations. It is not possible to quantify this overestimation.
- Not surprisingly for a large country like Sweden, there are large geographical variations. In general, however, there are more suitable areas for PTES in the south than in the north.
- The majority of district heating areas have significant amounts of suitable areas. For scenario 1 (conservative), only 136 district heating areas have no suitable areas while in the progressive scenario this figure is 86. The main difference between the two scenarios is that scenario 4 allows most forest areas while scenario 1 does not.
- In terms of storage capacity, all the other district areas have a potential heat storage capacity in the suitable areas for PTES that is (far) larger than the annual district heating demand in the area. Thus, it is likely that good sites for PTES can be found in most of these, despite the fact that there are several practical aspects that mean that many of these would in practice not be suitable.

Estimation of potential for solar and PTES in Sweden:

- Limited to systems with a minimum PTES size and the district heating areas with enough suitable area for PTES identified in the screening process, delivered solar heat for 20%, 40% and 60% solar fractions was calculated.
- For the progressive scenario 4, 31 district heating areas could have solar and PTES with a solar fraction of 20%, providing 8.0 TWh – assuming that all of these possible systems are built. This is 15% of total demand in Sweden's district heating systems. For 40% solar fraction, the figures are 135 district heating areas and 19.1 TWh (36% of total demand).
- Values for 60% solar fraction are not reliable as the results from the case studies show that this level is difficult to achieve in the north of Sweden.
- In order to make sure that a site is in fact viable for a PTES, further on-site examinations for amongst other things ground water and its flow as well as uniformity of soil type over the whole site are necessary.

Case studies:

- Of the seven district heating companies that were interested in having techno-economic studies made, only three had suitable sites for PTES based on the screening process and land ownership.
- In two of the three cases, the site for the PTES was on the periphery of the district heating area some distance away from a connection point with sufficient pipe size in the network. This existing pipe in the network limits the heat discharge capacity from the store and thus the size of the solar and PTES system, i.e. solar fraction. It is likely that a majority of the district heating areas would fall into this category.
- The same two cases have exhaust gas condensation, and the solar heat cannot be added to the return pipe but rather needs to be added to the supply pipe at the current operating temperature. The maximum temperature of 90°C allowed in the PTES means that an additional heat pump to boost this temperature results in a better and more cost-effective system.
- The cost of heat (LCOH) was calculated for a number of scenarios for each of the three cases, the scenarios being dependent on the wishes of the district heating companies and the possible location of the PTES.
- With current cost data the LCOH is slightly higher than the existing heating costs for all three cases. However, if there is an annual increase in fuel costs of 1% or more over the lifetime of the system, the solar and PTES system in Söderhamn has a positive net present value.
- The lowest LCOH of the scenarios studied was 75 €/MWh for the solar, PTES and heat pump system in Söderhamn that delivers 29% of the district heating areas annual demand.
- Scale of system impacts the LCOH significantly, as shown in the case studies. However, it is difficult in practice to achieve large solar fractions of 60% in the north of Sweden due to the extreme mismatch of solar resource and heat loads and thus needs for storage.
- LCOH values are not surprisingly very dependent on the available interest rate and economic lifetime chosen for a project. Experiences from Denmark emphasize the need for constructive discussions with banks to get lower interest rates.
- If a market is to be created, subsidies or loans with guaranteed low interest rates would be needed.

Future work

This project has generated a lot of theoretical results that show that there is a large theoretical potential for PTES and the combination with solar collectors. More detailed analyses of the use of the PTES for flexibility on the electricity markets as well as for co-generation is needed to understand the full potential. More studies on the benefits and limitations of heat pumps in the system are also needed as well as the practical limitations of connecting to parts of the network where reversed flow is required.

An important step would, however, be to build a first system in Sweden, thereby generating a lot of detailed knowledge as well as experience in the practical aspects that do not exist in Sweden. The large potential and close to parity heat costs suggest that this a logical next step.

Publications

The following scientific articles were written and published during the project, but do not contain more information than is contained in this final report. A final journal article on the screening process and results will be submitted just after the projects end, but it will also not contain anything in addition to this report.

Saini, P., et al., *Evaluating the Potential for Solar District Heating with Pit Thermal Energy Storage in Sweden*, in *International Sustainable Energy Conference - Proceedings*. 2024: Graz, Austria. Available at (2024-07-08): https://www.tib-op.org/ojs/index.php/isec/article/view/1214

Persson, U., et al. *Data categories and selection criteria for an evaluation of the potential for solar district heating with pit thermal energy storage in Sweden*. in *Book of Abstracts: 10th International Conference on Smart Energy Systems*. 2024. 10-11 September 2024, Aalborg, Denmark: Aalborg University and Energy Cluster Denmark. Available at (2025-03-17): https://urn.kb.se/resolve?urn=urn:nbn:se:hh:diva-55640.

References

1. Energimyndigheten, *Solvärme i Sverige - En studie med fokus på potential, ekonomi och bidrag till energi- och klimatmål*, in *ER*. 2021, Energimyndigheten: Eskilstuna. p. 60.
2. Perez de la Mora, N., et al., *Solar district heating and cooling: A review.* International journal of energy research (Print), 2017: p. 1-23.
3. Gao, L., J. Zhao, and Z. Tang, *A Review on Borehole Seasonal Solar Thermal Energy Storage.* Energy Procedia, 2015. **70**: p. 209-218.
4. Xiang, Y., et al., *A comprehensive review on pit thermal energy storage: Technical elements, numerical approaches and recent applications.* Journal of Energy Storage, 2022. **55**: p. 105716.
5. Helden, W., et al., *Giga-scale thermal energy storage for renewable districts - Publishable Final Report*. 2021.
6. EU-Treasure. *Demonstrating large pit thermal energy storages*. 2024 [cited 2024 2024-03-03]; Available from: https://www.treasure-project.eu/.
7. EU-Uses4Heat. *Underground Large Scale Seasonal Energy Sotrage for Decarbonised and Reliable Heat*. 2024 [cited 2024 2024-03-03]; Available from: https://www.uses4heat.eu/the-project/.
8. EU-Interstores. *International Innovation Network for the Development of Cost- and Environmentally Efficient Seasonal Thermal Energy Storages*. 2024 [cited 2024 2024-03-03]; Available from: https://interstores.eu/.
9. IEA-ES-Task45. *Accelerating the Uptake of Large Thermal Energy Storages*. 2024 [cited 2024 2024-03-03]; Available from: https://iea-es.org/task-45/.
10. HRE4. *Heat Roadmap Europe Resource Center*. 2020. Available at: https://heatroadmap.eu/.
11. Möller, B., et al., *The Pan-European Thermal Atlas (Peta, version 5.2)*. 2022, Developed as part of the sEEnergies project. Europa-Universität Flensburg: Flensburg. Available at (2022-10-01): https://euf.maps.arcgis.com/apps/webappviewer/index.html?id=8d51f3708ea54fb9b732ba0c94409133.
12. HUDHC, *Halmstad University District Heating and Cooling Database_version 5 (2016 update by date 2019-09-30)*. 2019: Halmstad University, Sweden.
13. Danish Energy Agency, *Technology Data – Energy storage*. 2018: Version number: 0009. Danish Energy Agency and Energinet. Available at (2025-03-12): https://ens.dk/en/analyses-and-statistics/technology-data-energy-storage.
14. PlanEnergi, *SUNSTORE 3, Phase 2, Implementation*. Final Report. PlanEnergi. Available at (2025-03-12): https://planenergi.eu/wp-content/uploads/2023/09/SUNSTORE-3-Phase-2-Implementation.pdf.
15. Dannemand Andersen J., Bødker L., and Jensen M.V. *Large Thermal Energy Storage at Marstal District Heating*. in *Proceedings of the 18th International Conference on Soil Mechanics and Geotechnical Engineering, Paris*. 2013. Available at (2025-03-12): https://www.cfms-sols.org/sites/default/files/Actes/3351-3354.pdf.
16. Saini, P., et al., *Evaluating the Potential for Solar District Heating with Pit Thermal Energy Storage in Sweden*, in *International Sustainable Energy Conference - Proceedings*. 2024: Graz, Austria. Available at

(2024-07-08): https://www.tib-op.org/ojs/index.php/isec/article/view/1214.
17. sEEnergies, *sEEnergies - Quantification of Synergies between Energy Efficiency First Principle and Renewable Energy Systems*. 2020: Horizon 2020 Project No. 846463. Available at (2021-06-21): https://www.seenergies.eu/.
18. sEEnergies Open Data Hub, *sEEnergies Open Data Hub. Referenced dataset: "D5 1 District Heating Areas"*. 2022: Europa-Universität Flensburg, ArcGIS Online. sEEnergies: Quantification of synergies between Energy Efficiency first principle and renewable energy systems. Available at (2022-05-28): (https://s-eenergies-open-data-euf.hub.arcgis.com/search?categories=d5.1).
19. PETA 4.3. *Pan-European Thermal Atlas 4 (PETA 4.3). Dataset: "Heat Demand Densities 2015 (HRE4)"*. 2018.
20. Persson, U., B. Möller, and E. Wiechers, *Methodologies and assumptions used in the mapping. Deliverable 2.3: A final report outlining the methodology and assumptions used in the mapping. August 2017*. 2017: Heat Roadmap Europe 2050, A low-carbon heating and cooling strategy. Available at (2018-12-10): (https://heatroadmap.eu/wp-content/uploads/2018/11/D2.3_Revised-version_180928.pdf).
21. Swedenergy, *Energy supply to cogeneration, district heat production, and district heat deliveries 2015 (SE: Tillförd energi till kraftvärme och fjärrvärmeproduktion och fjärrvärmeleveranser 2015). Downloaded dataset: Tillförd energi till kraftvärme och fjärrvärmeproduktion och fjärrvärmeleveranser 2015.xlsx*. 2024: Swedenergy - Energiföretagen Sverige. Available at (2024-02-26): https://www.energiforetagen.se/statistik/fjarrvarmestatistik/tillford-energi/tillford-energi-till-fjarrvarme-och-kraftvarme/.
22. Energimarknadsinspektionen, *Tekniska uppgifter - fjärrvärme (Technical information - district heating)*. 2024: Energimarknadsinspektionen (Energy Market Inspectorate). Available at (2024-03-01): https://ei.se/om-oss/statistik-och-oppna-data/tekniska-uppgifter---fjarrvarme.
23. Swedish Energy Markets Inspectorate, *Delivered heat by price area, technical data. Ver: 3.00, Datum: 221129 (SE: Levererad värme per prisområde, tekniska uppgifter. Ver: 3.00, Datum: 221129). Downloaded dataset: Levererad värme per prisområde tekniska uppgifter - fjärrvärme.xlsx*. 2023: Energimarknadsinspektionen (Ei). Swedish Energy Markets Inspectorate. Available at (2024-02-26): https://ei.se/om-oss/statistik-och-oppna-data/tekniska-uppgifter---fjarrvarme.
24. Swedenergy, *Personal communication with N. Burstein 2023-03-16. Shared internal dataset: District heat deliveries per location and per year 1996-2021.xlsx (SE: Fjärrvärmeleveranser per ort och per år 1996-2021.xlsx)*. 2023: Swedenergy - Energiföretagen Sverige.
25. Fleiter, T., et al., *D5.1: Excess heat potentials of industrial sites in Europe (Revised version). Documentation on excess heat potentials of industrial sites including open data file with selected potentials*. 2020: sEEnergies - Quantification of synergies between Energy Efficiency first principle and renewable energy systems. DOI: (https://doi.org/10.5281/zenodo.4785411).

26. European Commission: Joint Research, C., et al., *The European settlement map 2017 release – Methodology and output of the European settlement map (ESM2p5m)*. 2016: Publications Office.
27. JRC, *European Settlement Map (ESM). Copyright European Commission, European Settlement Map 2016*. 2017: Joint Research Centre, Institute for the Protection and Security of the Citizen, Global Security and Crisis Management Unit. European Commission, Brussels. Retrieved originally 2017-07-21 from (https://land.copernicus.eu/pan-european/GHSL/european-settlement-map/EU%20GHSL%202014?tab=download). Updated address (2024-03-04): (https://ghsl.jrc.ec.europa.eu/datasets.php).
28. Geonames, *Features for country with iso code SE (Download date: 2023-05-23). Licensed under Creative Commons BY 4.0 (CC BY 4.0). Link to licence: https://creativecommons.org/licenses/by/4.0/. No changes made.* 2023: Opendatasoft. St. Gallen, Switzerland. Available at: https://download.geonames.org/export/dump/.
29. IEA, *World Energy Balances (2019 Edition)*. 2019: International Energy Agency, Paris.
30. Persson, U. and S. Werner, *Quantifying the Heating and Cooling Demand in Europe. Work Package 2. Background Report 4*. 2015: Stratego: Multi-level actions for enhanced Heating & Cooling plans. Project No: IEE/13/650. Available at (2024-02-23: https://heatroadmap.eu/wp-content/uploads/2018/09/STRATEGO-WP2-Background-Report-4-Heat-Cold-Demands.pdf).
31. Persson, U., et al., *Heat Roadmap Europe: Heat distribution costs.* Energy, 2019. **176**: p. 604-622.
32. sEEnergies Open Data Hub, *sEEnergies Open Data Hub. Referenced datasets: "BL2015 HD100 total"*. 2022: Europa-Universität Flensburg, ArcGIS Online. sEEnergies: Quantification of synergies between Energy Efficiency first principle and renewable energy systems. Available at (2022-05-28): (https://s-eenergies-open-data-euf.hub.arcgis.com/maps/886d9e7864ca4c53a67172d523a588c0/about).
33. Nielsen, J.E. 2012.
34. Dadi Sveinbjörnsson, P., Denmark Niels From, PlanEnergi, Denmark Per Alex Sørensen, PlanEnergi, Denmark, et al. 2020 [cited 2025; Available from: https://www.greenonetec.com/en/.
35. *Technical report on model validation, cost functions and results of an exemplary base case study*.
36. 2025; Available from: https://www.trnsys.com/.
37. Xiang, Y., et al., *Assessment of inlet mixing during charge and discharge of a large-scale water pit heat storage.* Renewable energy, 2023. **217**: p. 119170.
38. Volkova, A., H. Koduvere, and H. Pieper, *Large-scale heat pumps for district heating systems in the Baltics: Potential and impact.* Renewable & sustainable energy reviews, 2022. **167**: p. 112749.
39. Østergaard, P.A. and A.N. Andersen, *Economic feasibility of booster heat pumps in heat pump-based district heating systems.* Energy (Oxford), 2018. **155**: p. 921-929.
40. Geoffroy Gauthier, P. *HEATSTORE Benchmarking, and improving models of subsurface heat storage dynamics*. 2020.

41. Tosatto, A., A. Dahash, and F. Ochs, *Simulation-based performance evaluation of large-scale thermal energy storage coupled with heat pump in district heating systems.* Journal of energy storage, 2023. **61**: p. 106721.
42. Persson, U., et al. *Data categories and selection criteria for an evaluation of the potential for solar district heating with pit thermal energy storage in Sweden*. in *Book of Abstracts: 10th International Conference on Smart Energy Systems*. 2024. 10-11 September 2024, Aalborg, Denmark: Aalborg University and Energy Cluster Denmark. Available at (2025-03-17): https://urn.kb.se/resolve?urn=urn:nbn:se:hh:diva-55640.
43. Lantmäteriet, *Höjddata, grid 50+ NH 2020 (tif) Elevation data, grid 50+*. 2023: © Lantmäteriet. GSD Geografiska Sverigedata. Available at (2023-08-22): SLU GET (Geodata Extraction Tool) Service.
44. Lantmäteriet, *Terrain Model Download, grid 50+ NH*. 2022: Product description. Document version: 1.6. Lantmäteriet (Swedish Land Survey). Available at (2024-08-12): (https://www.lantmateriet.se/globalassets/geodata/geodataprodukter/hojddata/e_grid50plus_nh.pdf).
45. SGU, *Produkt: Jorddjupsmodell*. 2024: Produktbeskrivning. Sveriges geologiska undersökning (SGU). Available at (2024-08-12): (https://resource.sgu.se/dokument/produkter/jorddjupsmodell-beskrivning.pdf).
46. SGU, *Jorddjup_10x10m (tif)*. 2023: Raster dataset. Produkt: Jorddjupsmodell. © Sveriges geologiska undersökning (SGU). Available at (2023-08-24): SLU GET (Geodata Extraction Tool) Service.
47. SGU, *Produkt: Jordarter 1:25 000 – 1:100 000*. 2024: Produktbeskrivning. Sveriges geologiska undersökning (SGU). Available at (2024-08-13): (https://resource.sgu.se/dokument/produkter/jordarter-25-100000-beskrivning.pdf).
48. SGU, *Jordarter_25_100k_jg2*. 2023: Vector dataset (Jordart, grundlager JG2). Produkt: Jordarter 1:25 000 - 1 000 000. © Sveriges geologiska undersökning (SGU). Available at (2023-09-27): SLU GET (Geodata Extraction Tool) Service.
49. European Environment Agency, *CORINE Land Cover 2018 (vector/raster 100 m), Europe, 6-yearly - version 2020_20u1, May 2020*. 2020: © European Union, Copernicus Land Monitoring Service 2024, European Environment Agency (EEA). "Available at (2024-05-29): (https://land.copernicus.eu/en/products/corine-land-cover/clc2018#general_info).
50. Copernicus, *Corine Land Cover*. 2024: Copernicus: Europe's eyes on Earth. Available at (2024-08-13): (https://land.copernicus.eu/pan-european/corine-land-cover).
51. Sköldberg, H., J. Holm, and A. Rensfeldt, *Värdet av säsongslager i regionala energisystem – modellberäkningar av sex typsystem (The Value of Seasonal Storage in Regional Energy Systems - Model Calculations of Six Type Systems)*. 2019: Rapport 2019:624. Energiforsk. Available at (2025-03-04): https://energiforsk.se/media/27170/vardet-av-sasongslager-i-regionala-energisystem-energiforskrapport-2019-624.pdf.

52. Epp, B. *Seasonal pit heat storage: Cost benchmark of 30 EUR/m³*. 2019; Available from: https://solarthermalworld.org/news/seasonal-pit-heat-storage-cost-benchmark-30-eurm3/.
53. Epp, B. *A guideline for industrial heat pumps adapted to district heating networks*. 2024 [cited 2025 March 19]; Available from: https://solarthermalworld.org/news/a-guideline-for-industrial-heat-pumps-adapted-to-district-heating-networks/.

Appendices

Input datasets for the screening process

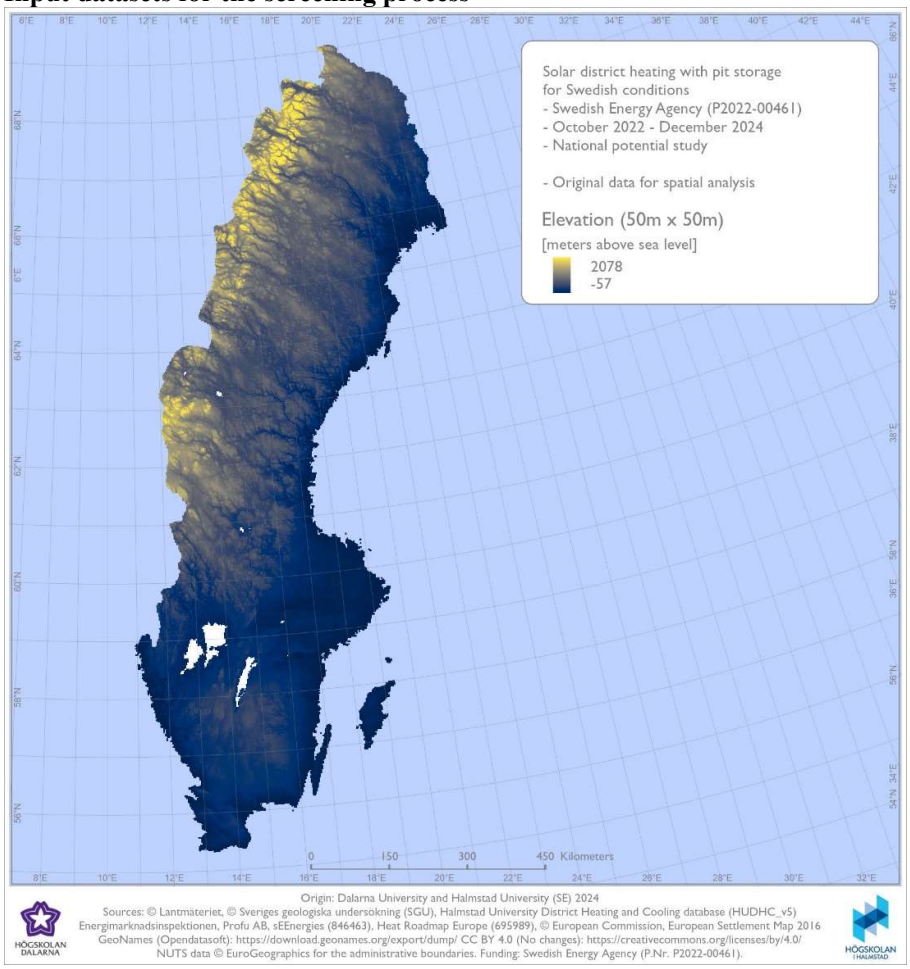

Figure 48. Input datasets for the screening process: Elevation.

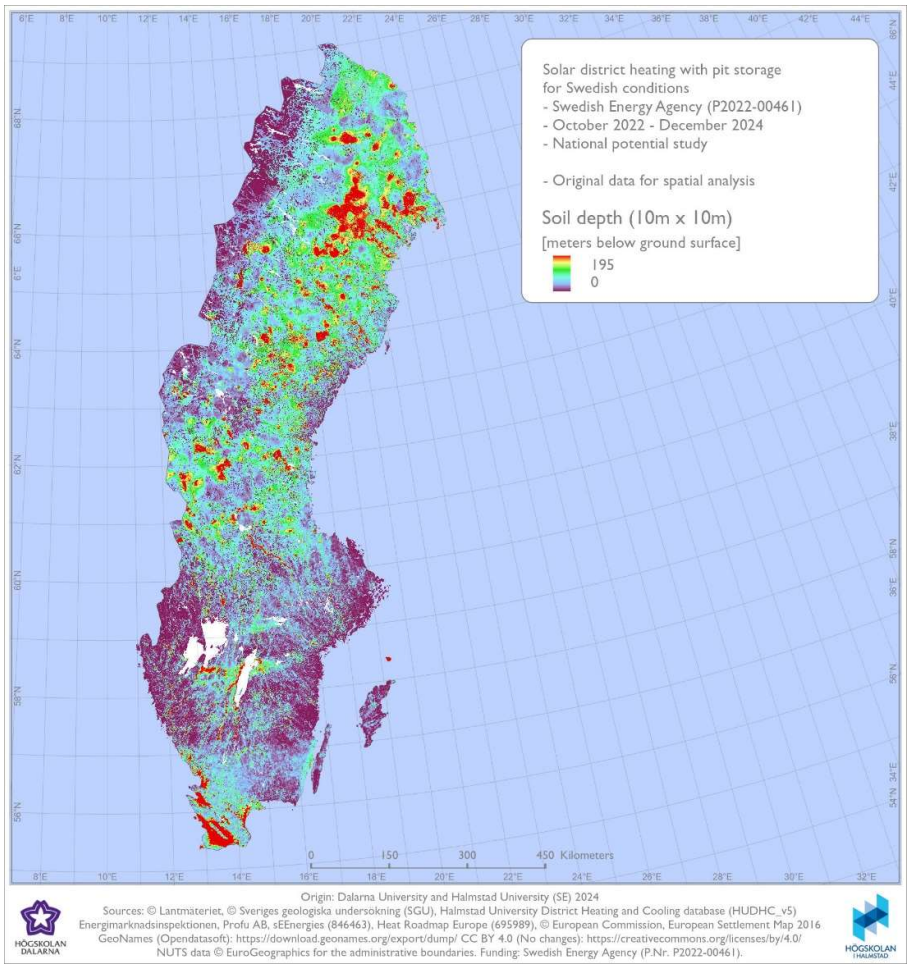

Figure 49. Input datasets for the screening process: Soil depth.

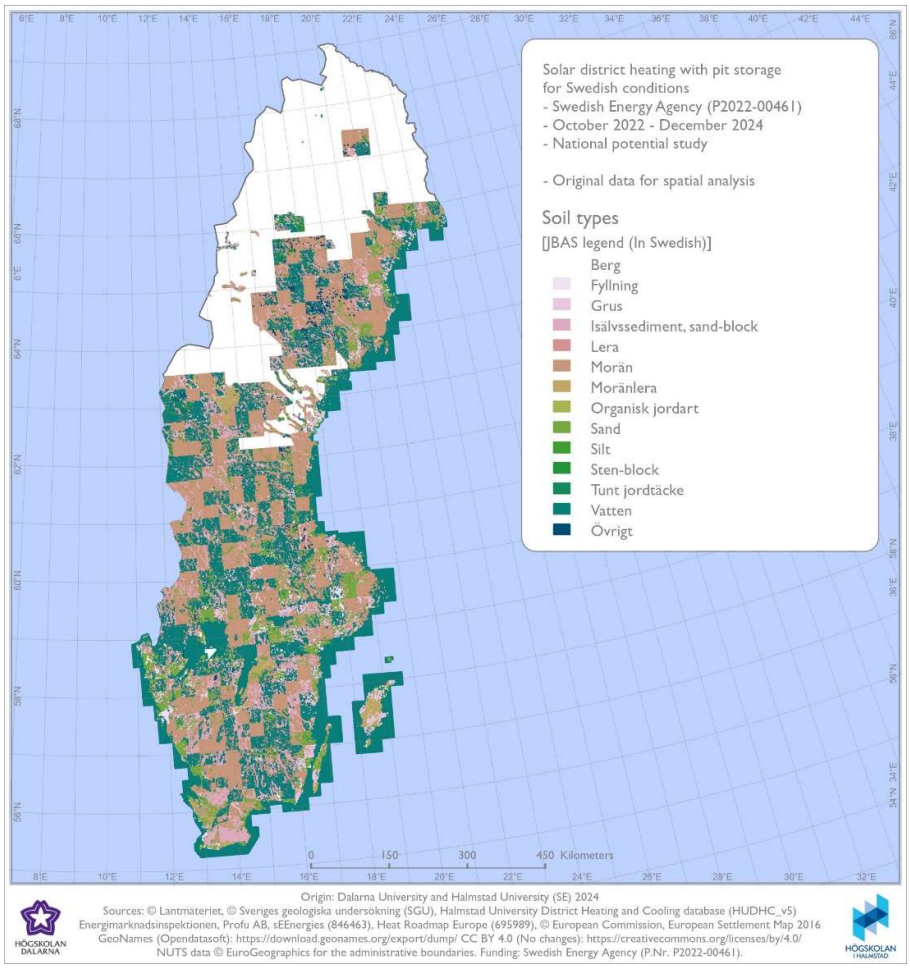

Figure 50. Input datasets for the screening process: Soil types.

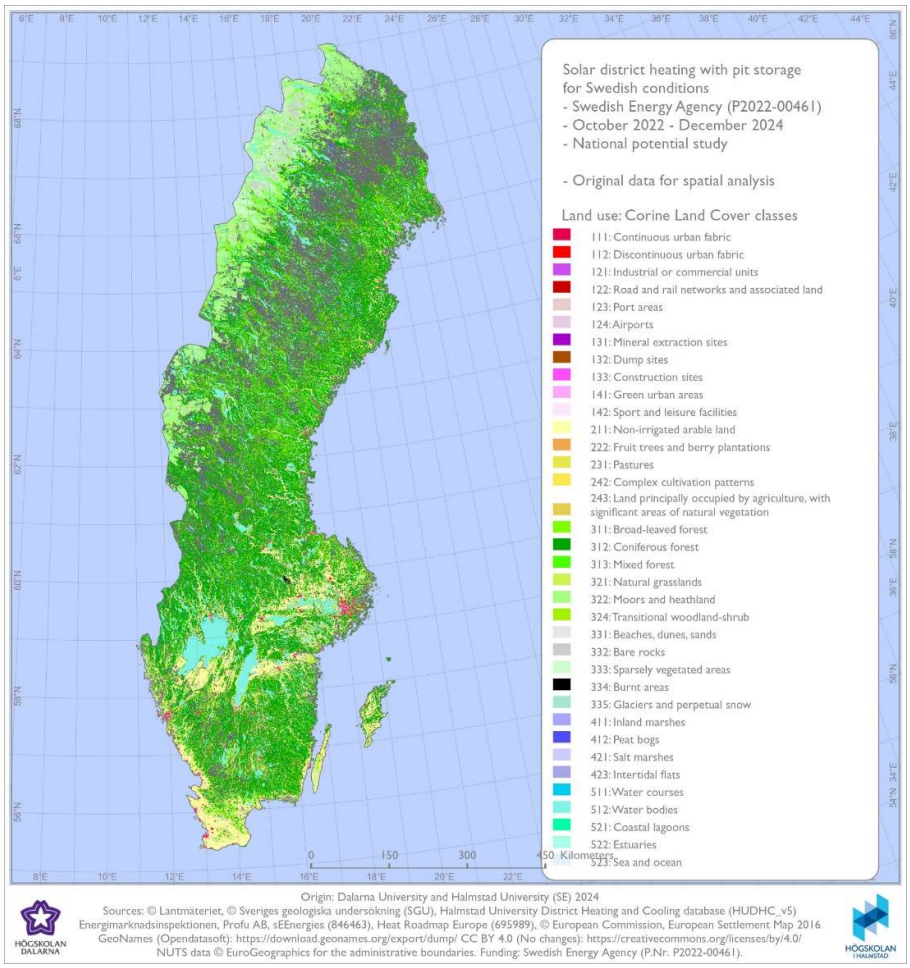

Figure 51. Input datasets for the screening process: Land use.

Complementary datasets for the screening process

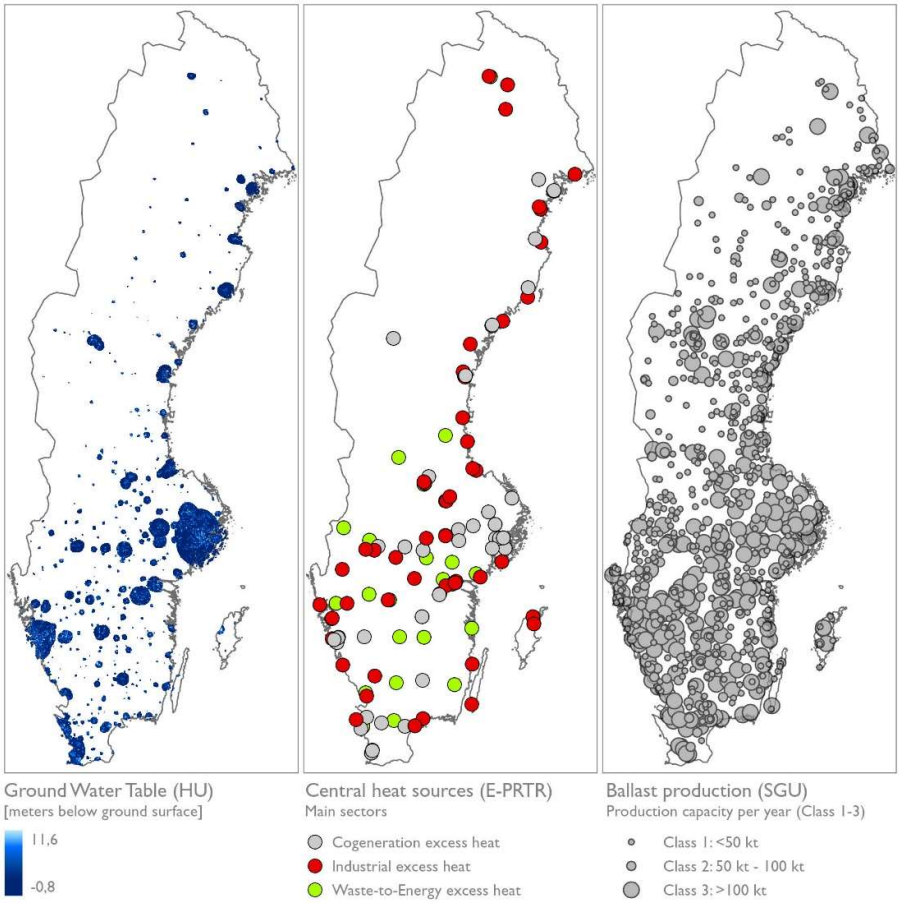

Figure 52. Complementary datasets for the screening process: Modelled ground water table (within boundary layer), central heat sources, and ballast production sites.

Selection criteria for required soil type

Table 24. Selection criteria for required soil type by screening 1 and 2

JBAS_TX	JG2_TX	JG2_ Code	Suitability (Yes/ No) First screening	Suitability (Yes/ No) Second screening
Berg	Berg	888	No	No
	Fanerozoisk diabas	823	No	No
	Rösberg	849	No	No
	Sedimentärt berg	850	No	No
	Skålla av sedimentärt berg	9950	No	No
	Urberg	890	No	No
	Vittringsjord	82	No	No
	Vittringsjord, sand--grus	8950	No	No
Fyllning	Fyllning	200	Yes	Yes
	Fyllning, rödfyr	322	Yes	Yes
Grus	Svallsediment, grus	33	Yes	Yes
	Svämsediment, grus	62	Yes	Yes
	Älvsediment, grus	8803	Yes	Yes
Isälvssediment, sand-block	Isälvssediment	50	Yes	Yes
	Isälvssediment, grus	57	Yes	Yes
	Isälvssediment, sand	55	Yes	Yes
	Isälvssediment, sten--block	51	Yes	Yes
Lera	Glacial finlera	43	No	No
	Glacial grovlera	44	No	Yes
	Glacial lera	40	No	No
	Lera	85	No	No
	Lera--silt	86	No	No
	Lera--silt, tidvis under vatten	8186	No	No
	Postglacial finlera	19	No	No
	Postglacial grovlera	22	No	Yes
	Postglacial lera	17	No	No
Morän	Grusig morän	93	Yes	Yes
	Morän	100	Yes	Yes
	Sandig morän	95	Yes	Yes
	Sandig-siltig morän	97	Yes	Yes

Moränlera	Lerig morän	9794	Yes	Yes
	Moränfinlera	99	No	Yes
	Morängrovlera	98	Yes	Yes
	Moränlera	101	Yes	Yes
	Moränlera eller lerig morän	9792	Yes	Yes
Organisk jordart	Bleke och kalkgyttja	2306	No	No
	Gyttja	6	No	No
	Gyttjelera (eller lergyttja)	16	No	No
	Kärrtorv	5	No	No
	Mossetorv	1	No	No
	Torv	75	No	No
	Torv, tidvis under vatten	8175	No	No
Sand	Flygsand	13	Yes	Yes
	Postglacial finsand	28	Yes	Yes
	Postglacial sand	31	Yes	Yes
	Sand	21	Yes	Yes
	Svämsediment, sand	10	Yes	Yes
	Älvsediment	8804	Yes	Yes
	Älvsediment, sand	8809	Yes	Yes
Silt	Glacial grovsilt--finsand	9060	No	No
	Glacial silt	48	No	No
	Postglacial grovsilt-finsand	79	No	Yes
	Postglacial silt	24	No	No
	Silt	39	No	No
	Svämsediment	8937	No	No
	Svämsediment, grovsilt--finsand	9010	No	Yes
	Svämsediment, ler--silt	9	No	No
	Vittringsjord, ler--silt	8919	No	No
	Älvsediment, grovsilt--finsand	8802	No	Yes
	Älvsediment, ler--silt	8806	No	No
Sten-block	Blockmark	66	No	No
	Klapper	34	No	No
	Sten--block	92	No	No
	Talus (rasmassor)	81	No	No
	Älvsediment sten--block	8814	No	Yes
Vatten	Vatten	91	No	No
Övrigt	Flytjord eller skredjord	2372	No	No
	Kalktuff	1950	No	No

	Morän omväxlande med sorterade sediment	9147	Yes	Yes
	Oklassat område	90	No	No
	Oklassat område, tidvis under vatten	8114	No	No
	Skaljord	36	No	No
	Slamströmssediment, ler--block	2368	No	No

Selection criteria for available areas

Table 25. Selection criteria for available areas by screening 1 and 2

CLC_CODE	LABEL1	LABEL3	1st screening	2nd screening	Suitability (Yes/No/Maybe)
111	Artificial surfaces	Continuous urban fabric			No
112	Artificial surfaces	Discontinuous urban fabric			No
121	Artificial surfaces	Industrial or commercial units		SDH	Maybe
122	Artificial surfaces	Road and rail networks and associated land		SDH	Maybe
123	Artificial surfaces	Port areas		SDH	Maybe
124	Artificial surfaces	Airports		SDH	Maybe
131	Artificial surfaces	Mineral extraction sites		SDH	Maybe
132	Artificial surfaces	Dump sites		SDH	Maybe
133	Artificial surfaces	Construction sites		SDH	Maybe
141	Artificial surfaces	Green urban areas		SDH	Maybe
142	Artificial surfaces	Sport and leisure facilities		SDH	Maybe
211	Agricultural areas	Non-irrigated arable land	SDH	SDH	Yes
212	Agricultural areas	Permanently irrigated land	SDH	SDH	Yes
213	Agricultural areas	Rice fields	SDH	SDH	Yes
221	Agricultural areas	Vineyards			No
222	Agricultural areas	Fruit trees and berry plantations			No
223	Agricultural areas	Olive groves			No
231	Agricultural areas	Pastures	SDH	SDH	Yes
241	Agricultural areas	Annual crops associated with permanent crops	SDH	SDH	Yes

242	Agricultural areas	Complex cultivation patterns	SDH	SDH	Yes
243	Agricultural areas	Land principally occupied by agriculture, with significant areas of natural vegetation	SDH	SDH	Yes
244	Agricultural areas	Agro-forestry areas	SDH	SDH	Yes
311	Forest and semi natural areas	Broad-leaved forest		SDH	Maybe
312	Forest and semi natural areas	Coniferous forest		SDH	Maybe
313	Forest and semi natural areas	Mixed forest		SDH	Maybe
321	Forest and semi natural areas	Natural grasslands	SDH	SDH	Yes
322	Forest and semi natural areas	Moors and heathland	SDH	SDH	Yes
323	Forest and semi natural areas	Sclerophyllous vegetation	SDH	SDH	Yes
324	Forest and semi natural areas	Transitional woodland-shrub	SDH	SDH	Yes
331	Forest and semi natural areas	Beaches, dunes, sands	SDH	SDH	Yes
332	Forest and semi natural areas	Bare rocks			No
333	Forest and semi	Sparsely vegetated areas	SDH	SDH	Yes

	natural areas				
334	Forest and semi natural areas	Burnt areas	SDH	SDH	Yes
335	Forest and semi natural areas	Glaciers and perpetual snow			No
411	Wetlands	Inland marshes			No
412	Wetlands	Peat bogs			No
421	Wetlands	Salt marshes			No
422	Wetlands	Salines			No
423	Wetlands	Intertidal flats			No
511	Water bodies	Water courses			No
512	Water bodies	Water bodies			No
521	Water bodies	Coastal lagoons			No
522	Water bodies	Estuaries			No
523	Water bodies	Sea and ocean			No

Aggregated District Heating Areas (DHA*) for different administrative areas

As for district heating areas, aggregated and unique, Table 26 summarizes the numbers by NUTS2 and NUTS3 administrative areas in a similar way as was done for DHS above.

Table 26. Total count of aggregated district heating areas (DHA*) and the corresponding total count of district heating areas (DHA) and district heating systems (DHS) within them, by administrative areas. Note that the DHS summation by administration area was done based on a different spatial join operation compared to that in Table 11

Administrative areas	DHA* [n]	DHA [n]	DHS [n]	Pop. [kn]	Qs [GWh/a]
Mellersta Norrland	**36**	**40**	**41**	**248**	**2,226**
Jämtlands län	18	18	18	76	743
Västernorrlands län	18	22	23	172	1,483
Norra Mellansverige	**66**	**76**	**74**	**541**	**4,339**
Dalarnas län	23	26	26	178	1,504
Gävleborgs län	24	30	28	195	1,646
Värmlands län	19	20	20	168	1,189
Östra Mellansverige	**53**	**70**	**69**	**1,022**	**7,901**
Örebro län	14	18	16	248	1,584
Östergötlands län	13	19	19	369	2,845
Södermanlands län	8	9	9	89	612
Uppsala län	9	9	10	22	111
Västmanlands län	9	15	15	294	2,749
Övre Norrland	**42**	**50**	**48**	**389**	**3,861**
Norrbottens län	19	21	21	158	2,081
Västerbottens län	23	29	27	231	1,779
Småland med öarna	**69**	**72**	**69**	**529**	**4,043**
Gotlands län	5	5	5	28	209
Jönköpings län	22	23	25	231	1,625
Kalmar län	22	23	19	136	1,182
Kronobergs län	20	21	20	134	1,028
Stockholm	**3**	**34**	**47**	**2,509**	**14,890**
Stockholms län	3	34	47	2,509	14,890
Sydsverige	**34**	**51**	**53**	**1,054**	**6,180**
Blekinge län	8	10	9	128	641
Skåne län	26	41	44	926	5,538
Västsverige	**53**	**71**	**75**	**1,384**	**8,451**
Hallands län	9	9	7	138	812
Västra Götalands län	44	62	68	1,246	7,639
Grand Total	**356**	**464**	**476**	**7,677**	**51,891**

From Table 26, it is clear that the aggregation of 464 unique – but partly overlapping – district heating areas, resulted in 356 aggregated DHA*. It

may further be seen that the effect of aggregation is more profound in regions which host larger city areas, relative to regions with a more rural character. For example, in Jämtlands län and Hallands län, no aggregation occurs at all (18 DHA* and 18 DHA, 9 DHA* and 9 DHA, respectively), whereas in Stockholm, a total of 34 unique district heating areas (harboring 47 DHS) is reduced to three aggregated district heating areas.

Screen capture map illustrations of the 1st and 4th scenario

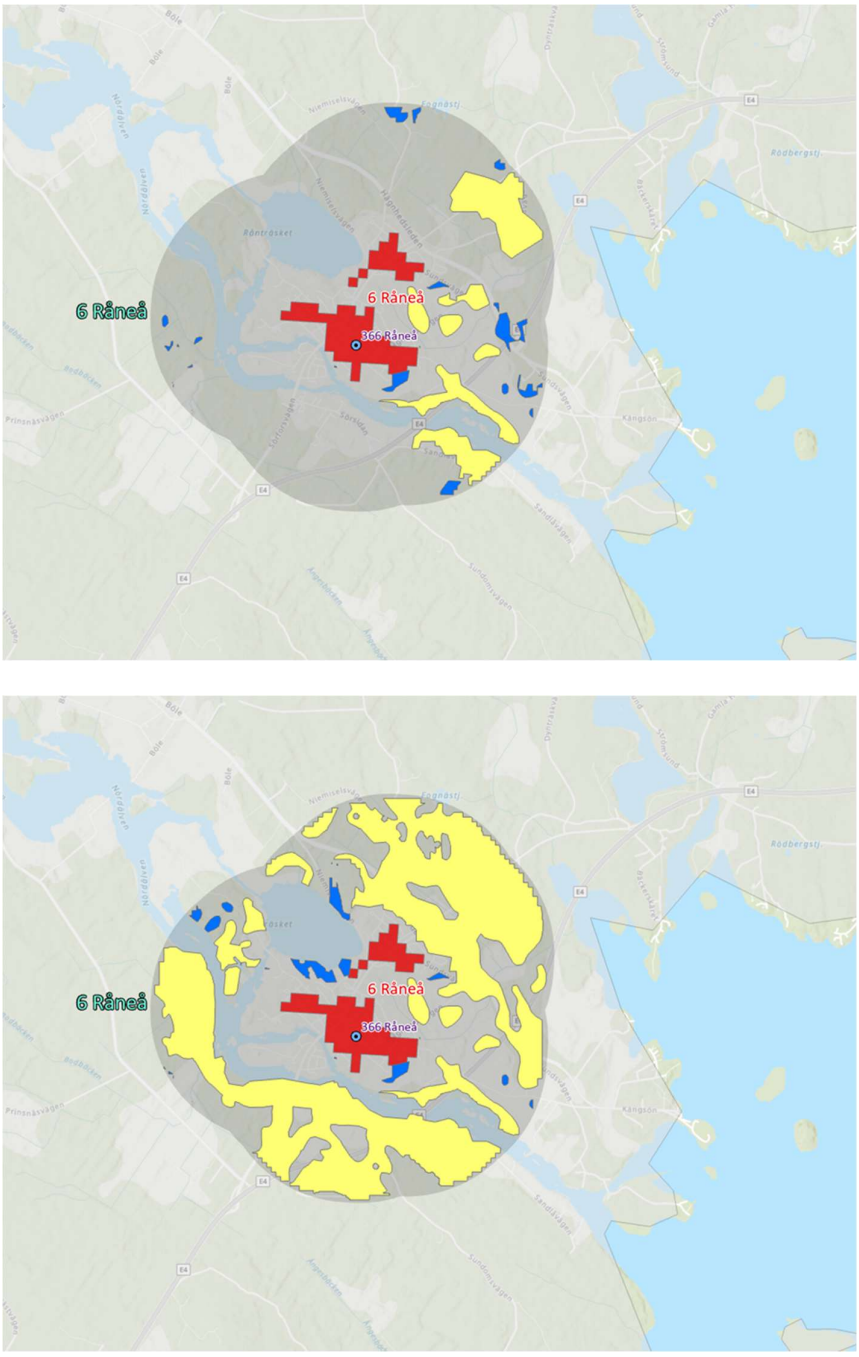

Figure 53. Screen capture map illustrations of suitable areas (yellow) identified in the town of Råneå under the 1st scenario (top) and 4th scenario (bottom). Blue polygons indicate suitable area candidates which did not meet roundness criteria.

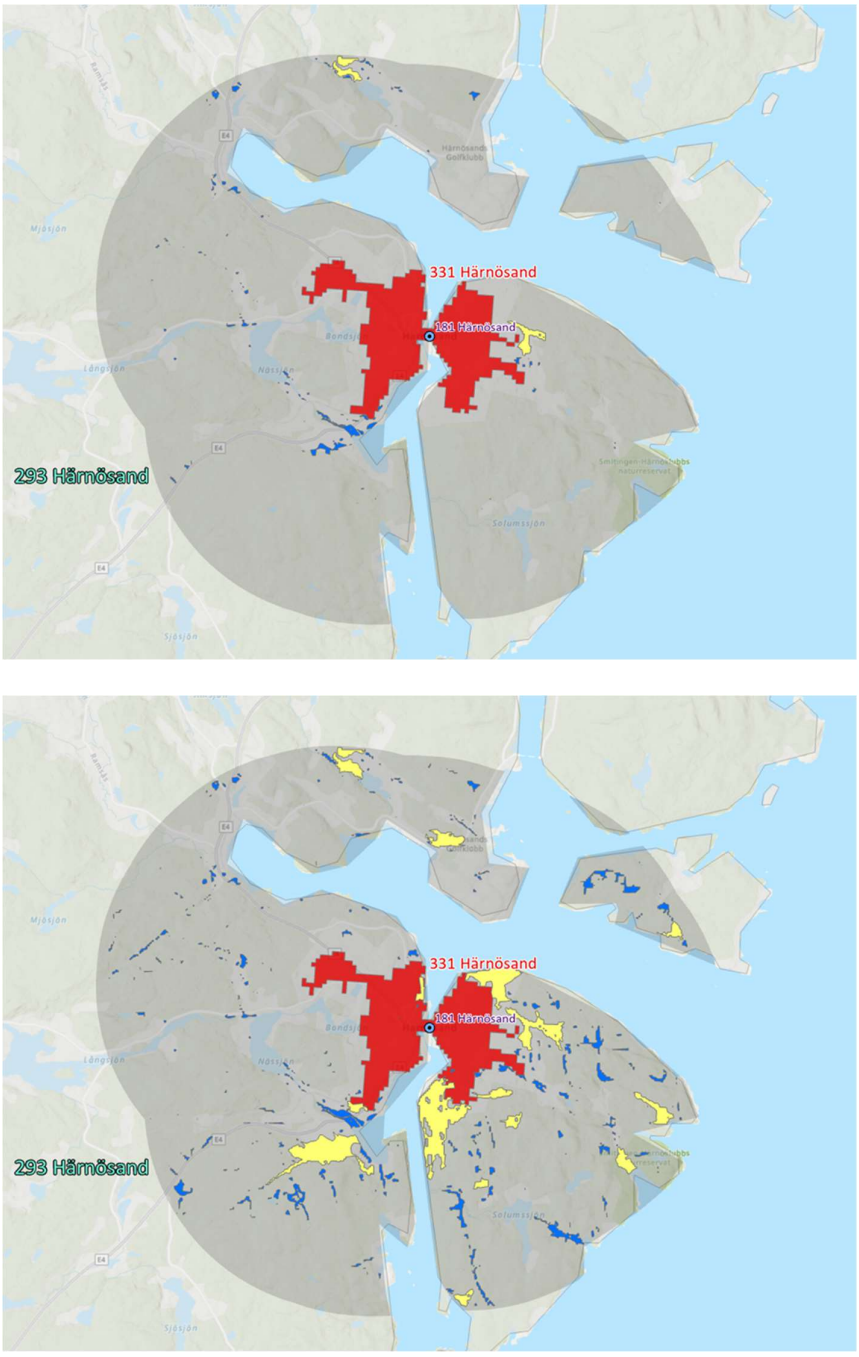

Figure 54. Screen capture map illustrations of suitable areas (yellow) identified in the town of Härnösand under the 1st scenario (top) and 4th scenario (bottom). Blue polygons indicate suitable area candidates which did not meet roundness criteria.

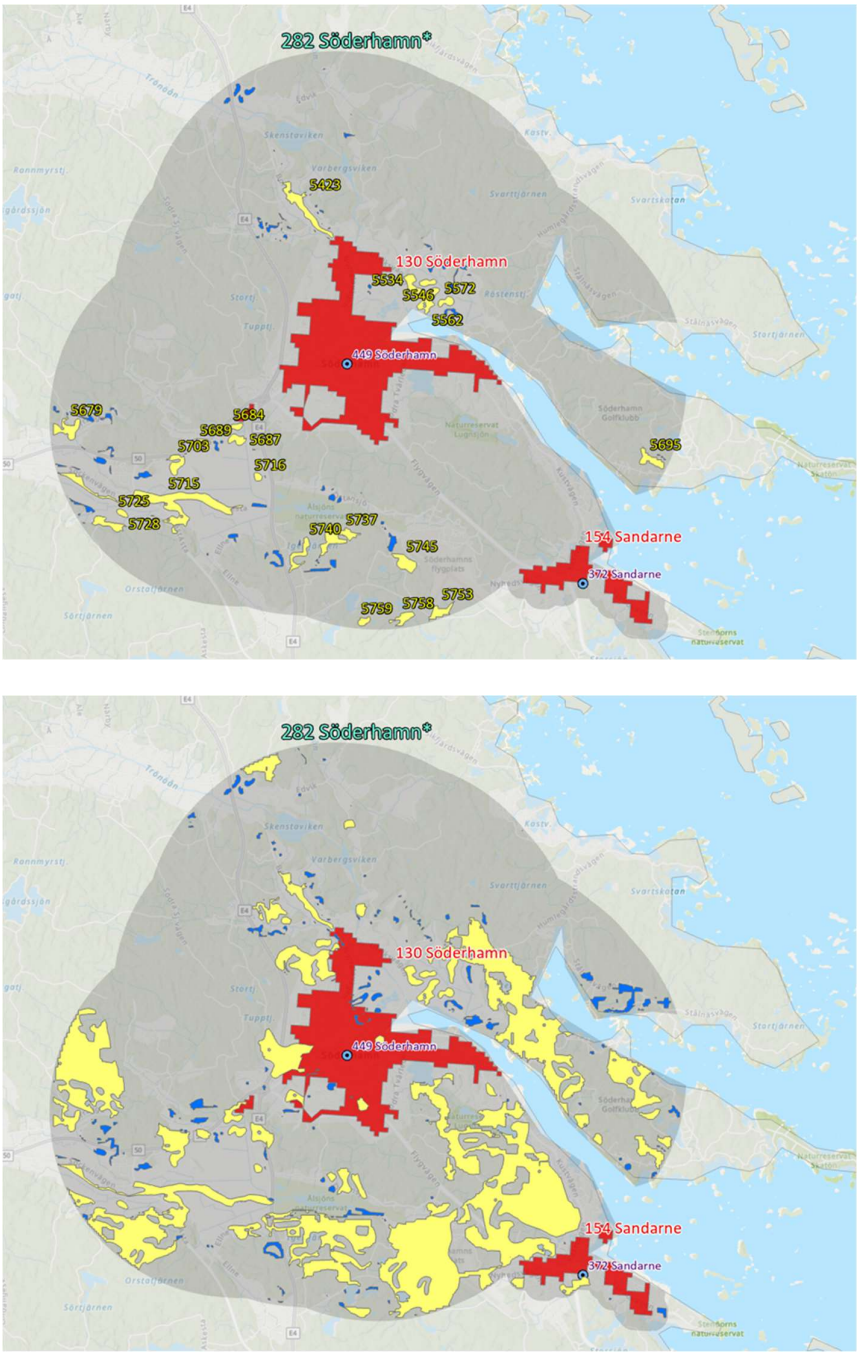

Figure 55. Screen capture map illustrations of suitable areas (yellow) identified in the town of Söderhamn under the 1st scenario (top, with SA ID-numbers) and 4th scenario (bottom). Blue polygons indicate suitable area candidates which did not meet roundness criteria.

Result tables for the 2nd and 3rd scenarios

Table 27. Scenario 2 (Total): Count of aggregated district heating areas (DHA*) and the corresponding total count of district heating areas (DHA) and district heating systems (DHS) within them, as well as count of suitable areas (SA) by NUTS2 and NUTS3 administrative units, with average and max ratio of suitable areas summed area [km2] by summed annual district heat deliveries [GWh/a]

NUTS2/NUTS3	DHA* [n]	DHA [n]	DHS [n]	SA [n]
Mellersta Norrland	**20**	**24**	**28**	**191**
Jämtlands län	11	11	12	42
Västernorrlands län	9	13	16	149
Norra Mellansverige	**46**	**56**	**55**	**433**
Dalarnas län	18	21	21	163
Gävleborgs län	17	23	22	196
Värmlands län	11	12	12	74
Östra Mellansverige	**31**	**48**	**50**	**632**
Örebro län	8	12	12	226
Östergötlands län	10	16	16	294
Södermanlands län	3	4	5	20
Uppsala län	5	5	6	13
Västmanlands län	5	11	11	79
Övre Norrland	**27**	**35**	**35**	**461**
Norrbottens län	11	13	13	260
Västerbottens län	16	22	22	201
Småland med öarna	**34**	**37**	**39**	**359**
Gotlands län	1	1	1	3
Jönköpings län	17	18	20	189
Kalmar län	9	10	10	101
Kronobergs län	7	8	8	66
Stockholm	**2**	**33**	**45**	**153**
Stockholms län	2	33	45	153
Sydsverige	**32**	**49**	**52**	**690**
Blekinge län	7	9	9	28
Skåne län	25	40	43	662
Västsverige	**35**	**53**	**60**	**661**
Hallands län	5	5	5	144
Västra Götalands län	30	48	55	517
Grand Total	**227**	**335**	**364**	**3580**

Table 28. Scenario 3 (Total): Count of aggregated district heating areas (DHA*) and the corresponding total count of district heating areas (DHA) and district heating systems (DHS) within them, as well as count of suitable areas (SA) by NUTS2 and NUTS3 administrative units, with average and max ratio of suitable areas summed area [km2] by summed annual district heat deliveries [GWh/a]

NUTS2/NUTS3	DHA* [n]	DHA [n]	DHS [n]	SA [n]
Mellersta Norrland	**25**	**29**	**32**	**397**
Jämtlands län	11	11	12	61
Västernorrlands län	14	18	20	336
Norra Mellansverige	**52**	**62**	**61**	**722**
Dalarnas län	21	24	24	260
Gävleborgs län	20	26	25	368
Värmlands län	11	12	12	94
Östra Mellansverige	**39**	**56**	**58**	**723**
Örebro län	10	14	14	278
Östergötlands län	12	18	18	273
Södermanlands län	4	5	6	34
Uppsala län	5	5	6	19
Västmanlands län	8	14	14	119
Övre Norrland	**32**	**40**	**40**	**823**
Norrbottens län	11	13	13	403
Västerbottens län	21	27	27	420
Småland med öarna	**43**	**46**	**48**	**452**
Gotlands län	1	1	1	1
Jönköpings län	19	20	22	233
Kalmar län	12	13	13	119
Kronobergs län	11	12	12	99
Stockholm	**2**	**33**	**45**	**315**
Stockholms län	2	33	45	315
Sydsverige	**32**	**49**	**52**	**1029**
Blekinge län	7	9	9	43
Skåne län	25	40	43	986
Västsverige	**43**	**61**	**67**	**763**
Hallands län	8	8	7	122
Västra Götalands län	35	53	60	641
Grand Total	**268**	**376**	**403**	**5224**

Distribution of suitable area sizes by bin areas

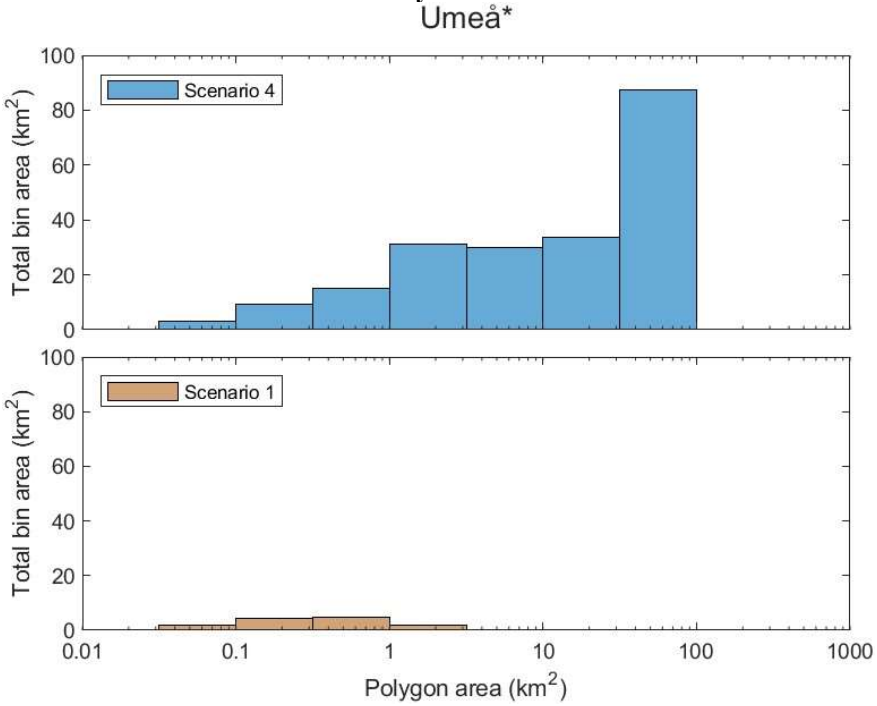

Figure 56. Distribution of suitable area polygon areas (km^2) in the 1st scenario (bottom) and the 4th scenario (top) for the aggregated district heating area of Umeå*.

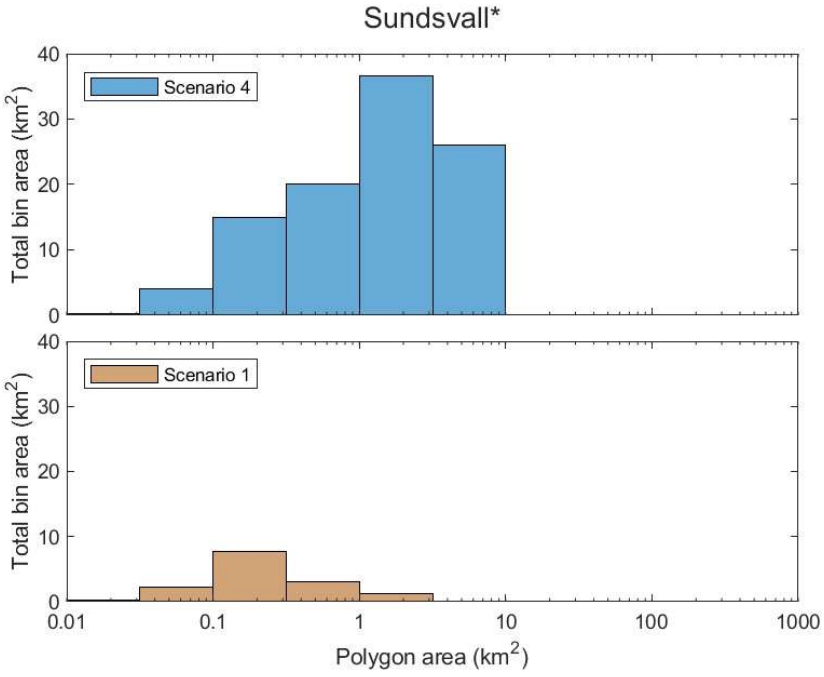

Figure 57. Distribution of suitable area polygon areas (km^2) in the 1st scenario (bottom) and the 4th scenario (top) for the aggregated district heating area of Sundsvall*.

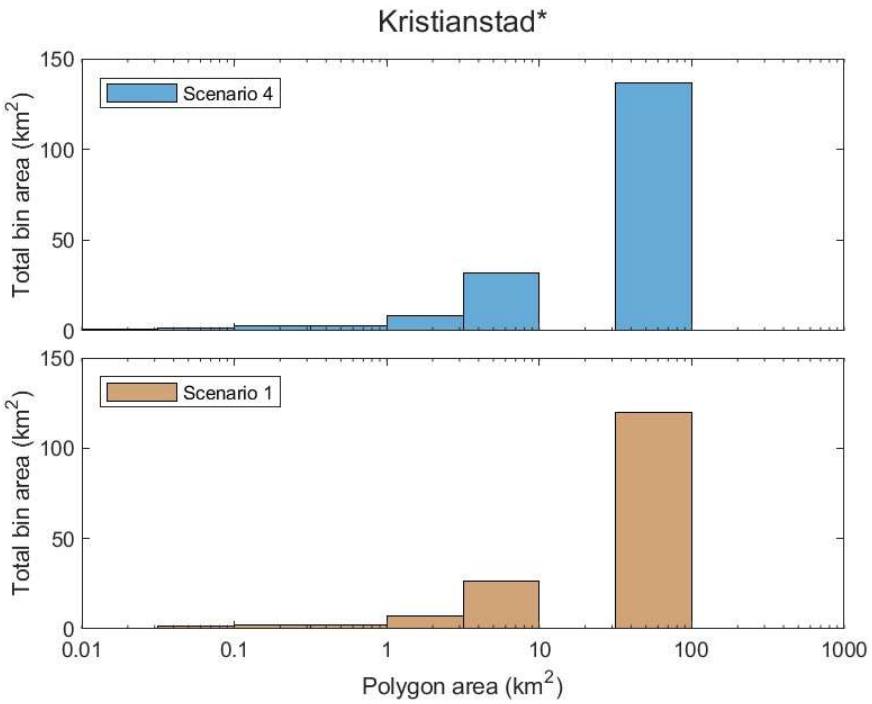

Figure 58. Distribution of suitable area polygon areas (km^2) in the 1st scenario (bottom) and the 4th scenario (top) for the aggregated district heating area of Kristianstad*.